Chapter 6

6 Seismic Vulnerability in Mérida

6.1 Introduction

As explained previously in chapter 3: Vulnerability Assessment Methods, several approaches are available to assess the seismic vulnerability of buildings. In this research, the study is performed at two levels, globally, for Mérida city, and locally, for the "La Milagrosa" Barrio. For this last evaluation, and to acquire knowledge, a structural analysis is carried out (through prototype buildings) for one of the most vulnerable typologies, to forwardly apply both a score assignment approach (the Italian Vulnerability Index Method) and a typology matrix based method (LM1).

6.2 Preliminary vulnerability and damage in Mérida.

In Venezuela, building inventories for the principal cities of the country are not yet available, and cadastral data is very limited where it exists. The information available on buildings is the result of national census performed through the last two decades, where this information does not have the level required for the purpose of vulnerability assessment. The city of Mérida is not an exception in Venezuela; the local government in Mérida does not have a building inventory or a cadastral database. For the case pertaining to this research, a methodology based in Capacity Spectrum is not practical, due to the unavailability of enough information of the buildings to build-up the curves (Capacity-Fragility). The information available for the assessment of seismic vulnerability for the city of Mérida is that of the building's typological descriptions in a macroseismic scale, which is not enough to build-up capacity and fragility models, consequently, an empirical-expert opinions approach is used in the assessment of seismic vulnerability for the buildings in Mérida City. For these reasons, the information used for vulnerability assessments in this research corresponds to surveys performed by previous studies in the city; the general data on population is that from the last National Census in October 2001 [INE, 2001].

6.2.1 Building typology matrix

For the case of Mérida city, a survey performed by Laffaille (1996) is used; the author classified the buildings based in the MSK-1964 scale, considering a division of the surveyed zone in 28 sectors, accounting for a total number of 14,565 buildings. The criteria used for

sectorization comprise the homogeneity of the building classes present in the sub-sectors, and the physical barriers and accessibility, such as rivers, bridges and roads/streets.

The MSK-64 scale describes three structural typologies within which Laffaille (1996) establishes the classification:

A- Buildings of fieldstone, rural structures, adobe houses, clay houses.

B- Ordinary brick buildings, large block construction, half-timbered structures, and structures of hewn blocks of stone, also including in this vulnerability class the non-engineered (self-constructed) Reinforced Concrete frame with hollow clay block infill walls building type, observed in the city of Mérida. This last typology is used extensively in Venezuela´s urban zones, and for the case of this research it will be considered as representative of the tackled vulnerability class. The preponderance of this RC frame typology among the non-engineered constructions finds its justification in several factors accounted by Papanikolau and Taucer, (2004). Such factors involve, in the choice of RC buildings before other typologies: (1) a social issue, as the earthen and wooden houses have been associated by the population to poverty and inferior social status; (2) a security issue, as the consequences of historical earthquakes have proven that these typologies have a high risk of homeless and mortality; and (3) economic and practical issues, such as the scarcity of natural materials (wood, soil) in the periphery of the urban centers, and additionally, the shortage of building lots in urban areas (especially the legally owned ones) where these lots have usually a limited surface resulting in a need for multi-storey residential buildings not practicable through the use of traditional construction techniques (earthen-wooden architecture).

C- Reinforced Concrete and Steel buildings.

Under the structural type C, Laffaille (1996) establishes additional subtypes for several construction groups in Mérida city, based in the assumption that buildings of this type may resist a certain amount of lateral forces. Sub-classification for the type C is:

C5: One or several levels steel frame structure, with one-way slabs as floors and roofs and unreinforced hollow brick walls.

C6: One or several levels reinforced concrete structures with one-way slabs as floors and roofs and with unreinforced hollow brick walls.

C7: Several levels reinforced concrete flat slab buildings.

C8: Several levels reinforced concrete cast-in-situ walls and slabs.

Additionally, the author includes another type of construction, under the designation of "*Rancho*" (R), a self-constructed building type disseminated over urban areas in Venezuela fabricated with waste materials (aluminum sheets, cardboard, sticks, and any other waste material available in urban areas) with a very low quality of workmanship and consequently with a very high vulnerability.

Analyzing this classification, equivalence to EMS-98 scale vulnerability classes is performed by the different building types (in Table 3.3), and by means of the "*Guidelines for Seismic Vulnerability of Construction Types*" in [EERI/IAEE, 2001], which describes, in more detail, building types based in the EMS-98 scale (Table 6.1).

Proposed equivalences are shown in Table 6.2, and the criteria used for this equivalence are explained as follows:

- The "Rancho" (R) building type is classified as A, because of its inherent low quality that may result in a very poor seismic performance.
- A and B building types correspond to the same vulnerability classes as in MSK-64, including in type B the non-engineered (non-engineered/self-constructed) Reinforced Concrete frame with hollow clay block infill walls building type, corresponding to the EMS-98 RC frame without seismic features building type in Table 6.1, to which is assigned, preliminarily, a vulnerability class C; however, other studies [Castillo and Almansa, 2001; Schwarz et. al., 2000; Mejía, 2001] show that a better compliance to a vulnerability class is represented by class B. The reasons to lower the vulnerability class responds, in the first place, to post-earthquake investigations performed after the 1997 Caríaco earthquake [Schwarz et. al., 2000], where macroseismic studies for the Caríaco area identified the non-engineered RC-frame buildings into vulnerability class B. In second place, [Castillo and Almansa, 2001] recommend, after a qualitative analysis of the building type and the detection of several flaws in member detailing, to assign vulnerability class B.
- C5 building type corresponds to steel structures in the EMS-98 structural type with a vulnerability class E.
- C6 building type corresponds to RC frame designed with seismic features in the EMS-98 structural type with a vulnerability class D.
- C7 building type corresponds to the RC flat slab subtype in Table 6., with the vulnerability class C.
- C8 building type corresponds to the RC shear wall structure cast in-situ, in Table 6., with a vulnerability class E.

Observing the proposed equivalence in Table 6.2, the Rancho and the Adobe Block Walls-Rubble Stone building types fall both into the vulnerability class A, although it is expected a better seismic performance in the second building type. Also, the Steel Moment Resisting Frame and the RC Shear Wall building types fall in the same vulnerability class (Class E) although the expected behavior of the Steel Frame should be better than the one of the RC Shear walls. These typological identifications and its relationship to vulnerability classes may introduce an erroneous or at least imprecise appraisal of some building types, as some differentiation should be established in order to take into account differences in seismic performance for different building types.

Material	Type of Load-Bearing Structure	No	Subtypes	Vulnerability Class					
				A	B	C	D	E	F
Masonry	Stone Masonry Walls	1	Rubble stone (field stone) in mud/lime mortar or without mortar (usually with timber roof)	O					
		2	Massive stone masonry (in lime/cement mortar)		|-	O	-|		
	Earthen/Mud/	3	Mud walls	O					
	Adobe/Rammed Earthen Walls	4	Mud walls with horizontal wood elements	|-	O	-|			
		5	Adobe block walls	O					
		6	Rammed earth/Pise construction						
	Clay brick/block masonry walls	7	Unreinforced brick masonry in mud mortar	|-	O	-|			
		8	Unreinforced brick masonry in mud mortar with vertical posts						
		9	Unreinforced brick masonry in cement mortar with reinforced concrete floor/roof slabs		|-	O	-|		
		10	Confined brick/block masonry with concrete posts/tie columns and beams			|-	O	-|	
	Concrete block masonry	11	Unreinforced in lime/cement mortar (various floor/roof systems)						
		12	Reinforced, in cement mortar (various floor/roof systems)			|-	O	-|	
Structural concrete	Moment resisting frame	13	Designed for gravity loads only (predating seismic codes i.e. no seismic features)	|-	-	O	-|		
		14	Designed with seismic features (various ages)			|-	-	O	-|
		15	Frame with unreinforced masonry infill walls						
		16	Flat slab structure		|-	O	-|		
		17	Precast frame structure						
		18	Frame with concrete shear walls-dual system						
	Shear wall structure	19	Walls cast in-situ				|-	O	-|
		20	Precast wall panel structure		|-	O	-|		
Steel	Moment-resisting frame	21	With brick masonry partitions						
		22	With cast in-situ concrete walls						
		23	With lightweight partitions						
	Braced frame	24					|-	O	-|
Wooden structures	Load-bearing timber frame	25	Thatch		|-	O	-|		
		26	Post and beam frame			|-	O	-|	
		27	Walls with bamboo/reed mesh and post (Wattle and Daub)						
		28	Frame with (stone/brick) masonry infill						
		29	Frame with plywood/gypsum board sheathing						
		30	Frame with stud walls				|-	O	-|

Table 6.1: Guidelines for Seismic Vulnerability of Construction Types [EERI/IAEE, 2001].

As explained in Subsection 3.3.1, the LM1 Methodology can overcome this kind of problems through an intermediate classification of buildings using both the typological identification and its index rating (*vulnerability index*). This double entry to vulnerability assignment allows the differentiation required between different building types falling inside the same vulnerability class in the EMS-98 (as previously explained in Chapter 3). In order to establish this differentiation the Building Typology Matrix (BTM) considered in the LM1 method (shown in Table 6.3) must be used and performed with the recommended procedures for vulnerability analysis.

Number	Laffaille Classification [Laffaille, 1996]	EMS-98 Building Type	EMS-98 Vulnerability Class					
			A	B	C	D	E	F
1	Rancho- auto-constructed building fabricated with waste materials.	N/A	o					
2	A- Buildings of fieldstone, rural structures, adobe houses, clay houses.	Adobe block walls, Rubble stone (field stone)	o	-|				
3	B- Non-engineered one or several levels reinforced concrete frame with unreinforced hollow brick walls.	RC moment resisting frame designed for gravity loads only (no seismic features) or confined masonry	|-	o	-|			
4	C5- One or several levels steel frame structure, with one-way slabs as floors and roofs and unreinforced hollow brick walls	Steel moment-resisting frame with brick masonry partitions			|-	-	o	-|
5	C6- One or several levels RC structure, with one-way slabs as floors and roofs and unreinforced hollow brick walls.	RC frame designed with seismic features.		|-	-	o	-|	
6	C7- Several levels reinforced concrete flat slab buildings.	RC Flat slab structure.		|-	o	-|		
7	C8- Several levels reinforced concrete cast in situ walls and slabs.	RC Shear wall structure, cast in-situ.				|-	o	-|

Most Probable Class Possible Class Unlikely Class (exceptional cases)

Table 6.2: Proposed equivalence for Laffaille (1996) and EMS-98 building Types Classification.

General recommendations in vulnerability analysis through the LM1 methodology are exposed in [Multinovic and Trendafiloski, 2003]. Instructions state that if the building typologies may be identified directly within the BTM, then the vulnerability index values may be assigned univocally from Table 6.3. On the other hand, if the available information is not enough to perform a direct typological identification or the construction does not match any of the typologies in Table 6.3, more general categories may be defined based on both the experience and knowledge of the construction tradition and the similitude with a building typology (BTM_i) in the BTM. For each of the proposed categories, the vulnerability index values (most probable value V_I^*, lower bound of the uncertainty range V_I^-, upper bound of the uncertainty range V_I^+, lower bound of the possible values $V_I^{\min}$ and upper bound of the possible values $V_I^{\max}$), are evaluated knowing the percentage of the different building types recognized inside the category by the weighed average expression for the most probable value:

$$V^*_{I_{CAT\,i}} = \sum_t p_t \, V^*_{I_{BTM\,i}} \qquad \text{eq. 6.1}$$

Where, p_t is the ratio of the buildings inside category CAT_i supposing to belong to a certain building typology BTM_i.

Following the procedure described in [Multinovic and Trendafiloski, 2003], the next step is to estimate the Regional Vulnerability and the Behavior Modifier factors (ΔV_R, ΔV_m, see eq. 3.14), relying in the knowledge of the interest building typology.

Typology	Description	V_I representative values				
		$V_{I,BTM}^{min}$	$V_{I,BTM}^{-}$	$V_{I,BTM}^{*}$	$V_{I,BTM}^{+}$	$V_{I,BTM}^{max}$
M1.1	Rubble stone, fieldstone	0.62	0.81	**0.873**	0.98	1.02
M1.2	Simple stone	0.46	0.65	**0.74**	0.83	1.02
M1.3	Massive stone	0.3	0.49	**0.616**	0.793	0.86
M2	Adobe	0.62	0.687	**0.84**	0.98	1.02
M3.1	Wooden slabs	0.46	0.65	**0.74**	0.83	1.02
M3.2	Masonry vaults	0.46	0.65	**0.776**	0.953	1.02
M3.3	Composite steel and masonry slabs	0.46	0.527	**0.704**	0.83	1.02
M3.4	Reinforced concrete slabs	0.3	0.49	**0.616**	0.793	0.86
M4	Reinforced or confined masonry walls	0.14	0.33	**0.451**	0.633	0.7
M5	Overall strengthened	0.3	0.49	**0.694**	0.953	1.02
RC1	Concrete Moment Frames	-0.02	0.047	**0.442**	0.8	1.02
RC2	Concrete shear walls	-0.02	0.047	**0.386**	0.67	0.86
RC3.1	Regularly infilled walls	-0.02	0.007	**0.402**	0.76	0.98
RC3.2	Irregular frames	0.06	0.127	**0.522**	0.88	1.02
RC4	RC Dual systems (RC frame and wall)	-0.02	0.047	**0.386**	0.67	0.86
RC5	Precast Concrete Tilt-Up Walls	0.14	0.207	**0.384**	0.51	0.7
RC6	Precast C. Frames, C. shear walls	0.3	0.367	**0.544**	0.67	0.86
S1	Steel Moment Frames	-0.02	0.467	**0.363**	0.64	0.86
S2	Steel braced Frames	-0.02	0.467	**0.287**	0.48	0.7
S3	Steel frame+unreinf. mas. infill walls	0.14	0.33	**0.484**	0.64	0.86
S4	Steel frame+cast-in-place shear walls	-0.02	0.047	**0.224**	0.35	0.54
S5	Steel and RC composite system	-0.02	0.257	**0.402**	0.72	1.02
W	Wood structures	0.14	0.207	**0.447**	0.64	0.86

Table 6.3: Vulnerability Indices for BTM buildings [Multinovic and Trendafiloski, 2003].

For the case of this research, each of the studied typologies is sought within the BTM, in order to find a direct typological description. From the seven typologies detected in Mérida city, only two of them are not univocally identified: the Rancho, and the non-engineered Reinforced Concrete frame with hollow clay block infill walls building typologies. For these two, different evaluations are performed based in the information available about each of them.

- In the case of the Rancho building typology, the index should be considered greater than the Adobe building typology (M2 in Table 6.3), and even bigger as the typology is considered very vulnerable. As the knowledge of this typology is very limited, the greatest index value is considered as adequate, using the vulnerability class A values in Table 3.6, which is larger than the most vulnerable typology in the BTM.
- The non-engineered Reinforced Concrete frame with hollow clay block infill walls building typology is analysed in a different way, due to the detailed information obtained by means of a field survey performed in a representative settlement of the city with high concentrations of such typology. That settlement is the La Milagrosa Barrio, which has been surveyed by the Italian Vulnerability Index Method, as explained in detail in the next

section. This building typology is considered to be similar to the Concrete Moment Frame (RC1 in Table 6.3) typology, where the index values in the BTM are used as the typologic vulnerability index ($V^*_{I_{BTMi}}$) of equation 6.1, the Behavior Modifier (ΔV_M) is applied to the different building typology categories within the settlement, by means of the scores for the vulnerability factors V_m, and the weighed average in equation 6.1; the regional vulnerability factor (ΔV_R) has not been considered as no additional information over the building type is available.

The resulting equivalence between the EMS-98 and the LM1 Building Typology Matrix is shown in Table 6.4, where the non-engineered Reinforced Concrete frame with hollow clay block infill walls building typology is identified as NENG-RC, and the Rancho building typology as R. The comparison between the two different seismic vulnerability assessment approaches evidences the differentiation sought through the application of the LM1 approach, which considers seven vulnerability classes, with a grading of the vulnerability indices describing the different expected behavior of the building typologies, instead of the five proposed by the use of EMS-98 scale.

As in [Laffaille, 1996], the Mérida metropolitan area is divided in sectors (42 in total), taking into account homogeneity (similarity between predominant buildings), physical barriers (mostly the two rivers) and accessibility (bridges and roads). Each sector is divided in several sub-sectors; generally most constructions in each sub-sector belong to the same vulnerability class (according to the considered classifications). The latter implies that no information about specific location of the buildings is available; however, an analysis of the sectors and sub-sectors supply useful information over the different building classes's distribution within these and the probable damage inflicted among the class groups due to the occurrence of a certain seismic event.

A review of the building stock is performed through a fast survey over the information available, completing several sectors (14 in total) that were not considered in the Laffaille (1996) dataset. A revised dataset is built with a total number of 16,147 buildings distributed over 42 sectors, with a total of 494 sub-sectors, covering most of Mérida's tableau surface. The distribution of vulnerability classes in the building stock based in the EMS-98 vulnerability classes is shown in Figure 6.1, where the greater percentage is accumulated by vulnerability class B with a 35% of total buildings, followed by vulnerability classes D, A and C with a 36%, 17% and a 10% of total building stock, respectively. The higher vulnerability class E accounts for 1% of building stock, and class F has no examples in Mérida city. The distribution of the vulnerability classes performed by means of the LM1 Methodology is shown in Figure 6.2. The comparison between Figure 6.1 and Figure 6.2 shows that the EMS-98 vulnerability class A is separated into R and M2 Typologies (with the respective indices for the identification of such classes), and that the EMS-98 vulnerability class E is separated into RC5 and S1 typologies.

Laffaille Classification [Laffaille, 1996]	EMS-98 Vulnerability Class and Building Type	WP4-LM1 Methodology Building Typology Matrix		V_I representative values				
		Typology	Description	$V_{I,BTM}^{min}$	$V_{I,BTM}^{-}$	$V_{I,BTM}^{*}$	$V_{I,BTM}^{+}$	$V_{I,BTM}^{max}$
Rancho- auto-constructed building fabricated with waste materials.	N/A, considered as A	***R***	*Rancho*	0.78	0.86	**0.9**	0.94	1.02
A- Buildings of fieldstone, rural structures, adobe houses, clay houses.	A- Adobe block walls, Rubble stone (field stone)	***M2***	*Adobe*	0.62	0.687	**0.84**	0.98	1.02
B- Non-engineered one or several levels reinforced concrete frame with unreinforced hollow brick walls.	B- RC moment resisting frame designed for gravity loads only (no seismic features) or confined masonry	***NENG-RC***	*Based on Concrete Moment Frames*	0.23	0.29	**0.685**	0.97	1.02
C5- One or several levels steel frame structure, with one-way slabs as floors and roofs and unreinforced hollow brick walls	E- Steel moment-resisting frame with brick masonry partitions	***S1***	*Steel Moment Frames*	-0.02	0.467	**0.363**	0.64	0.86
C6- One or several levels RC structure, with one-way slabs as floors and roofs and unreinforced hollow brick walls.	D- RC frame designed with seismic features.	***RC3.1***	*Regularly infilled walls*	-0.02	0.007	**0.402**	0.76	0.98
C7- Several levels reinforced concrete flat slab buildings.	C- RC Flat slab structure.	***RC3.2***	*Irregular frames*	0.06	0.127	**0.522**	0.88	1.02
C8- Several levels reinforced concrete cast in situ walls and slabs.	E- RC Shear wall structure, cast in-situ.	***RC5***	*Precast Concrete Tilt-Up Walls*	0.14	0.207	**0.384**	0.51	0.7

Table 6.4: Equivalence between EMS-98 and LM1 BTM.

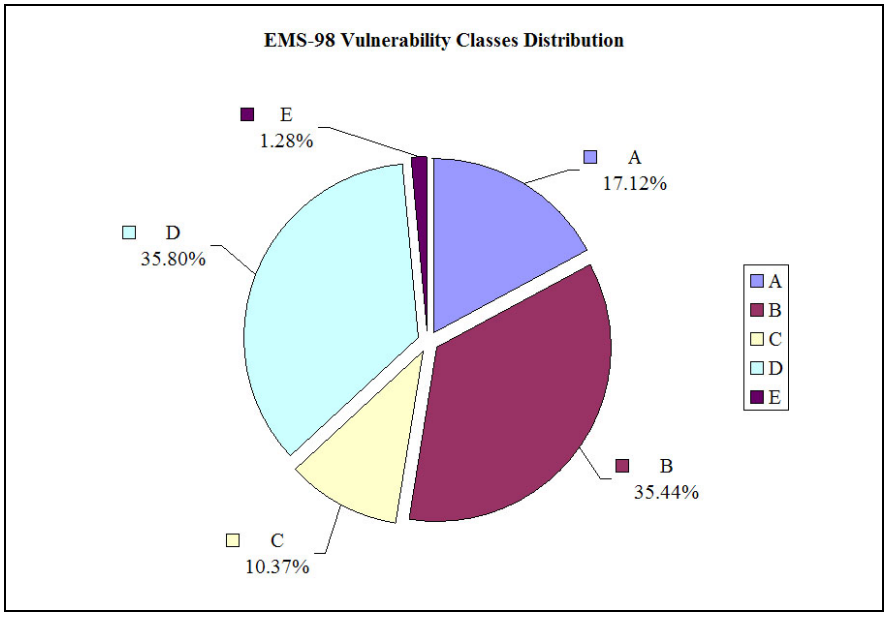

Figure 6.1: EMS-98 Vulnerability Classes distribution.

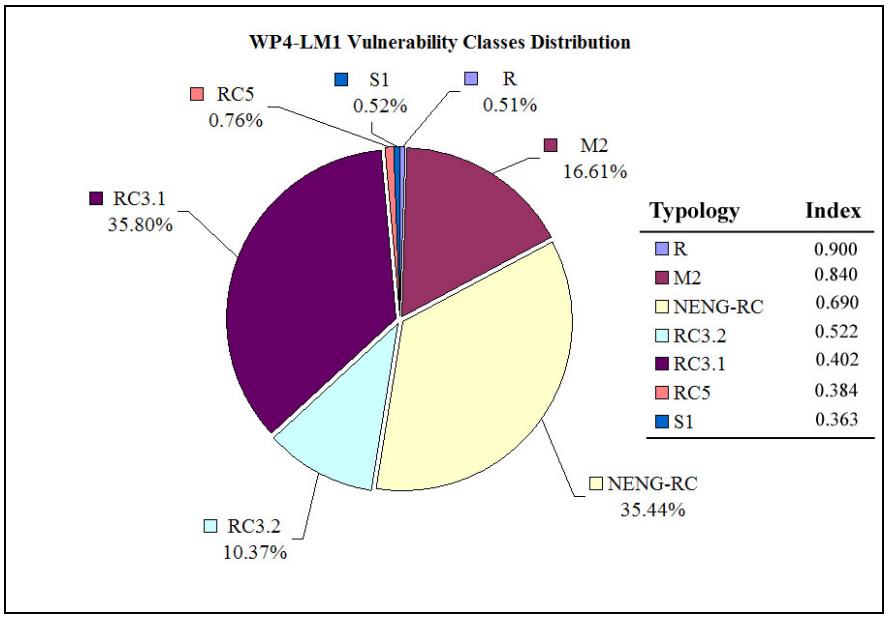

Figure 6.2: LM1 Vulnerability Classes distribution.

Operations may be performed with the dataset (through GIS) to detect vulnerability class-predominant zones in the city, such as the percentage of a certain vulnerability class with respect to the total number of buildings in each Sub-sector. In the following Maps, the vulnerability class distribution is shown as the percentage of this class with respect to the total number of buildings in every sub-sector considered (represented as fractions of 1). In Map 6.1, Rancho typology distribution is shown, it may be verified how the greater concentrations of this class (around 6% in several sub-sectors) are located in perimetral zones in Mérida, inside informal settlements. M2 typology distribution (shown in Map 6.2), representing the oldest buildings in the survey, concentrates (over 60% and up to a 100% in some cases) in sub-sectors of the city located downtown, at the original foundation site of the city, these sub-sectors contain most of the historical heritage buildings in Mérida.

The typology defined as NENG-RC is concentrated (with more than a 50% of the buildings) inside sub-sectors defined as “Barrios”, which are informal urban settlements, usually containing non-engineered buildings (Map 6.3).

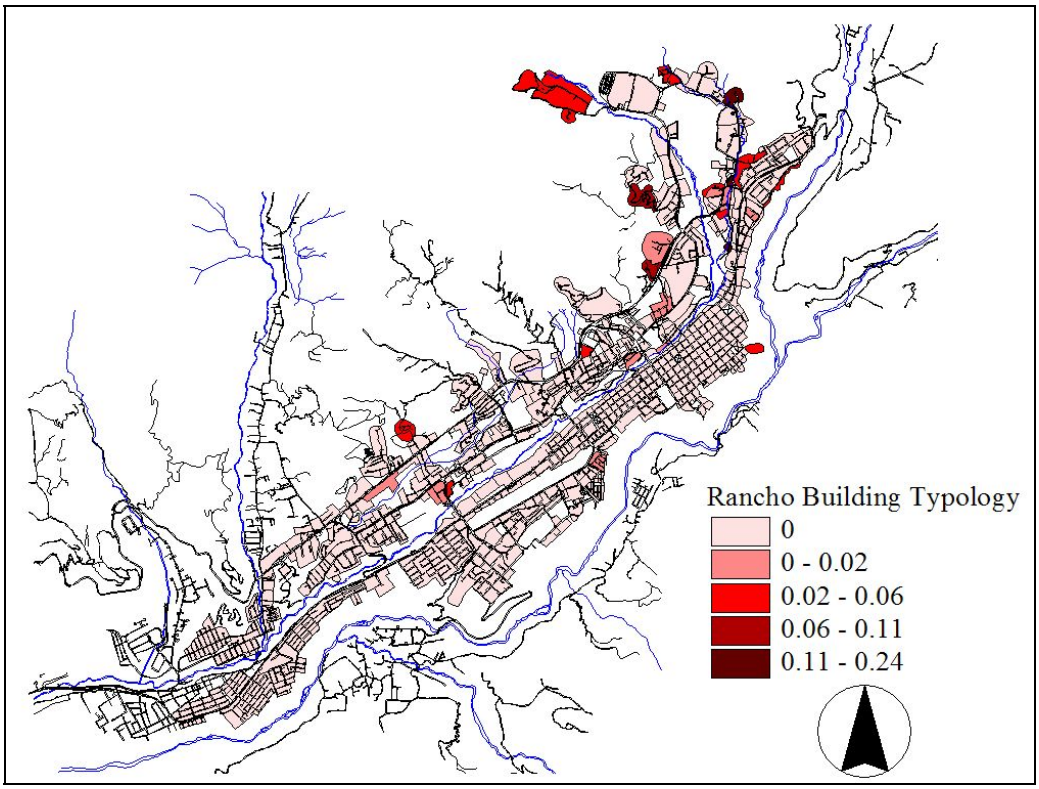

Map 6.1: Percentage of Rancho building typology in sub-sectors for Mérida.

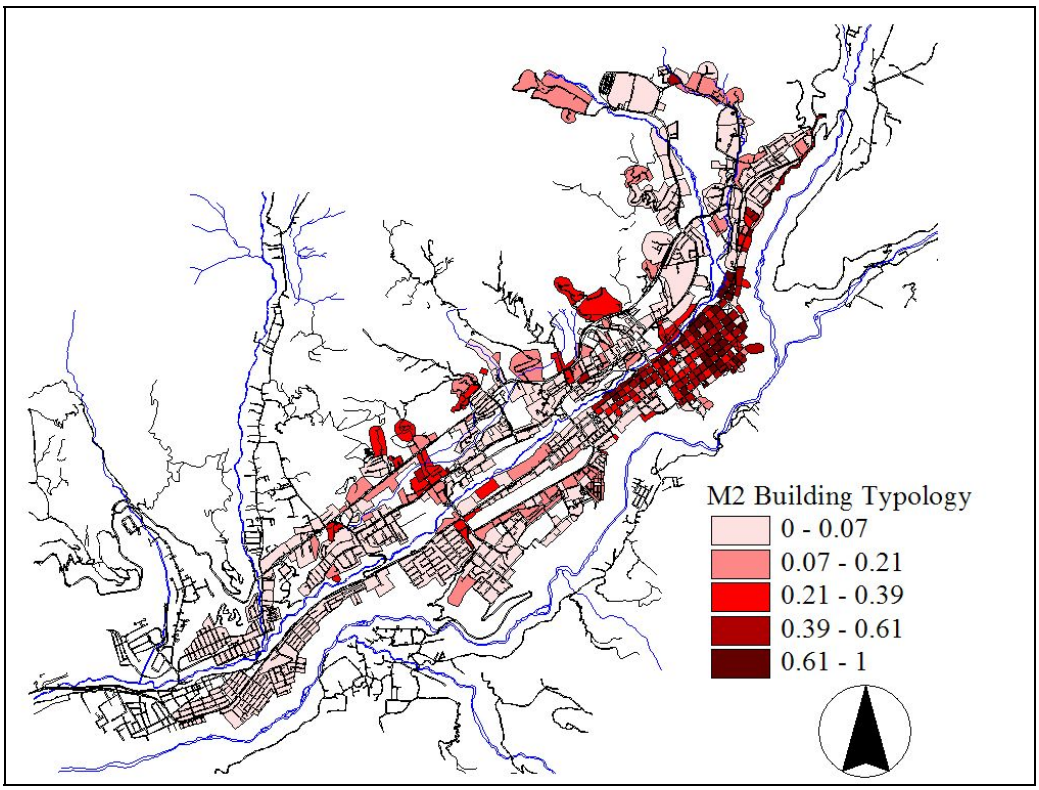

Map 6.2: Percentage of M2 typology in sub-sectors for Mérida.

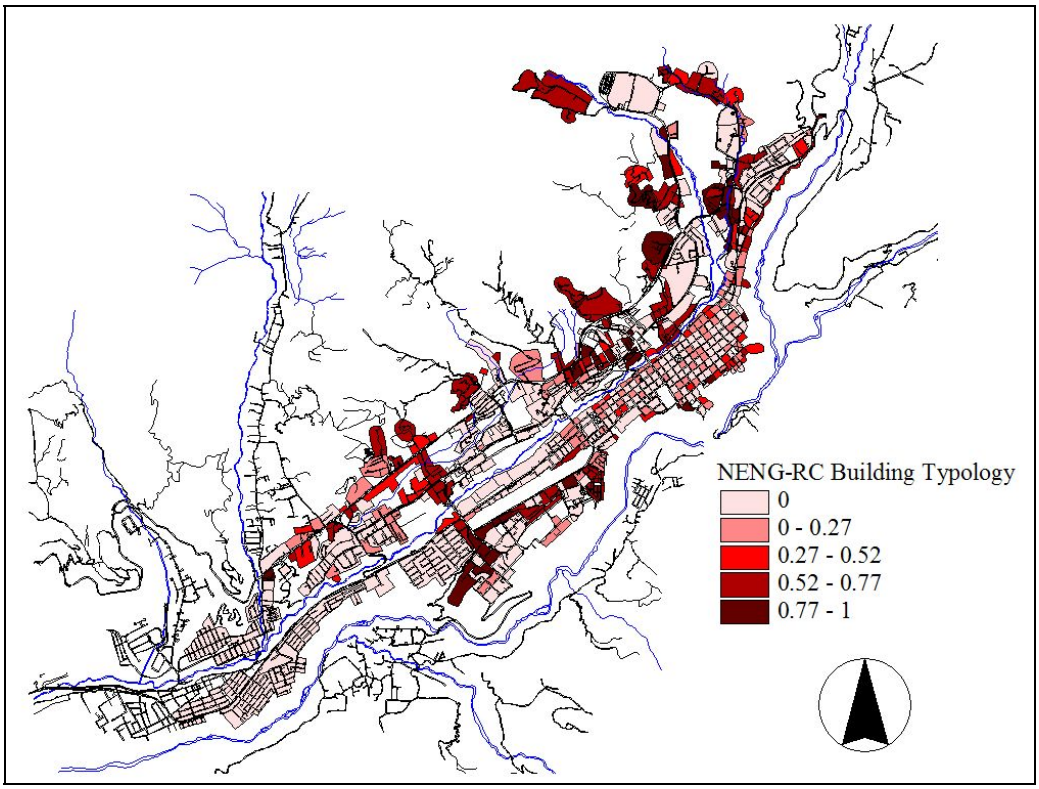

Map 6.3: Percentage of NENG-RC typology in sub-sectors for Mérida.

The RC3.2 typology concentrates (with percentages greater than 50% per sub-sector) over the southerly zone of the city's downtown developed mostly in the first half of the 20th century (Map 6.4). For typology RC3.1, concentrations (over 80% by sub-sector) are mostly located over the urban dwelling developments performed in the last four decades, at the northerly and southerly limits of the tableland (see Map 6.5). The RC5 building typology represents the most recent building typology in Mérida, with not more than 20 years of practice, corresponding to high-density dwellings (average 10 level apartment buildings), and mostly located over the northern side of the Albarregas River (see Map 6.6); the concentrations rise up to more than a 80% due to the fact that these buildings conform private dwellings with around 10 buildings with parking lots, green areas and commercial buildings with no more than 2 levels, as complementary services. Finally, typology S1 is shown disseminated in very few sub-sectors in different locations of the city (Map 6.7).

The previous analyses of the dataset, showing the different LM1 building typologies percentages inside the sub-sectors, allow distinguishing high concentration zones for one of the most common typology: NENG-RC. These zones correspond to informal urban settlements called "Barrios", which have the particularity of high density of non-engineered buildings with an also high density of low-income inhabitants. These informal urban settlements are mostly located in lands inappropriate for construction, due to steep slopes of the terrain and/or the presence of water-courses (streams and rivers).

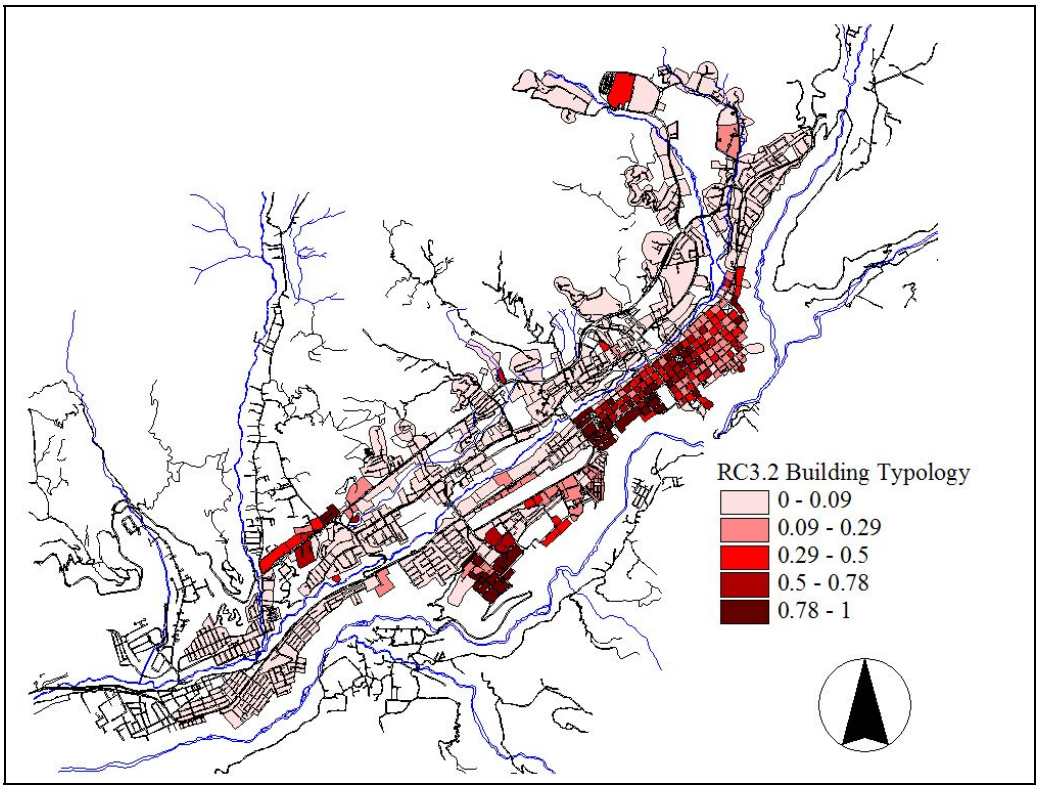

Map 6.4: Percentage of RC3.2 typology in sub-sectors for Mérida.

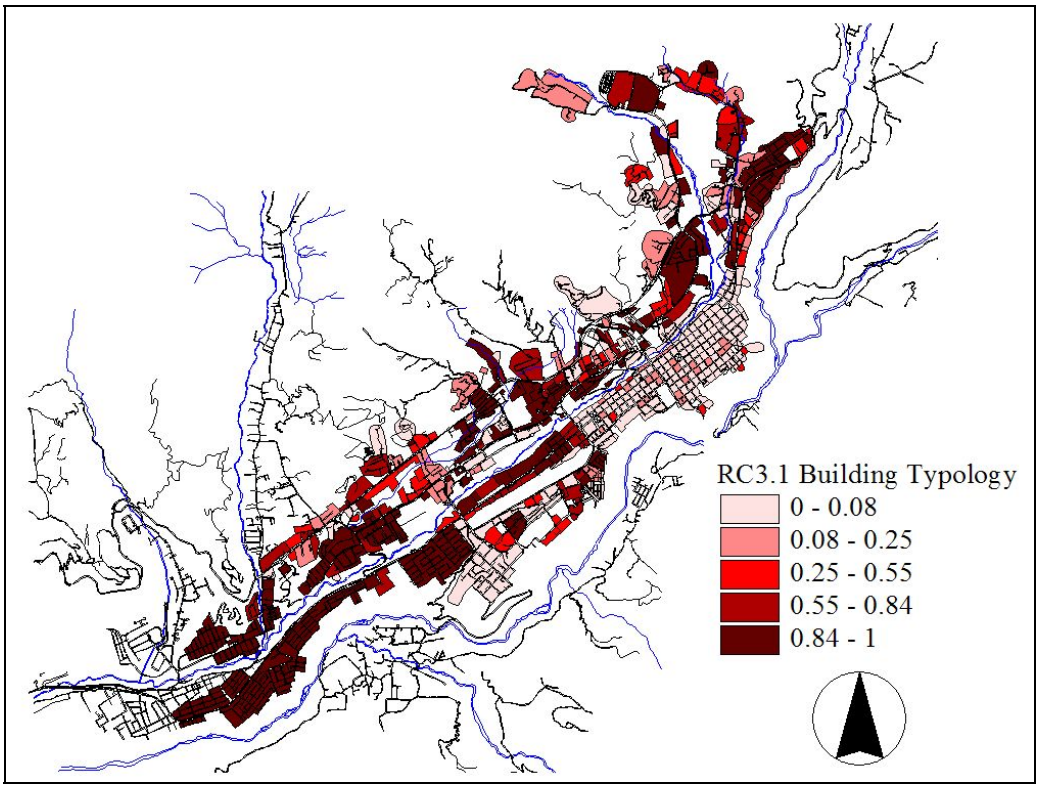

Map 6.5: Percentage of RC3.1 typology in sub-sectors for Mérida.

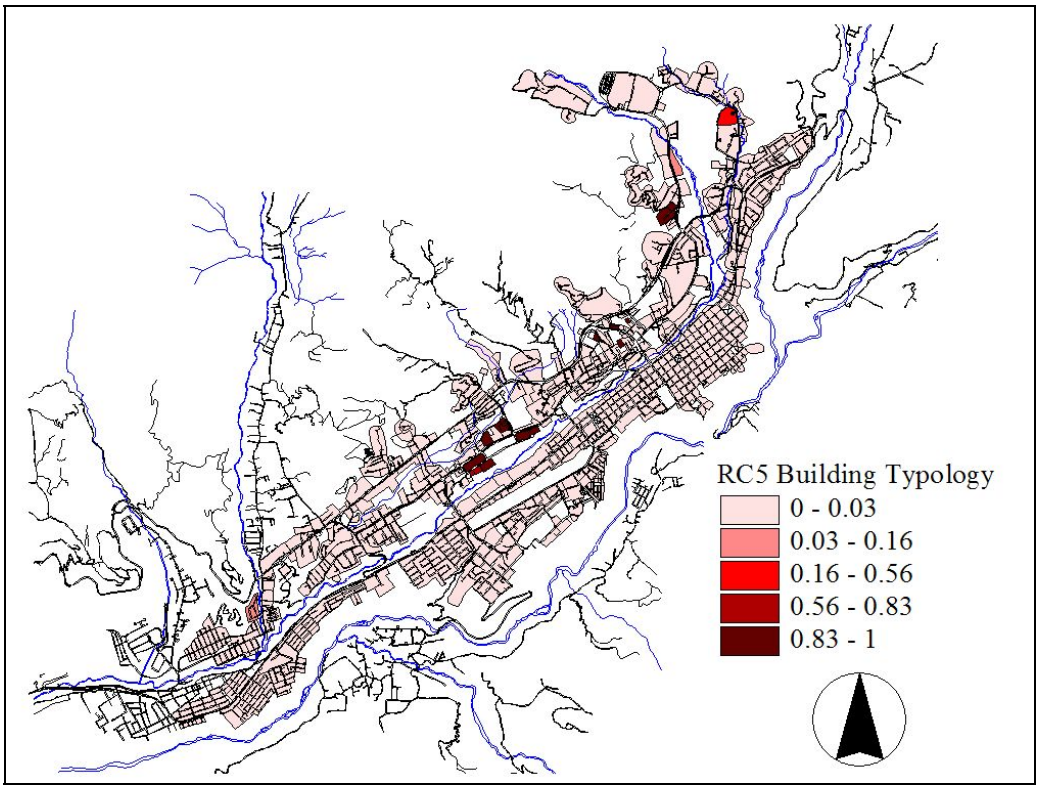

Map 6.6: Percentage of RC5 typology in sub-sectors for Mérida.

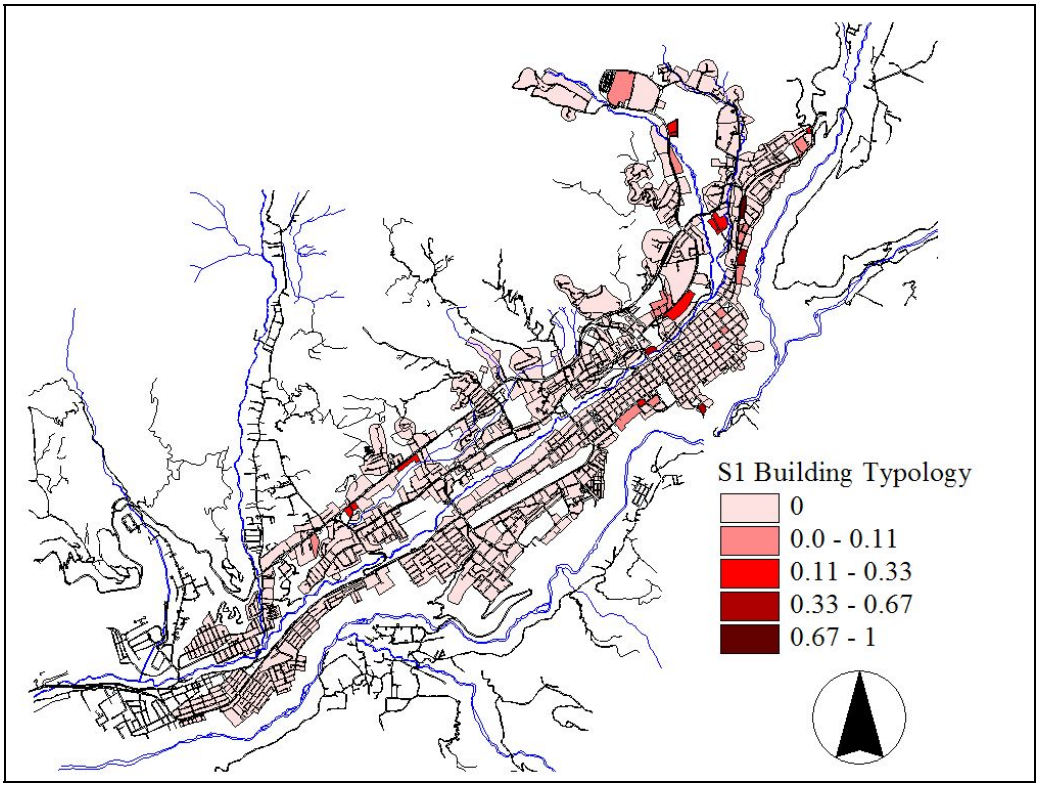

Map 6.7: Percentage of S1 typology in sub-sectors for Mérida.

In Venezuela, informal settlements have been growing around the cities since the mid 20th century, occupying urban lands not adequate for construction, and with very little attention in public services (water, electricity, drainages, and streets). Actually, the "Barrios" represents a

very severe problem not only of a social nature (high density of impoverished population), but also as a problem pertaining the security of this population, and their homes. The vulnerability of these settlements is very high, not only to earthquakes, but to any other natural phenomena capable of generating disasters. As an example, the 1999 rains that impacted the central coast of Venezuela, turned up into a disaster with catastrophic consequences. The death toll rose to several thousands and the economic loss to hundreds of million dollars. Most of the loss and casualties were concentrated over the hills, where informal settlements of the kind described above occupied the land [Muguerza, 2001]. The perverse economic and social impact generated by the catastrophe has not yet been measured, and sufficient countermeasures have not been taken either, as new informal settlements are growing over the ruins left by the catastrophe, where people are occupying semi-destructed buildings in a very hazardous zone [Cañizales, 2000].

6.2.2 General Damage Forecast

This general damage forecast is a preliminary estimation of the damage distribution in all the sub-sectors, the LM1 methodology is used for this purpose (applied to the typologies in Mérida city). The instructions in the document "*WP4: Vulnerability of current buildings*" [Multinovic and Trendafiloski, 2003] requires the estimation of the vulnerability index as the first step in damage estimation, which has been performed in the previous section. The following step is to estimate the mean damage grade (μ_D) for the different vulnerability indices in the Building typologies and the corresponding seismic intensity I, by means of equation 3.14. The results of this procedure applied to the vulnerability classes in Mérida are shown in Figure 6.3, for Intensities from I = VI to I = XII, where the curves represent the mean (semi-empirical) vulnerability functions for the building typologies considered in this study.

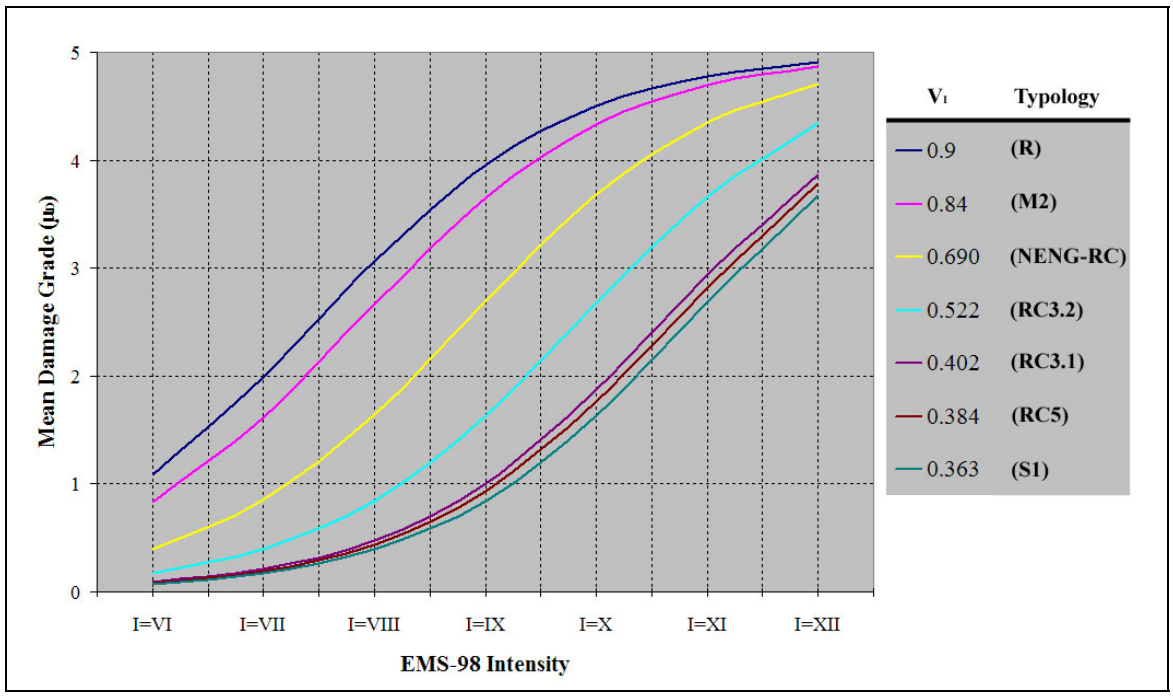

Figure 6.3: Mean semi-empirical vulnerability functions for the building typologies in survey.

The next step is to estimate the discredited Beta probability function to obtain the elements of the damage matrices for the building typologies studied, where each of the elements define,

given an intensity degree, the discrete probability (equation 3.10) associated with the different damage grades considered (from Grade 0, no damage, to Grade 5, collapse). The resulting Damage Probability Matrices (DPM) are shown in Table 6.5, for the scenario events considered in this risk assessment, from *I* = VI to *I* = IX (Table 5.8), and also considering the intermediate intensity degrees which take into account the local amplification effects (Map 5.8).

The DPM's constitute the vulnerability functions for the damage forecast; in Mérida, based on the survey dataset described previously. The total damage grades distribution for the building stock is shown in Figure 6.4. The percentage (from all the building stock) of damaged buildings with a certain Damage Grade *i*, for the scenario events considered (from *I* = VI to *I* = IX), describes the evolution of damage grades through intensities.

The greater percentages in each of the intensities considered are distributed over increasing damage grades (as shown in Table 6.6 containing the same information than Figure 6.4). Last column in Table 6.6 contains the sum of the percentages of the damaged buildings (Damage Grades ranging from 1 to 5). The sums of the values inside each row (percentages of buildings undergoing a certain Damage Grade for a given intensity) is slightly lower than 100 (99.00 for *I* = VI, 98.46 for *I* = VII, 98.18 for *I* = VIII and 98.70 for *I* = IX) because the number of buildings are expressed as integers. In this figure the distribution of damage shows, a concentration with respect to damage grades (from 1 to 5) for each of the scenario events, in this case, this damage grade may not be considered as the mean damage grade, as the percentages accumulate all the vulnerability classes in the survey. However, the stock shows a behavior ranging from a central damage grade in *I* = VI, considered as Damage Grade 1 (as it contains the greater percentage of damaged buildings in the survey), to a central Damage Grade 2 in *I* = IX (representing around a 23% of the buildings in the survey). The distribution also includes the appearance of the other damage grades in lower percentages for each of the scenario events considered (Table 6.6), where Damage Grade 5 (collapse) accounts for around a 1% at scenario event *I* = VIII, and for around a 6% at the higher considered intensity (*I* = IX).

Typology	Intensity	DG0	DG1	DG2	DG3	DG4	DG5
	I=VI	0.372	0.398	0.18	0.046	0.005	0
	I=VI-VII	0.194	0.4	0.282	0.106	0.018	0
R	I=VII	0.079	0.311	0.353	0.202	0.053	0.003
VI* =0.900	I=VII-VIII	0.025	0.188	0.344	0.304	0.126	0.012
	I=VIII	0.007	0.09	0.263	0.359	0.24	0.042
	I=VIII-IX	0.001	0.034	0.158	0.33	0.358	0.119
	I=IX	0	0.011	0.076	0.239	0.412	0.263
	I=IX-X	0	0.003	0.031	0.14	0.369	0.457
	I=VI	0.454	0.37	0.141	0.031	0.002	0
	I=VI-VII	0.261	0.412	0.24	0.077	0.011	0
	I=VII	0.118	0.356	0.331	0.159	0.034	0.001
M2	I=VII-VIII	0.042	0.239	0.358	0.264	0.091	0.006
VI* =0.840	I=VIII	0.012	0.125	0.303	0.345	0.19	0.026
	I=VIII-IX	0.003	0.052	0.201	0.352	0.313	0.08
	I=IX	0.001	0.017	0.105	0.281	0.401	0.195
	I=IX-X	0	0.005	0.046	0.178	0.397	0.374

Typology	Intensity	DG0	DG1	DG2	DG3	DG4	DG5
	I=VI	0.772	0.185	0.038	0.005	0	0
	I=VI-VII	0.622	0.285	0.079	0.014	0	0
	I=VII	0.429	0.38	0.152	0.035	0.003	0
NENG-RC	I=VII-VIII	0.239	0.41	0.253	0.085	0.012	0
VI* =0.690	I=VIII	0.105	0.344	0.339	0.172	0.039	0.001
	I=VIII-IX	0.036	0.223	0.356	0.277	0.101	0.008
	I=IX	0.01	0.114	0.291	0.35	0.205	0.03
	I=IX-X	0.002	0.046	0.187	0.347	0.327	0.091
	I=VI	0.928	0.063	0.009	0	0	0
	I=VI-VII	0.875	0.106	0.017	0.001	0	0
	I=VII	0.784	0.176	0.036	0.004	0	0
RC3.2	I=VII-VIII	0.639	0.274	0.074	0.013	0	0
VI* =0.522	I=VIII	0.449	0.372	0.144	0.032	0.003	0
	I=VIII-IX	0.256	0.411	0.243	0.078	0.011	0
	I=IX	0.115	0.354	0.333	0.162	0.035	0.001
	I=IX-X	0.041	0.235	0.358	0.267	0.092	0.007
	I=VI	0.965	0.032	0.003	0	0	0
	I=VI-VII	0.944	0.049	0.006	0	0	0
	I=VII	0.906	0.082	0.013	0	0	0
RC3.1	I=VII-VIII	0.835	0.137	0.025	0.002	0	0
VI* =0.402	I=VIII	0.719	0.223	0.051	0.007	0	0
	I=VIII-IX	0.548	0.327	0.104	0.02	0.001	0
	I=IX	0.349	0.403	0.191	0.051	0.006	0
	I=IX-X	0.177	0.394	0.293	0.115	0.02	0
	I=VI	0.968	0.029	0.003	0	0	0
	I=VI-VII	0.95	0.044	0.006	0	0	0
	I=VII	0.916	0.073	0.011	0	0	0
RC5	I=VII-VIII	0.855	0.122	0.021	0.002	0	0
VI* =0.384	I=VIII	0.75	0.201	0.044	0.006	0	0
	I=VIII-IX	0.591	0.303	0.089	0.016	0.001	0
	I=IX	0.394	0.392	0.169	0.042	0.004	0
	I=IX-X	0.211	0.405	0.271	0.098	0.016	0
	I=VI	0.971	0.026	0.003	0	0	0
	I=VI-VII	0.956	0.039	0.005	0	0	0
	I=VII	0.927	0.063	0.009	0	0	0
S1	I=VII-VIII	0.874	0.107	0.017	0.001	0	0
VI* =0.363	I=VIII	0.782	0.177	0.036	0.004	0	0
	I=VIII-IX	0.637	0.276	0.074	0.013	0	0
	I=IX	0.447	0.373	0.145	0.033	0.003	0
	I=IX-X	0.254	0.411	0.244	0.079	0.011	0

Table 6.5: Damage Probability Matrices for the Building typologies in the survey.

This behavior may be explained through the mean semi-empirical vulnerability functions shown in Figure 6.3, where the mean damage grades at I = VI for the different building typologies are mostly below Damage Grade 1, except for the Rancho typology which is slightly over this value. On the other hand, observing the intersections of the curves at I = IX, it may be noticed how the building typologies S1, RC5 and RC3.1 have their mean damage grade values around $\mu_D = 1$, typology RC3.2 around $\mu_D = 2$, the NENG-RC typology's mean damage grade is around $\mu_D = 3$, and the Rancho and M2 typologies have their mean damage grade around $\mu_D = 4$. Accounting for the percentage distribution of the different typologies within the survey, the most common typologies are RC3.1 and NENG-RC, with around a 36% of the total number of buildings each, accumulating over a 70% of all the buildings in the survey and having their mean damage grades around values 2 and 3.

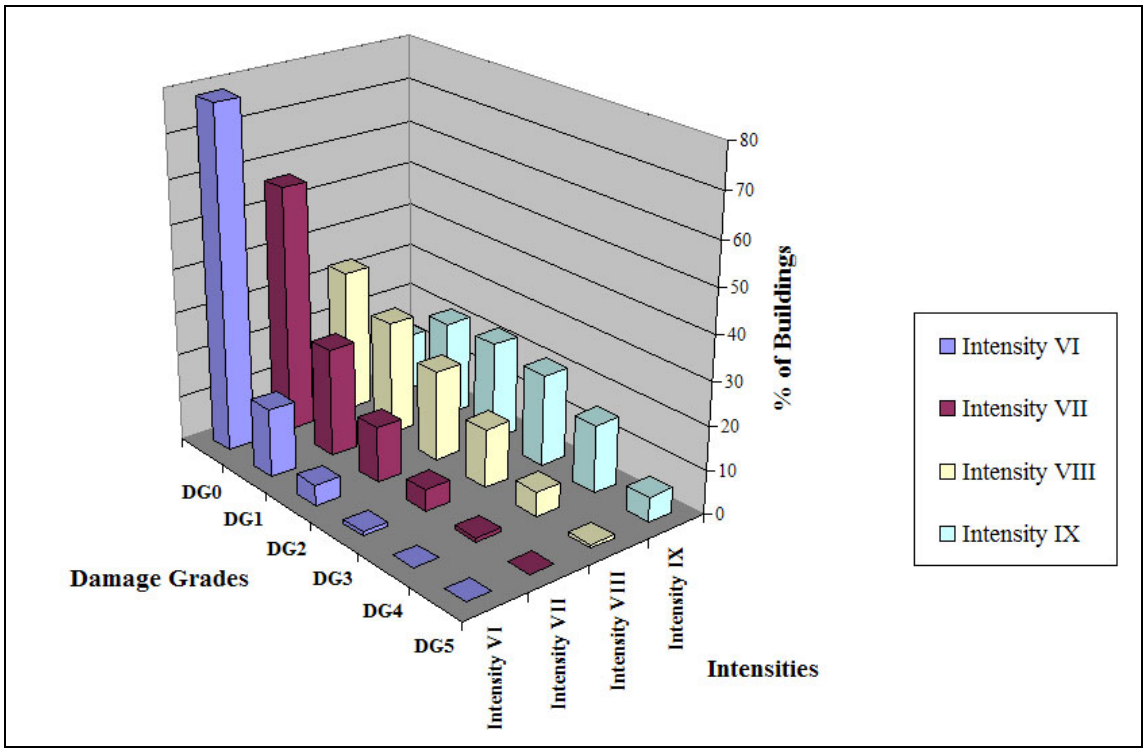

Figure 6.4: Percentage of Damaged Buildings by Damage Grades for the scenario events.

Intensity	Grade 0	Grade 1	Grade 2	Grade 3	Grade 4	Grade 5	Total
I=VI	78,56	15,32	4,34	0,77	0,01	0	20,44
I=VII	56,44	24,23	12,42	4,52	0,85	0	42,02
I=VIII	32,74	25,92	20,33	13,03	5,52	0,64	65,44
I=IX	12,61	21,18	22,32	20,73	15,26	5,6	85,09

Table 6.6: Percentage of Buildings by Damage Grades and Total Damage for Intensities.

The damage grades distribution (DG0 to DG5) for the considered typologies (seven, in total) as a percentage of the whole building stock by intensities is shown in Figure 6.5. From the observation of the different charts, it is evident that the most damaged vulnerability class (in percentage of the total number of buildings) is the one corresponding to the NENG-RC typology, which along with typology RC3.1 constitute the two most common ones in Mérida's survey (see Figure 6.2).

Information from these charts, which discriminate the damage distribution by building typologies for each of the intensities, is complemented with information in Table 6.6, where it

may be observed that for the greater concentration of damage in a certain damage grade, NENG-RC typology accounts for the major percentage of damaged buildings. As an example, at intensity $I = IX$, the greater concentrations of damage are produced in Damage Grades 1, 2 and 3 (Table 6.6); considering damage grades 2 and 3, the contribution of the NENG-RC typology (Figure 6.5) accounts for almost a half, and more than a half, of the total damage grades percentage, respectively.

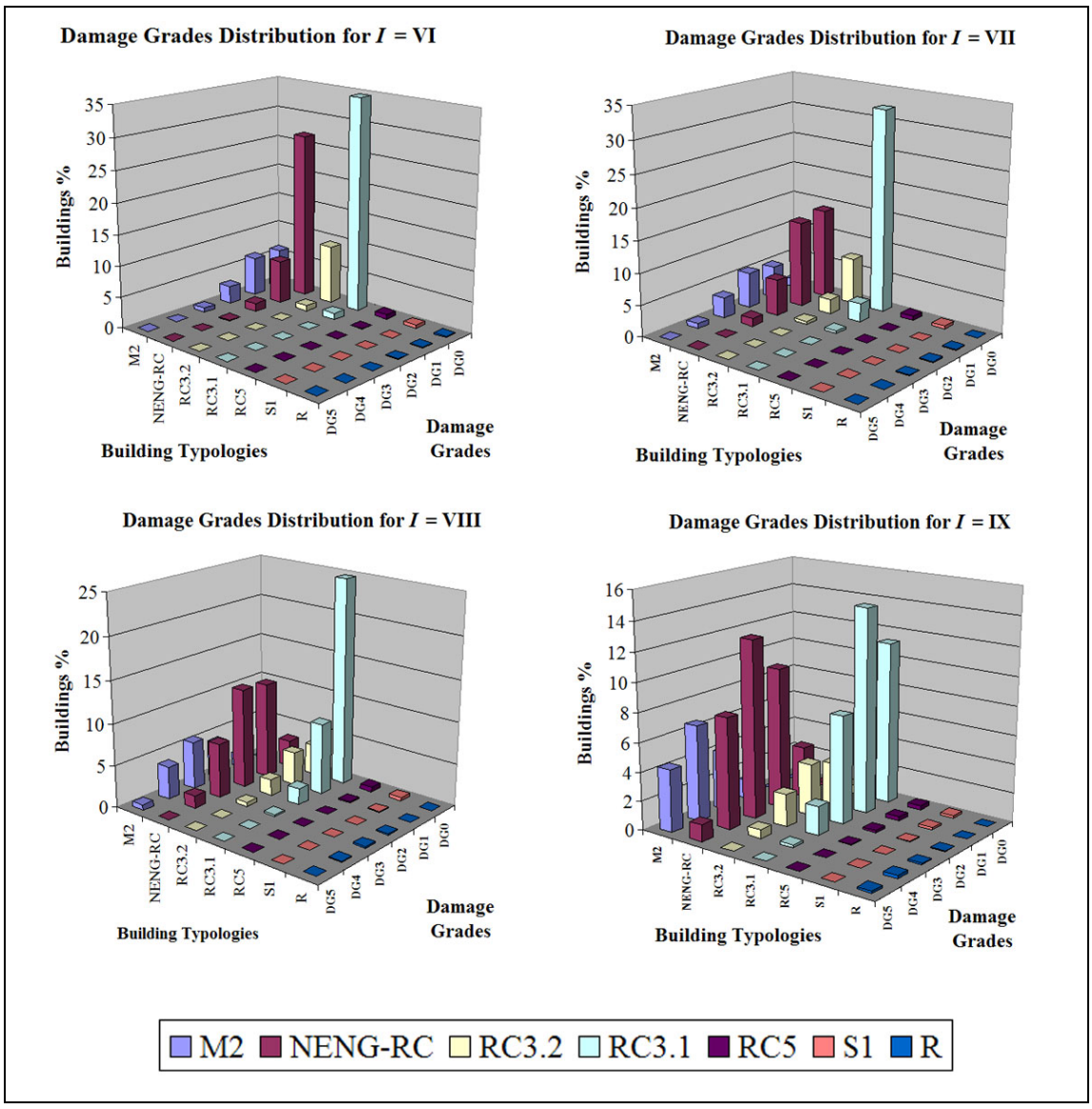

Figure 6.5: Damage Grades Distribution by Vulnerability Classes.

Due to the previous observations, the most critical vulnerability class in the city corresponds to the NENG-RC typology, which apart from being one of the most common in the survey (see Figure 6.2), its presence is verified in high concentrations over several urban zones identified as "Barrios" (as shown in Map 6.3). These informal settlements represent vulnerable parts of the city, where low-income population is also concentrated configuring probable high seismic risk zones in the city. These Barrios are chosen as the smallest urban areas selected to perform an assessment through the vulnerability index method, in order to establish the possible differences that within this building typology may arise (as a qualitative

approach to the differentiation of sub-typologies in a given building typology). Within the Barrios of Mérida city, a particular settlement is chosen, Barrio "La Milagrosa" based in the following three criteria: (1) terrain slope (Barrio with flat terrain and steeped one), (2) homogeneity of vulnerability class and (3) easy access to the premises (near a principal avenue of the city). The location, general description and other information of interest for the "La Milagrosa" Barrio are matter of Section 6.3 of this chapter.

6.3 A detailed study: Barrio "La Milagrosa"

For the case pertaining to this research, where the building type in study is non-engineered housing with RC frame and hollow clay block infill walls, a survey using the Vulnerability Index Assessment Method is performed in order to detect possible differences as to establish sub-types in such typology. The survey is applied over a smaller urban zone that is identified by the predominance of the building typology NENG-RC (see Section 6.2.1), using a Second Level Assessment Form created specifically for this study (ANNEX C). Through an inspection of Map 6.3, the darkest areas identify the zones with higher concentrations of buildings belonging to the NENG-RC typology, with ranges between 75% and 100% of the total number of buildings in the sub-sector; located northeasterly and southwesterly in Mérida City. The area selected to perform the Vulnerability Index assessment is a "Barrio" called "La Milagrosa", at the northeastern side of the city (Map 6.8); it is chosen because of the representativeness of its buildings and its proximity to a principal Avenue ("Los Próceres") and the presence of different slopes in the terrain ranging from near flat (0 to 5%) to steep (60%) (see Map 6.9).

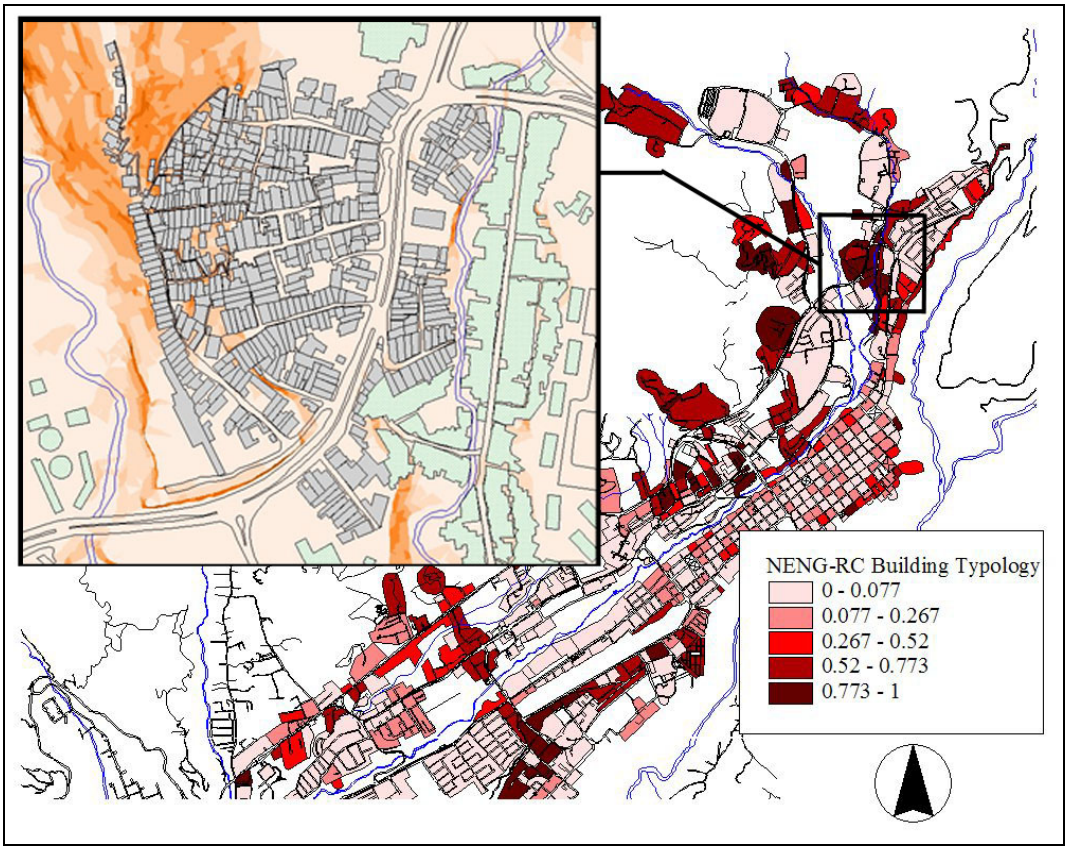

Map 6.8: "La Milagrosa" Barrio in Mérida.

6.3.1 Sectors in "La Milagrosa"

The settlement is divided into four different sectors: La Milagrosa, Cristo Rey, Los Molinos and Miranda; in Table 6.7, the surface, perimeter, number of buildings and year of foundation are described for each of those sectors. The oldest sector is La Milagrosa, founded in 1960, followed by Cristo Rey and Los Molinos, founded in 1962 and finally with Miranda, founded in 1965. In Map 6.9, these sectors are identified by their perimeters. For the four sectors, the steepest slope terrain appears in the Cristo Rey one, and in the other three sectors, slopes ranges are up to 10% and in some cases up to 20%.

The soil consists of clay rock outcrops in the steeper and upper parts and mid to good quality soil in the rest of the premises (as in the rest of Mérida, see chapter 5). The design stress can be estimated as 0.15 MPa; there are no available local tests. Apart from the risk of landsliding, the soil strength is not critical since the vertical stresses are rather low (both because of the lightness of the construction and the limited number of floors). In the lower parts the terrain topography would allow the formation of lagoons; however, they neither exist today nor have been reported for recent times.

Sector	Surface (Ha)	Perimeter (m)	Nº of Buildings	Population	Foundation Year
La Milagrosa	5.68	1,347	219	1,608	1960
Cristo Rey	2.83	887	199	1,232	1962
Los Molinos	0.82	601	37	280	1962
Miranda	1.31	571	78	620	1965
Total	11.36	1,653	533	3,740	

Table 6.7: Description of sectors in "La Milagrosa" Barrio.

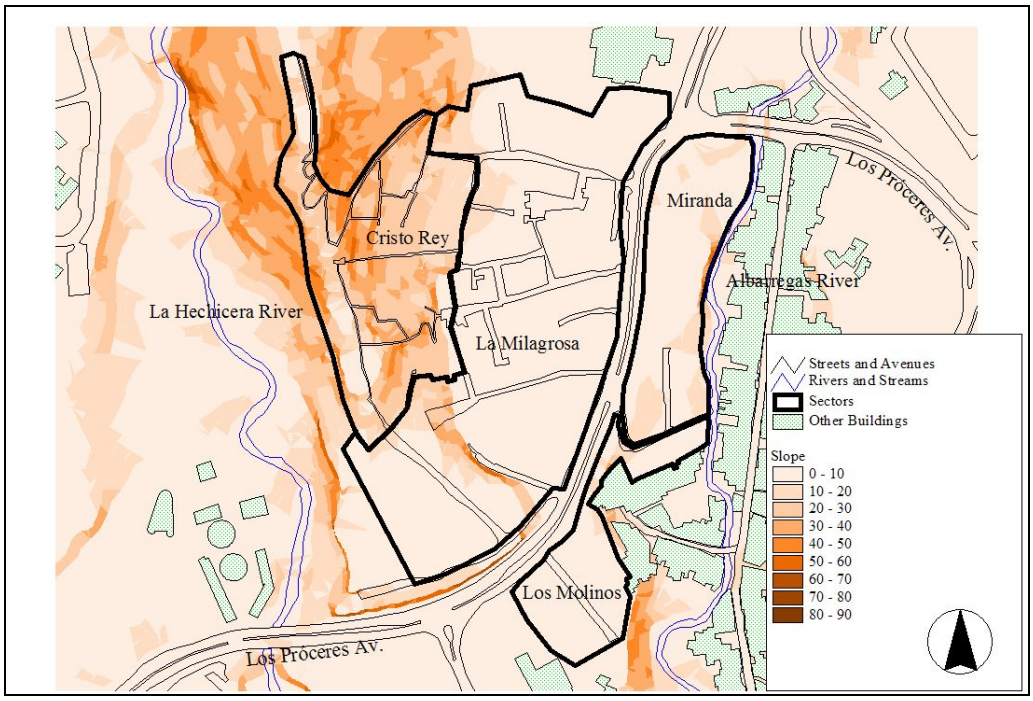

Map 6.9: Sectors in Barrio "La Milagrosa".

6.3.2 Public Services

The infrastructures for public services observed in "La Milagrosa" barrio are four: electricity supply, telephone, potable water supply, and sewage system. A brief description is presented:

- Electricity and telephone infrastructure: the supply of both services is performed by aerial cables supported by posts, no subterranean telephone or electric lines exist. Telephone service is only available in the sectors limiting with the Los Próceres Avenue, i.e. the La Milagrosa, Miranda and Los Molinos Sectors. The uncontrolled growth of informal settlements such as La Milagrosa barrio has produced an increment in the number of electric lines in the posts and the consequent entanglement of them (see Picture 1a), with hazardous line trajectories in front of windows and balconies and also at roof edges. These characteristics are observed in all sectors of La Milagrosa.
- Potable Water Supply: in the lower sectors (La Milagrosa, Los Molinos, and Miranda) the water supply pipes are subterranean (embedded in the street), incoming from a public pipe in the Los Próceres Avenue; in the upper sector of Cristo Rey the pipes are on the surface and usually at one side of stairways and paths (see Picture 1b), with diameters ranging from ½" to 2", incoming, either from a tank located in the uppermost side of the sector or from an extension of the public pipe from the Los Próceres Avenue.
- Sewage System: excretal waters are all embedded in the streets (with manholes) in the lower sectors; and under the stairways and paths in the upper sector (Cristo Rey), the latter without maintenance reach, unless a local destruction of stairways and paths is performed.

Picture 1: Electricity and water supply in La Milagrosa Barrio.

6.3.3 Building Types, Number of levels, and Plan Configuration of buildings

As the survey performed by means of the 2nd Level Assessment Form (see Subsection 6.3.9.1) describes every building with the eleven parameters considered in the Italian Vulnerability Index Method, the most relevant characteristics of the buildings (Building Types, Number of Levels and Plan Configuration) are described next.

The building types distribution in "La Milagrosa" barrio is shown in Map 6.10; five different types exist in the premises, with a predominance of non-engineered reinforced concrete frame with hollow clay block infill walls type, used as housing. Table 6.8 describes the number of buildings of each type in the barrio, and the percentages respect to the total number of buildings, where the type mentioned accounts for almost 95% of all buildings. It is important to remark that about the four other types of buildings, two of them are used as housing buildings (the non-engineered hollow clay block masonry and the RC Frame with seismic features), and the other two (Steel Frame and RC Columns and Steel Truss beams) have different uses, such as: churches, car mechanical workshops, and community services units.

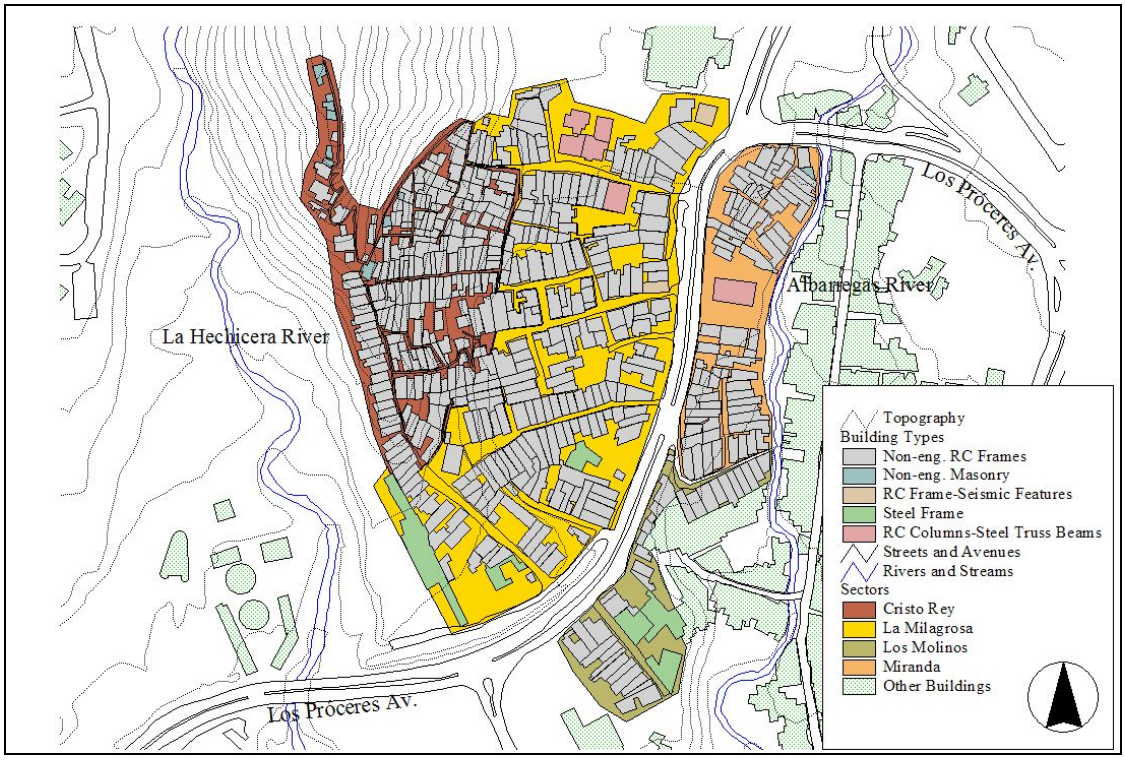

Map 6.10: Building types in Barrio "La Milagrosa".

Building Type	Nº of Buildings	Percentage of Total
Non-engineered RC frame with hollow clay block infill walls	506	94.93
Non-engineered hollow clay block masonry	10	1.87
RC Frame with seismic features	2	0.38
Steel Frame	9	1.69
RC Columns and Steel Truss beams	6	1.13
Total	533	100

Table 6.8: Distribution of building types in "La Milagrosa" Barrio.

The number of levels for each building and the total number of buildings with a certain level number are shown in Map 6.11, the predominant building heights are one and two levels with the 34.15% and the 50.28% respectively, of all the buildings. The number of stories is an important parameter to describe the total building height, as one level is equivalent to an average measure of 2.8 m; the building height is used in seismic codes to estimate the building's fundamental period. For example, in the Venezuelan seismic code [MINDUR and FUNVISIS, 1998] the expression for buildings capable to resist the seismic actions by means of deformation in columns and beams (classified as Type I in the code) is:

$$T = C_t \, h_n^{0.75} \qquad \text{eq. 6.2}$$

Where, T is the fundamental period (in s), C_t is 0.07 for reinforced concrete or combined reinforced concrete-steel buildings and 0.08 for steel buildings; and h_n is the total building height (in m) measured from the utmost level to the first level with total or partial displacement restrictions. This expression is similar to the one suggested by the part 1-2 of the

Eurocode 8 (ENV 1998-1-2:1994), C_t is 0.075 for reinforced concrete frames and 0.085 for steel moment resisting frames. Such code incorporates also some expressions to account (in a semi-empirical way) for the stiffening effect of the cladding and partitioning masonry walls, which significantly shortages the fundamental period of the building.

The plan configuration distribution inside the settlement's premises is predominantly regular, as the buildings are mostly built in rectangular sites with an occupation percentage of 100%; the regular or rectangular buildings represent an 84.24% of all the buildings. The average proportion between the sides of the rectangular sites for buildings is 1 to 3, where the smallest side is the building's access in front of the street/stairway/path (Map 6.12). This configuration is predominant for the different slopes in the terrain, i.e. in flat and sloped.

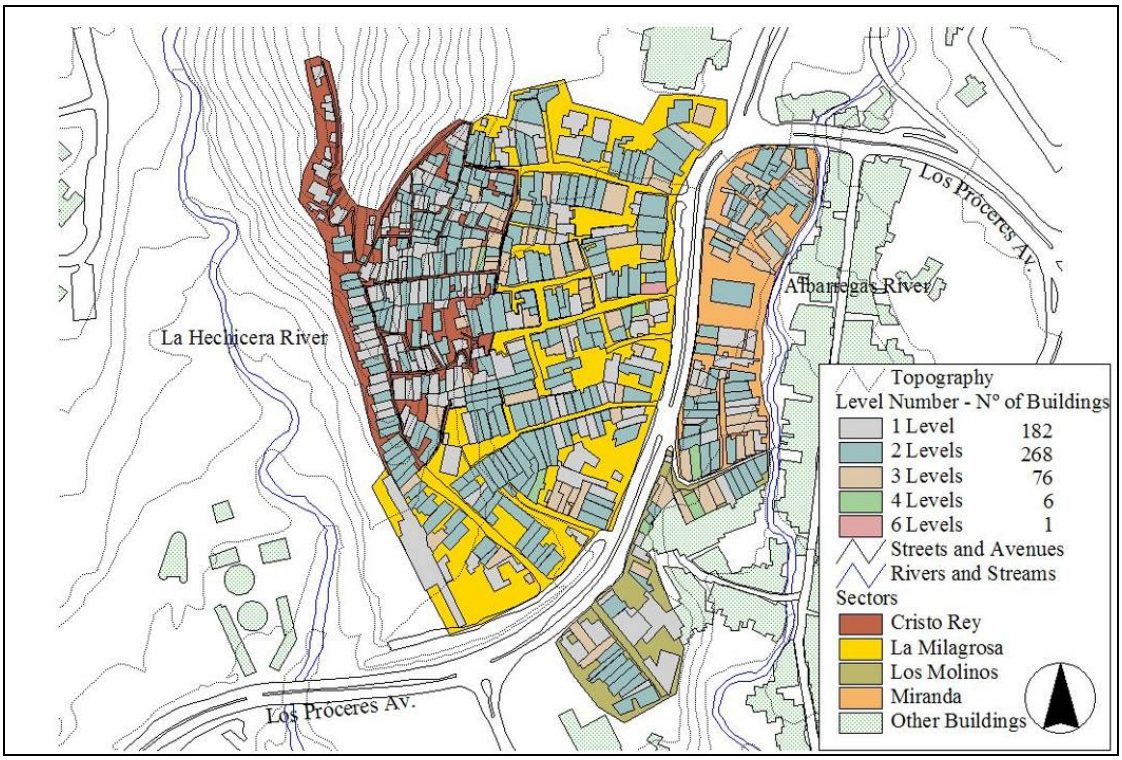

Map 6.11: Number of Levels in the buildings, Barrio "La Milagrosa".

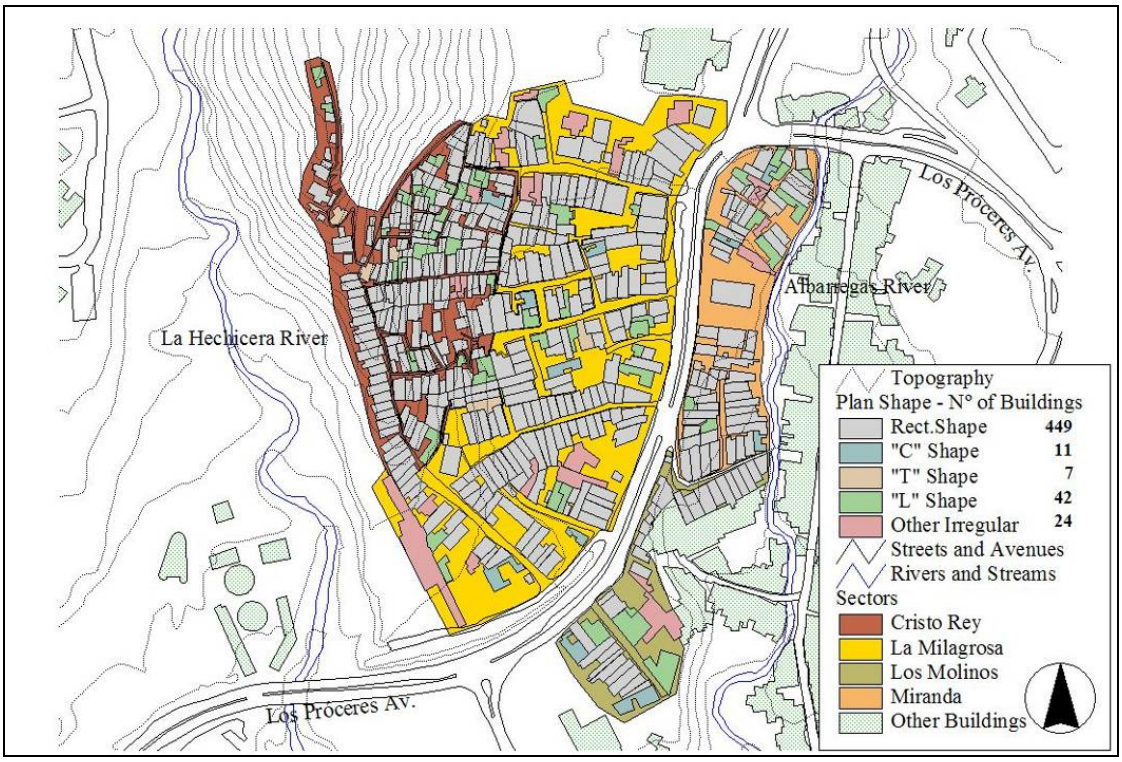

Map 6.12: Plan Configuration for buildings in "La Milagrosa".

6.3.3.1 Predominant typology

The high concentrations of the typology NENG-RC in settlements such as "La Milagrosa" (accounting for almost 95% of all the buildings), induces to focus on such typology.

An identification of the average features of the constructions in the settlement is performed next by means of a detailed survey of all the buildings belonging to the above mentioned typology.

The constructions are used for housing purposes, and although not very common also commercial uses are found mostly in the first level. Usually a family unit occupies a single floor; in average, they are composed by near five members (parents and three children). When a new generation establishes a new family, they move to a new flat, frequently built over the one of their parents. It generates a typical vertical growth, usually limited to three levels. The actual live loads are lower than the official design values (L = 1.75 kN/m^2, [COVENIN 2002-88, 1988]); it has been assumed as L = 1.50 kN/m^2.

The used materials consist in reinforced concrete for the frames; hollow clay block bonded with mortar for the walls (cladding and partitioning); steel I-shaped beams, hollow clay blocks and reinforced concrete for the slabs; and metal sheathing (usually zinc) with steel I-shaped or rectangular beams for the roof. The doors and windows are built in several different materials such as wood and/or steel; most of the windows have glasses. Protection against burglary is provided for the windows and doors by means of steel bars and grating.

The houses may be located in flat or sloped sites (See Picture 2). The plan configuration of the buildings is mostly rectangular with an aspect ratio of about 1/3, with the longest sides adjacent to the neighboring houses. This is a characteristic configuration of the informal settlements; very close neighboring constructions where the distances between them are just a few centimeters (mostly less than 4 cm). This feature may produce pounding effects between

the buildings when subjected to earthquake motion, becoming very critical when the buildings are in sloped sites, as the slabs are not horizontally aligned. The façades are in the shortest side of the plan with the openings for doors and windows; in the other direction there are no openings.

Figure 6.6 shows a sketch of the construction type.

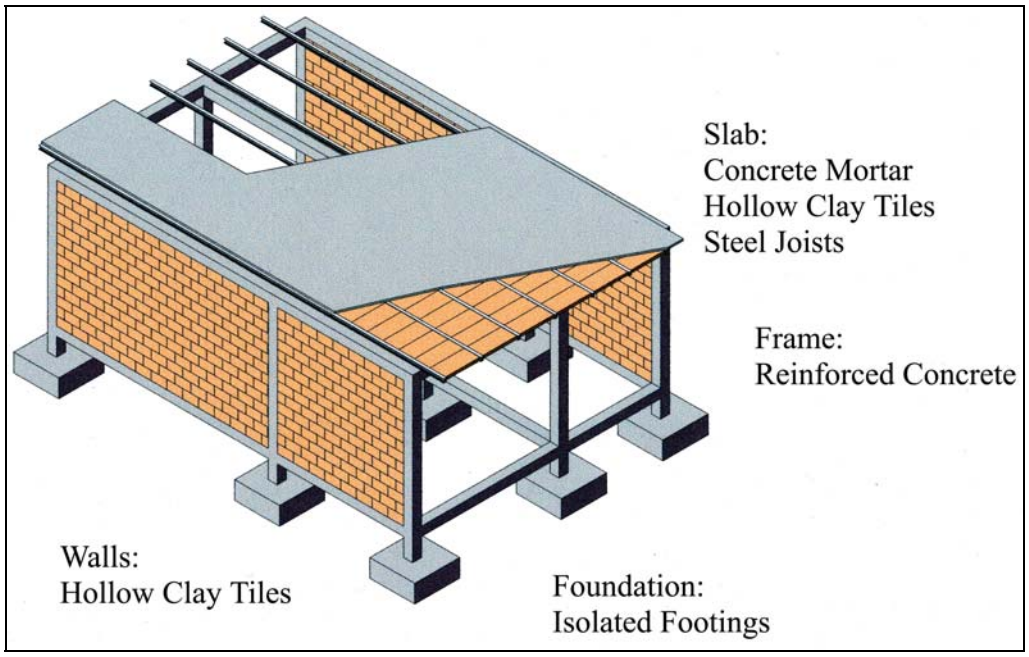

Figure 6.6: Construction system characteristics.

The foundation consists of isolated RC footings supporting the columns. The walls are erected without foundation; at most, a 20×20 cm^2 reinforced concrete tie beam (connecting the footings).

The structural system is a two-way RC frame (3-D), with an average square section in beams and columns of 20×20 cm^2, the steel used for reinforcement has a yielding point f_{yk} = 140 MPa (the cheapest steel in the Venezuelan market). The beam-column connections do not have special detailing, with absence of stirrups within it, however, the longitudinal rebar of the beams have hooks at its ends. The compressive strength of the concrete has been measured with a Schmidt Hammer in several columns of these buildings, the characteristic value is about f_{ck} = 10 MPa. In some cases alignment of the joined members is poor.

Picture 2: Buildings in flat and sloped sites.

The infill walls are built in running (stretcher) bond, without any reinforcement, bonded together with a low-quality mortar. The apparent unit weight for the masonry is $\gamma = 12$ kN/m^3; the weight per square meter is 1.8 kN/m^2. The characteristic value of the walls shear strength is conservatively assumed as $f_{wk} = 0.08$ MPa [IAEE, 2002], and the compression strength of the masonry as $f_{wck} = 0.35$ MPa [IAEE, 2002]. The cladding walls run around the entire perimeter and openings are produced only at front and back sides with usually one window and one door at front, and two windows in the rear (first level), in upper levels, the openings are two windows (or one door and one window if there is a balcony) for both the front and rear. Not all the partition walls are aligned with the frame; moreover they are not always vertically coincident (this leading to complicated loading paths). The walls under slabs are termed in the following "topped" while those under (light) roofs are termed "untopped" as the roof is both weak and untied; this distinction is relevant with respect the seismic behavior and strength (as discussed next).

The slabs are built with I-shaped steel beams (parallel to the longest side) and hollow clay blocks between them, and a RC topping (of around 3 to 4 cm) (See Picture 3); this configures a diaphragm encased between the columns of the next floor (Figure 6.17). The self weight of this slab is determined as 1.832 kN/m^2.

The stairs connecting the levels may be inside the building (parallel to the longitudinal axis) or outside of it over the façade, built in steel or reinforced concrete (See Picture 4). The roofing mostly consists of metal sheathing (usually zinc) over metallic beams (I-shaped or rectangular) which make it very light; however, the roofs are not well bonded to the surrounding support elements (columns and walls) (See Picture 5). Roofs are heterogeneous, with rather peculiar solutions. Water dripping is frequent. The weight of the light roof is considered as 0.4 kN/m^2.

Picture 3: Detail of a slab (balcony in a sloped site building).

The services are commonly connected to public networks. Treated water supply comes usually from a low pressured system supply; some users possess rather small auxiliary reservoirs (the added mass is not relevant for seismic design). The water is mostly permanently available. Waste water goes mostly to a public sewage network; in some cases informal septic tanks are used. Usually there is a bathroom per floor. Electricity supply is aerial; power shortages as well as voltage droppings are frequent. Propane gas in portable containers (canisters) is used for cooking and heating water. Neither heating nor air conditioning exist. TV signal comes from antennas; some houses near the "Los Próceres" Avenue receive aerial cable TV signal, phone and Internet.

Picture 4: Stair in the front of a building.

The buildings, as belonging to informal settlements are non-engineered and built by their owners, whom in this case work mainly in the local construction industry. The houses are usually built in phases, starting from a one-storey building enough to accommodate a single family, and progressively growing (a storey at a time) up to three stories (three families occupation). Few taller houses have been built. A peculiar growth pattern is observed, as the two-storey buildings are mostly topped with light roofs of metal sheathing, without collar RC beams at the top of the walls. For the next phase (third storey erection) some destruction of the upper walls and columns has to be performed to cast the RC beams and to place the slab, to forwardly build the third floor.

The first stage of construction starts with the isolated footings, from which emerge the longitudinal reinforcements of the columns; the next step is to cast the first level of the frame (columns and beams), leaving prominent longitudinal reinforcement bars at the top of the columns (not greater than 300 mm). Once the formwork (moulds) has been removed, the slabs are placed and the concrete floor-base is cast. After the slabs are built, the walls of the first storey are erected (cladding and partitioning walls).

The general level of quality, yet rather poor, is better than expected (taking into account the adverse conditions). The construction quality of many elements in the dwellings is not adequate; the self-constructed and phased feature does not allow quality control for the materials and their assemblage. For example, many broken masonry units and discontinuities are observed in the walls, the bonding mortar does not resist scratching, the running of the blocks are not horizontally aligned, the light roofs are not properly tied, there are shrinkage cracks in floors, and there are cavities and erosions in the frame members, with observed irregularities due to framework positioning. Reinforcement cover is not enough (even some of the bars are visible). In some cases soil erosion surrounding the foundations is observed in steep sites.

Picture 5: Metallic sheathing roofing. Poor bonding to frame and walls.

No relevant pathologies were observed. Minor problems are: humidity, water filtration and cracks in the walls plaster.

Based in the general characteristics of the buildings, some common features are identified:

- Regular plan configuration mostly rectangular, in a proportion width/length (aspect ratio) of around 1/3, with a single-bay transverse RC frame about 6 m wide, and a three-bay RC frame in the longitudinal direction with inter-column spacing of about 5 m.
- The reinforced concrete frames are built with hand-mixed concrete, where the dimensions of the members are common (columns and beams have a cross-section of about 200 × 200 mm^2). The detailing of the members consists of four longitudinal reinforcement bars (diameter ½" = 12.7 mm), with widely spaced ($s \geq 200$ mm) low diameter transverse reinforcement (stirrups with diameter 1/8" = 3.175 mm), the hooks are bent only 90º. No special detailing is observed in the column-beam joints. The splicing of the upper columns reinforcement is usually produced at the column base, with an average longitude of about 300 mm. These detailing features of the building's structural members do not provide ductility, since the excessive spacing and low diameter of stirrups guarantees neither the confinement of the core concrete nor the shear strength of the members.
- The masonry infill walls are unreinforced (URM) and are built with hollow clay blocks usually bonded with low-quality mortar. The walls are erected after the frames (columns and beams). The masonry units have width/longitude/height dimensions of 150/250/200 mm, with the cells disposed horizontally. This kind of URM is used both for cladding and partitioning.
- The slabs are built with I-shaped beams (IPN 80 mm in height) arranged parallel to the longitudinal axis of the building and supported by the transverse RC beams. The inter-axial spacing is around 800 mm allowing to place hollow clay blocks with a width/longitude/height of 200/800/60 mm. The slabs are topped with an upper concrete compressive layer (30 to 40 mm high) reinforced with a steel plain wire welded mesh (diameter 3.175 mm @ 20 mm). The yielding point of the steel of the IPN beams is f_{yk} = 250 MPa and the one of the welded mesh is unknown (probably is f_{yk} = 140 MPa). Usually, the first level has a front cantilever (in the longitudinal direction) ranging from 700 to 900 mm; this cantilever either supports masonry cladding walls in the first and second stories or balconies.
- The (light) roof is usually built with metal sheets (usually zinc sheathing) supported by steel beams (rectangular and "I" shaped) sustained directly by the upper walls and columns.
- The foundations are RC isolated square footings, mostly superficial, with average side-dimensions from 800 to 1000 mm.

Figure 6.7 shows some details about the reinforcement for columns and beams.

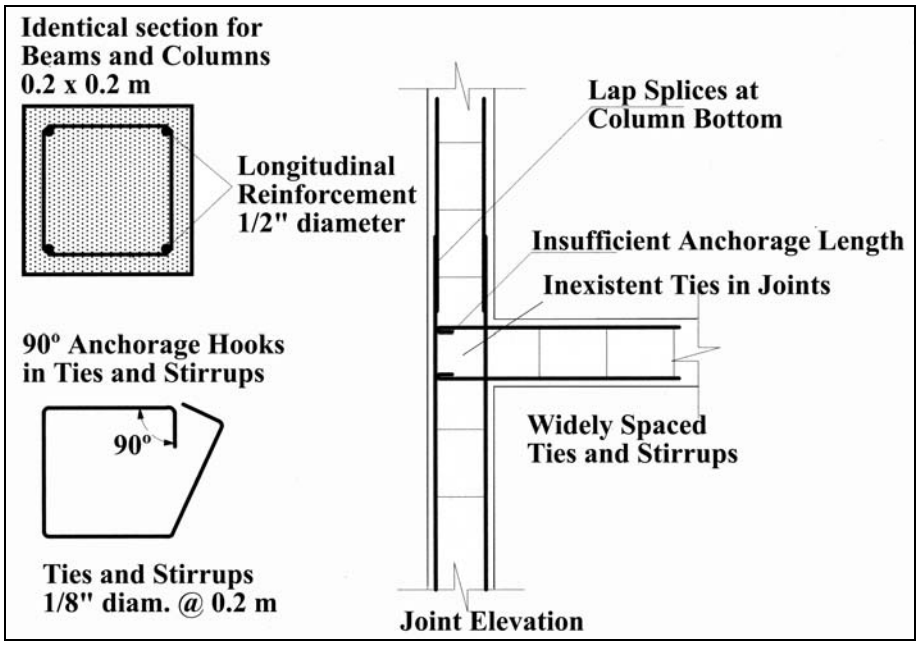

Figure 6.7: Frames steel reinforcement.

6.3.3.2 Representative prototype buildings

The number of levels is another feature used in the classification of buildings in "La Milagrosa". For the NENG-RC typology, the most common are the two-storey buildings (52%), followed by the single-storey ones (32%) and finally, by the three-storey (16%). The number of floors is used to select initially three building prototypes, one-, two- and three-storey buildings, termed B1, B2 and B3, respectively. All of them are symmetrical, e.g. the centroids and the stiffness centers are roughly coincident. The average storey height is about 2.80 m.

Buildings B2 and B3 are topped with light roofs while building B1 is topped with a conventional slab (since it represents a group of constructions intended to grow vertically) as discussed previously. A further distinction is incorporated in building B3, originating B3-b (with balconies) and B3-c (with cantilevered walls). When B3 term is used, it will refer to both B3-b and B3-c.

Four representative buildings are selected:

- **B1**. It is a building with one storey and topped with a slab.
- **B2**. It is a building with two stories and topped with a light roof. The second floor might have either a cantilever or a balcony; this distinction is considered irrelevant from the seismic behavior point of view since (1) the upper walls lack both of collar beam and of proper ties and, hence, their in plane strength will never be developed and (2) the roof is very light and, consequently, the demanding lateral forces on the upper walls are rather small.
- **B3-b**. It is a building with three stories and topped with a light roof. The second and third floors have a balcony; this is considered relevant from the seismic behavior point of view since the second floor front wall is coplanar with the frame, being fully able to cooperate in the seismic strength.

- **B3-c**. It is a building with three stories and topped with a light roof. The second and third floors have a cantilever; this is considered relevant from the seismic behavior point of view since the second floor front wall is not coplanar with the frame, being only partially able to cooperate in the seismic strength.

The representative buildings with average features are assumed to be built in the same fashion as in the previous descriptions, i.e. regular in plan with the characteristic common conditions, structural layout and dimensions and detailing of structural members, roofing, and infill walls (cladding and partitioning). An isometric drawing of the four representative buildings are shown in Figure 6.8 and Figure 6.9, where B1 is the single-storey building, B2 is the two-storey one, B3-b and B3-c are the three-storey buildings. The typical plans for the prototypes are shown in Figure 6.10.

It is remarkable that, in spite, building B3-c is asymmetric (e.g. there is an eccentricity among the center of stiffness and of gravity in the second and third floors), this has only a reduced influence on the torsional seismic behavior.

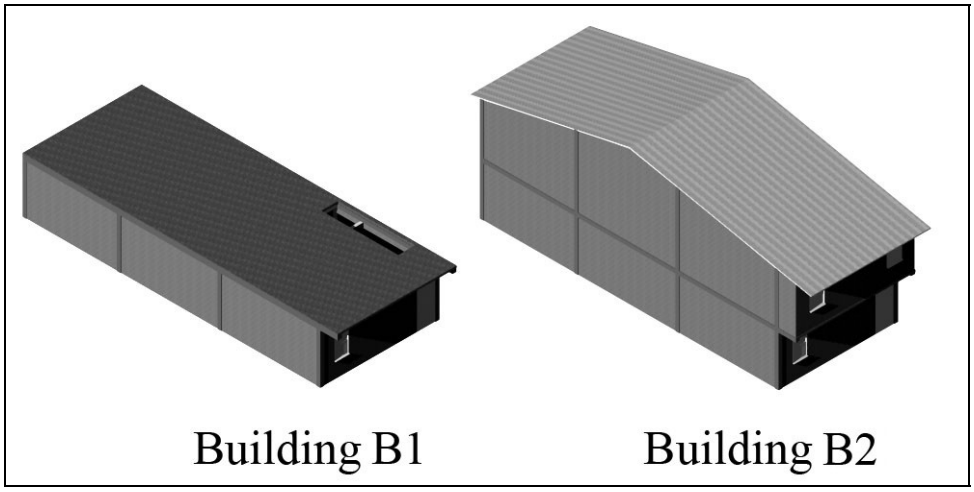

Figure 6.8: Isometric drawings for buildings B1 and B2.

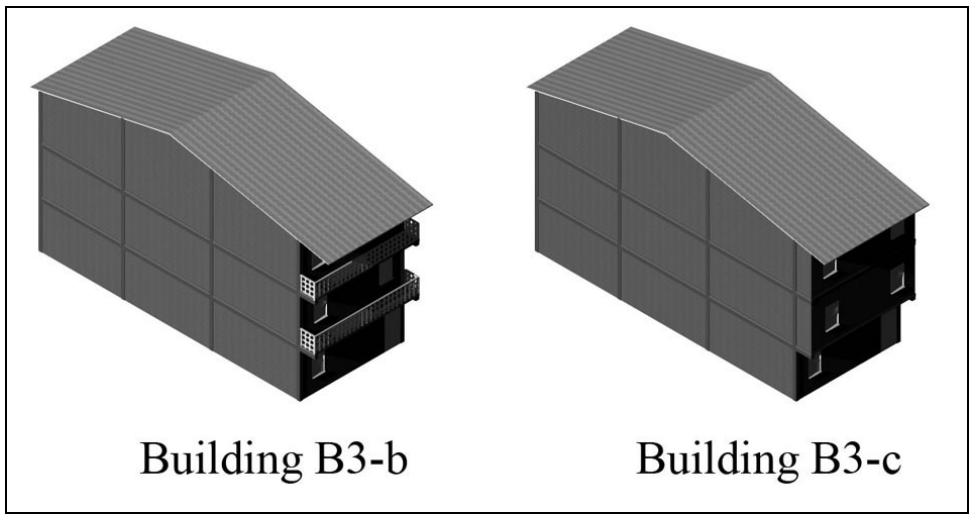

Figure 6.9: Isometric drawings for buildings B3-b and B3-c.

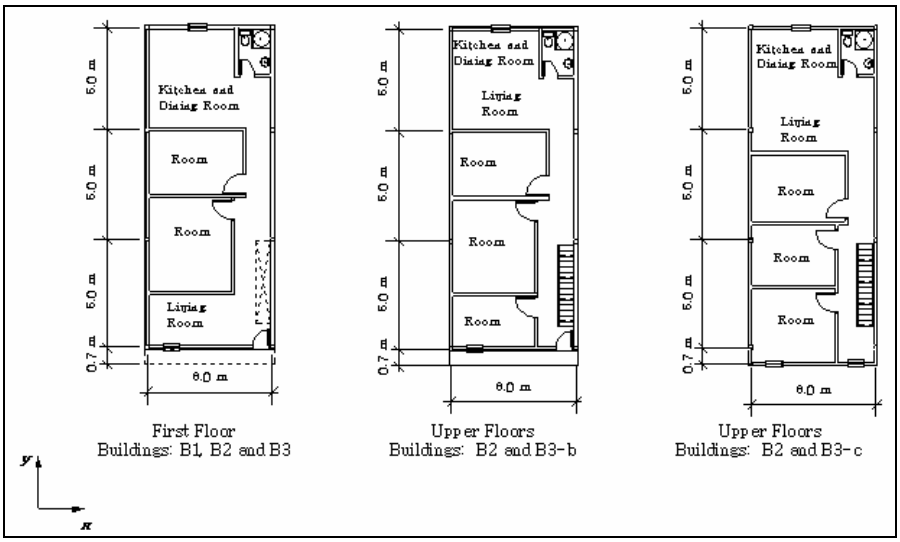

Figure 6.10: Typical plans for building prototypes.

6.3.4 Gravity loads behavior

6.3.4.1 General considerations

The purpose of this subsection is to assess the ability of the supporting structure to resist the vertical loads. Such loads are supported by the frame (the slabs might contribute to alleviate the demands on the beams) and the walls. The distribution between both systems is rather unclear and, hence, conservative criteria have to be considered:

- The frames weight is rather supported by themselves.
- The slabs weight is distributed among frames and walls (if they are continuous down to the supports). Initially the load is mainly carried by the frame but, once loads grow and the concrete of the beams creep, part of it is transferred to the walls.
- The walls (provided they are down to the supports) are mainly carried by the lower level walls as they are significantly more rigid (in the vertical direction) than the frames.
- The live loads are mainly carried by the walls as they are generated mostly after their erection and are (as discussed previously) significantly stiffer than the frames.

The approach considered in this subsection consists of assessing (conservatively) the capacity of the frames, slabs and walls to resist the gravity loads in order to understand the actual resisting mechanism.

Only ultimate limit states are checked, the serviceability conditions are not verified as they are not crucial.

6.3.4.2 Structural analysis of the frames

The *x* direction frames are more demanded than the longitudinal ones as they are intended to support the secondary beams of the slabs. Hence, only transversal frames are analyzed.

A linear first-order 2D analysis under ultimate limit states has been performed for the inner and outer transversal frames (x direction) of prototype buildings B2 and B3; B1 has not been considered as it is similar to B2 yet with smaller loads. Only the inner frames are shown here as they are more demanded because carry heavier loads and are less supported by the infill walls. No plastic bending moment laws redistribution has been considered.

Figure 6.11 shows the analyzed (inner) frames for buildings B2 and B3. The upper floor columns are not modeled as they are not tied and behave simply as a cantilever.

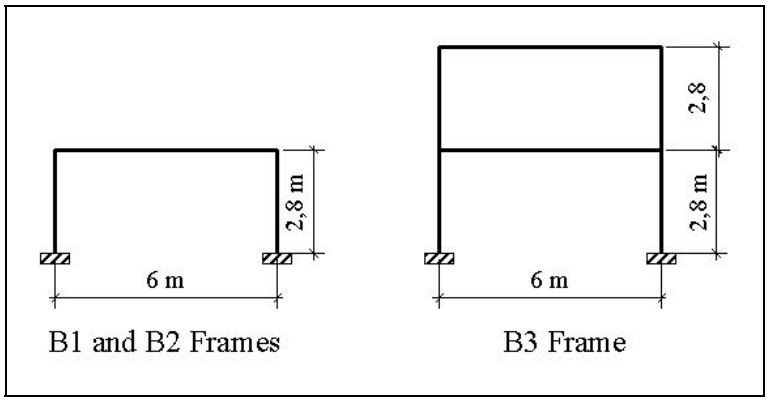

Figure 6.11: Transversal frames of buildings B2 and B3.

The concrete deformation modulus is $E_c = 4700\ (f_{ck})^{½} = 14863$ MPa [American Concrete Institute, 2002]. Its unit weight has been taken as $\gamma_c = 24$ kN/m^3 (since the reinforcement amount is rather low).

The following load combination has been considered: $1.4\ D + 1.7\ L$ where D and L account for dead and live loads, respectively. The live load has been taken as $L = 1.50$ kN/m^2, in spite that Venezuelan codes prescribe $L = 1.75$ kN/m^2 (as discussed previously) since such level fits more the actual situation. As discussed previously, the weight of the walls is not included as it is assumed to be withstood by the lower walls (they are significantly more stiff than the frame in vertical direction).

The contribution of walls and slabs in the structural behavior of the frames is neglected. The upper columns are not modeled as they are not tied at their tops and they merely exert vertical compression due to their self weight.

Figure 6.12 and Figure 6.13 show the design values of the internal forces (bending moments, shear and axial forces) laws for the inner frames (those supporting heavier loads) in buildings B2 and B3, respectively.

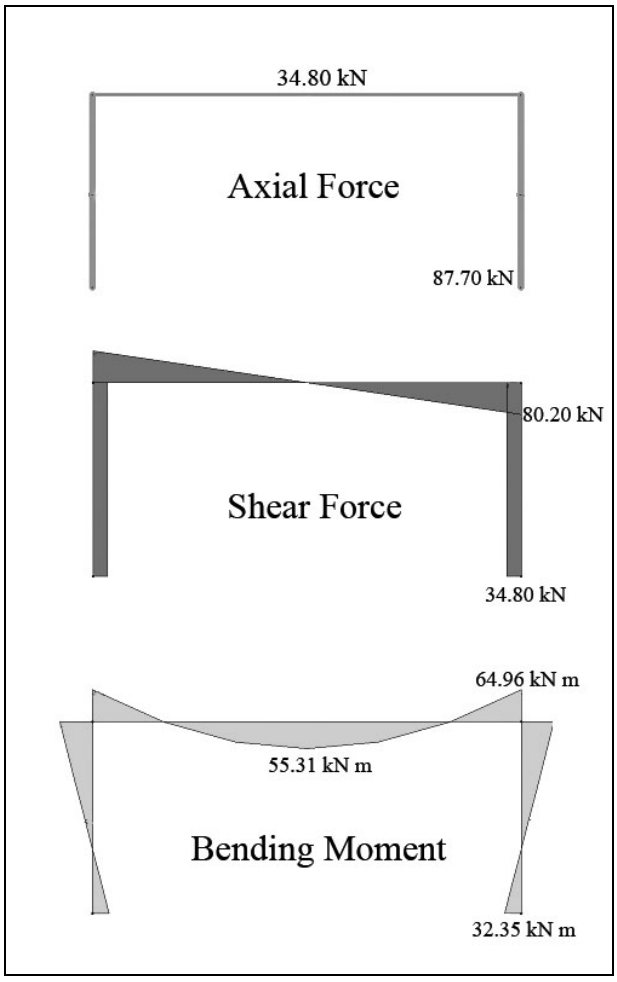

Figure 6.12 Internal forces for the inner frames in building B2.

No second order analysis has been performed since the side-sway motion is clearly prevented by the walls. Hence, the risk of buckling is extremely low and no special verifications are included.

The ability of the frame members to resist the internal forces at Figure 6.12 and Figure 6.13 is assessed next.

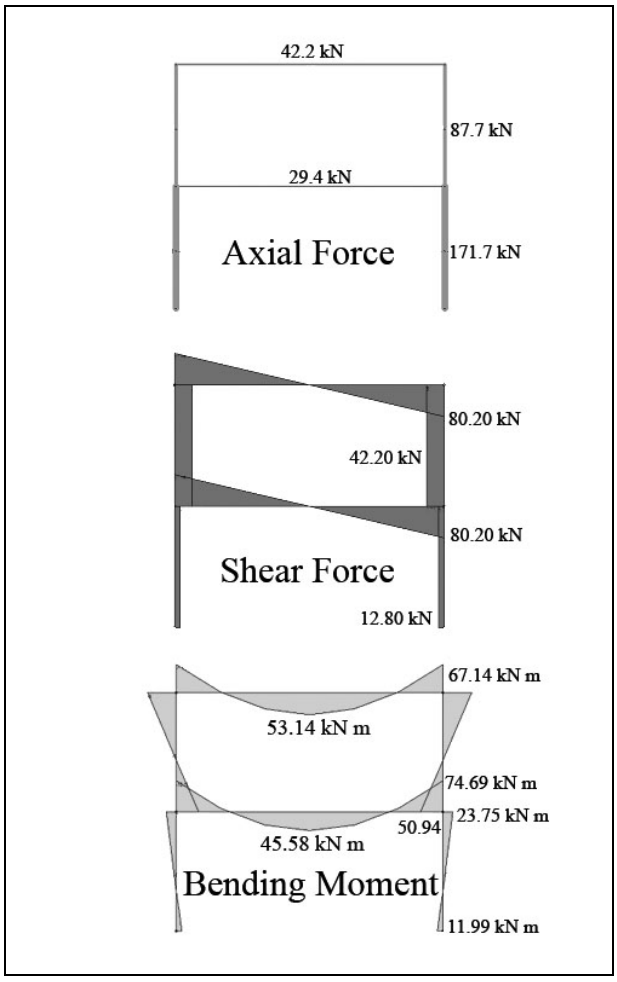

Figure 6.13 Internal forces for the inner frames in buildings B3.

6.3.4.3 Strength verifications in the transversal frames

Axial force and bending moment. The design values of N and M shown by ; the internal forces laws indicate that the bending moment is largely more demanding. The worst case corresponds to the end sections of the lower beam of the frame belonging to buildings B3. Such design greatest demanding moment is M_{Sd} = 74.69 kNm.

The section capacity is determined next following a classical limit analysis. The following (common) assumptions have been considered: (1) the section remains planar, (2) the tensile concrete strength is neglected, (3) the compressed concrete stresses distribution is constant along the upper 85% of the compression zone and (4) such stress is equal to 85% of the characteristic value of the concrete compressive strength. Figure 6.14 describes the strain and stress distributions along the section.

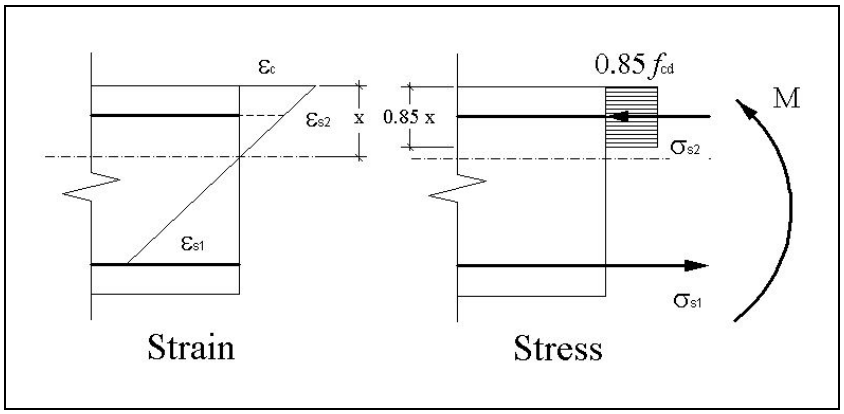

Figure 6.14: Ultimate state of the bent section.

At Figure 6.14 d is the effective depth, d' is the upper reinforcement cover, x is the distance from the neutral axis to the upper extreme fiber, b is the section width, A_{s1} and A_{s2} are the tension and compressed steel reinforcement areas and σ_{s2} is the compressed steel reinforcement stress.

The following failure criteria are considered: (1) maximum (compressed) concrete strain $\varepsilon_c = 0.003$ (no further strength is considered as the transversal reinforcement is clearly insufficient to confine the core concrete) and (2) maximum tensioned steel strain $\varepsilon_s = 0.1$. The obtained ultimate moment M_R is reduced by a safety factor $\phi = 0.90$ [American Concrete Institute, 2002].

Equilibrium equations are

$$0.85 f_{ck}\, b\, 0.85\, x + A_{s2}\, \sigma_{s2} = A_{s1} f_{yk} \qquad \text{eq. 6.3}$$

$$A_{s2}\, \sigma_{s2}\, (d - d') + 0.85 f_{ck}\, b\, 0.85\, x\, (d - 0.85\, x / 2) = M_R \qquad \text{eq. 6.4}$$

The combined use of the compatibility conditions and the (linear) steel constitutive law yields

$$E_s\, 0.003\, [(x - d') / x] = \sigma_{s2} \qquad \text{eq. 6.5}$$

The solution of equations 6.3, 6.4 and 6.5 provides $x = 20.75$ mm and $\sigma_{s2} = 21.69$ MPa, this last value is significantly smaller than the estimated steel yielding point (140 MPa) and, hence, it does not yield (as assumed previously). The strain of the tensioned steel is given by the compatibility condition $\varepsilon_{s1} = 0.003\ (d - x) / x = 0.0230$; it is clearly lower than the assumed threshold (0.1) and, hence, such steel has not failed. However, ε_{s1} largely exceeds the strain yielding point (given by $f_{yk} / E_s = 0.0007$); therefore, the tensioned steel has yielded. By substituting the above values of x and σ_{s2}, the maximum resisting bending moment is obtained

$$M_R = 6 \text{ kNm}$$

By using the reduction factor ϕ, the design value is

$$M_{Rd} = \phi\, M_R = 0.90 \times 6 \ = 5.40 \text{ kNm}$$

Since $M_{Rd} < M_{Sd}$ (largely), it can be concluded that the frame does not have the capacity to withstand the demand.

After checking the resistance to bending, the risk of buckling of the compressed rebars (spalling) is assessed. After preliminary calculations by assuming conservative hypotheses, it follows that there is no relevant risk of buckling of the longitudinal reinforcement bars in the columns.

Shear forces. The worst situation about the shear forces arise in the beam ends since such forces are greater and there are no relevant and reliable compressive axial forces (they improve the shear resistance). The greatest demanding force is $V_{Sd} = 80.20$ kN.

Instructions from the ACI 318 [American Concrete Institute, 2002] recommend estimating the shear resistance V_R for reinforced concrete members using the expression:

$$V_R = V_c + V_s \qquad \text{eq. 6.6}$$

where V_c is the concrete contribution and V_s is the shear strength due to the stirrups action. This last resistance is neglected as the spacing between stirrups is excessive ($s_2 \geq 200$ mm, so allowing the formation of transversal 45º cracks), the diameter is too small ($\phi = 3.175$ mm) and the steel yielding point is extremely low:

$$V_s = 0$$

The ACI 318 [American Concrete Institute, 2002] suggests that for members subjected only to shear and bending, the shear strength can be estimated using the expression:

$$V_R = b\, d\, (f_{ck})^{½} / 6 = 200 \times 180 \times (10)^{½} / 6 = 18.97 \text{ kN}$$

The obtained ultimate shear force V_R is reduced by a safety factor $\phi = 0.85$ [American Concrete Institute, 2002]:

$$V_{Rd} = \phi\, V_R = 0.85 \times 18.97 = 16.13 \text{ kNm}$$

Since $V_{Rd} < V_{Sd}$, it can be concluded that the frame does not have the capacity to withstand the demand. It is remarkable that this situation is dangerous as this type of failure is rather brittle and the inhabitants will not be probably able to detect it until it is too late.

Detailing. It is apparent that the detailing is extremely poor. Main detected facts and deficiencies are:

- The longitudinal reinforcement amount is greater than the minimum value indicated in the ACI 318 [American Concrete Institute, 2002].
- The transversal reinforcement is too weak as the separation between adjacent stirrups is even bigger than the effective depth, the diameter is too small, the steel yielding point is unclear and the stirrups are not well closed (90º instead of 135º).

- The overlapping length is smaller than the minimum value established in the ACI 318-02, as it is equal to the maximum of 400 mm and of $0.07\, f_{yk}\, d_b = 0.07 \times 140 \times 1.27 = 12.4$ cm (d_b is the diameter of the rebar).

6.3.4.4 Cantilevers

As discussed previously, buildings B3-c are cantilevered since the second and third floors walls extend around 70 cm beyond the outer frame plane. The strength is checked here.

The cantilever consists of steel beams laid orthogonally to (outer) transversal beams. Each of these beams supports the loads sketched at Figure 6.15.

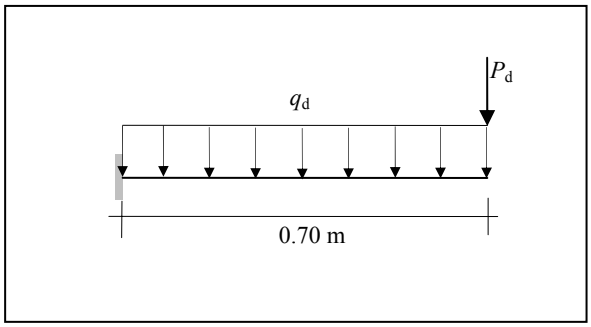

Figure 6.15: Loaded cantilever beam.

The design values of the loads shown at Figure 6.15 are:

$$q_d = 1.4 \times 1.832 \times 0.80 + 1.7 \times 1.50 \times 0.80 = 4.09 \text{ kN/m}$$

$$P_d = 1.4 \times 0.80 \times 2.80 \times 0.15 \times 12 = 5.64 \text{ kN}$$

These values have been derived for the first level beam assuming that it supports only the second floor wall.

The maximum bending moment is

$$M_{Sd} = 4.09 \times 0.7^2 / 2 + 5.64 \times 0.7 = 4.95 \text{ kNm}$$

Neglecting the contribution of the (tensioned) upper concrete layer, the maximum normal stress (assuming elastic behavior) is given by

$$\sigma_{max} = 4.95 / 19.5 = 253 \text{ MPa}$$

As this stress is (slightly) greater than the steel yielding point (250 MPa), these structural members are unsafe. It is remarkable that the design and construction manual [Sidetur, 2004] recommends this solution for cantilevers up to 0.90 m; apparently this suggestion is mostly intended for balconies.

6.3.4.5 Slabs

As described previously, the slabs are composed of steel IPN 80 beams topped with a reinforced concrete layer at least 3 cm deep. The characteristic value of the compressive concrete strength is assumed to be he same as the one of the columns: f_{ck} = 10 MPa. The role of the reinforcement is not crucial as this layer is mostly compressed; wherever it is tensioned (due to static redundancy) the yielding of the section would lead to an internal redistribution of the bending moments. In any case, the maximum (positive) moment will be given by

$$M_{Sd} = 4.09 \times 5^2 / 8 + 5.64 \times 5 / 4 = 19.83 \text{ kNm}$$

In this result, it has been assumed that there is a wall (perpendicular to the beam) in the mid of the span.

Neglecting the contribution of the upper concrete layer, the maximum normal stress (assuming elastic behavior) largely exceeds the steel yielding point, hence, it is required to consider its cooperation. As there are no shear connectors between the topping and the beams, it is not reliable to analyze each beam-topping assembly as a composite single member. At most, it might be assumed than the steel beam and the concrete layer share the moment, being distributed among them proportionally to their rigidities. In any case, it is clear that these slabs are unsafe. It is remarkable that the design and construction manual [Sidetur, 2004] recommends this solution for span length up to 3.45 m and requires a top layer 6 cm deep and cast with higher strength concrete (f_{ck} = 25 MPa).

6.3.4.6 Summary

After the verifications about the frame, walls and slabs strength and the member detailing, it is clear that the demands largely exceeds the resistances (e.g. in some beam ends the maximum resisted moment is about ten times smaller than the demand). However, in the site inspections, relevant pathologies have been neither observed nor reported. This significant disagreement has to be explained in order to better understand the actual structural behavior. A list of possible reasons follows.

- The limit analyses carried out in this section consider safety factors (both increasing the loads and decreasing the resistances of the materials) while the actual situation corresponds, obviously, to serviceability conditions.
- The real live load is still smaller than the assumed one.
- The slabs placed directly over the frame beams cooperate in their resistance.
- The actual values of the material parameters might be bigger than those assumed; in particular the rebars steel yielding point can be higher.
- There are some (common) conservative simplifications in the structural analysis of the frame and of the slabs. For instance, the lengths of the members are equal to the distances between the joints (while they are shorter), the assumed (maximum) values of the internal forces correspond actually to the joints (where the concrete is more confined) among others.
- The infill walls (both coplanar and not coplanar with the frame) take most of the dead and live load. It is remarkable that the assumed compression strength of the masonry is enough to cope with the gravity forces (at least under serviceability conditions, e.g. without safety factors), as taking the greatest value for the building weights (three levels) and distributing it uniformly over the wall plan area, renders an average

compression stress of σ_{cw} = 0.195 MPa, which is smaller than f_{wck}. The situation of the second floor (outer) transversal beams supporting the cantilever (Building B3-c) is particularly crucial as they are not supported by lower walls.

Among these considerations, the last one is probably the most relevant; it is crucial that the owners and occupants of the houses are aware that their weight is mainly carried by the walls (both the cladding and the partitioning ones) rather than by the frame. In any case, the constructions are clearly unsafe from the regular standards. Another practical conclusion is that it can be reasonably assumed that, under serviceability conditions, the columns are scarcely bent and their behavior is mostly compressive.

6.3.5 Seismic behavior

The horizontal and vertical seismic behavior is theoretically analyzed in this subsection.

About the seismic strength, there are two relevant drawbacks: there are no experimental results (other than the Schmidt hammer tests for concrete in columns and observed damage for similar typologies –as described next in subsection 6.3.8–) and the strength of the constructions is highly unreliable. Therefore, only (rather conservative) preliminary conclusions can be conjectured herein (from theoretical considerations); an experimental verification is strongly required and their features are described at the end of this subsection. However, the analyses carried out in this subsection are useful since will provide a valuable understanding of the seismic behavior of the buildings and will orientate the research required to inform about the hottest arisen issues.

No safety factors have been considered; this choice has been adopted because of the following reasons: the actual (average) behavior is of interest and, as the seismic action is considered by most of the worldwide regulations as accidental, the safety and combination factors are usually equal to 1. An important exception is the live load, only a given percentage of it (25% according to Venezuelan seismic code [MINDUR and FUNVISIS, 1998]) is assumed to be present in case of earthquake.

6.3.5.1 Failure modes

Identified failure modes for masonry infill frames are described in [Paulay and Priestly, 1992].

The infill walls are much stiffer (in the horizontal direction) than the RC frames (in fact, they are extremely flexible). It means that, prior to any damage, most of the lateral forces are carried by the walls rather than by the frames. For greater forces (corresponding to more intense earthquakes), several (global or local) failure modes are possible:

1. Shear failure of the topped walls accompanied by shear or bending failure of the frame. This mode describes the failure of the masonry along horizontal mortar courses, generally at mid-height of the panel.
2. Diagonal strut compression failure of the topped walls (which are coplanar with the frame, i.e. not cantilevered) accompanied by shear or bending failure of the frame.
3. Out of plane failure of the untopped walls.
4. Detachment of the (light) roofs from the supporting elements.
5. Collapse of vertical propless elements (cantilevered and vertically discontinuous walls).

The two first failure modes are described by Figure 6.16. The most relevant features for each of the individual possible failure modes as well as their combinations are described at the next subsections.

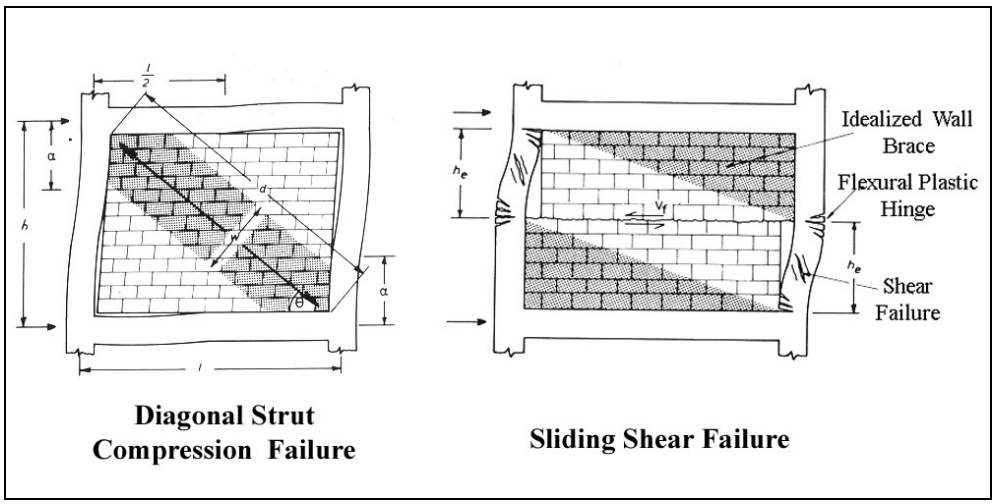

Figure 6.16: Global failure modes (after [Paulay and Priestley 1992]).

Figure 6.16 (left) shows that the resistance of the diagonal strut compresion failure mode is upper bounded by the shear strength of the columns.

It is remarkable that the shear failure through rather diagonal cracks is disregarded as such fissures would follow the mortar joints and, hence, more energy would be required (to break the vertical joints).

Other possible failure modes can be disregarded:

- Out of plane failure of the topped walls. These walls are rather confined and vertically compressed; hence, is improbable that this failure comes earlier than the in plane one.
- In plane failure (horizontal shear or diagonal strut compression) of the untopped walls. The out of plane strength of these walls is very small (since they are both laterally unrestrained and uncompressed) and clearly significantly lower than the in plane one.
- Tension failure of the columns. It is unfeasible as the elevation aspect ratios of the buildings are low and the masses are small.
- Diagonal tensile cracking of the walls. This is not properly considered as a failure as the construction keeps virtually all its resistant capacity.
- Detachment of the slabs from the supporting frames. This possibility is unfeasible as the slabs are rigid in its own plane (mainly because of the top concrete layer) and they are encased by the columns (as shown by Figure 6.17).

The contribution of the stairs (see Figure 6.10) to the horizontal strength is neglected because they are usually located near stiffer elements (longitudinal walls for internal stairs or transversal walls for external stairs) which take most of the lateral load prior to any failure. After wall failure, the additional resistance of the stairs might play a relevant role but it is not accounted for (conservatively) because of both the lack of reliability of the stairs contribution and because they are located in a completely asymmetrical way and would introduce relevant torsion effects in the building.

The repercussion of the openings in the slabs (mostly because of the stairs) is also neglected as they have little effect in their in-plane resistance. Hence, a full diaphragm effect is assumed and the lateral behavior of the building is represented by lumped masses models with one degree-of-freedom per floor (at each direction) as the building is rather symmetric.

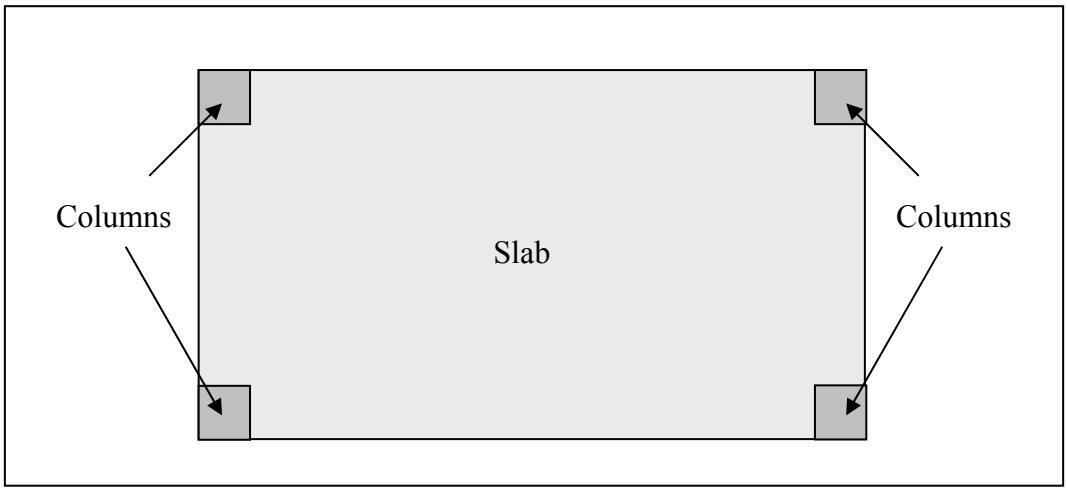

Figure 6.17: Building slab encased by the columns.

- Tension failure of the beams in the joints. This failure would mainly arise by slippage of the longitudinal reinforcement bars of the beams inside the columns. It is rather not viable as such bars are sufficiently anchored by conventional hooks.

6.3.5.2 Shear failure of the walls

The shear failure of the walls arises from horizontal sliding along courses of mortar beds. The strength of this failure mode comes from two sources: bonding and friction (due to vertical compression), according the classical Mohr-Coulomb criterion. Paulay and Priestley (1992) conservatively recommend not taking into account the vertical forces due to gravity as their values are hard to estimate and, prior to failure, the beams are separated from the walls (Figure 6.16). The vertical compression comes only from the vertical component of the diagonal strut compression. The shear strength of the coplanar and un-coplanar (partitioning or cantilevered) walls is different: in the first case, such compression can be taken into account while in the second one it does not exist since there are no columns in the sides of the wall (and, hence, the behavior described by Figure 6.16 is impossible).

For cyclic behavior, only the friction term can be accounted for as the cohesion is not reliable; such residual strength is also determined in this subsection. This is relevant when considering the joint behavior of walls ad frames as discussed forwardly.

The effect of openings is represented by an equivalent reduction in the length of the wall, as shown by Figure 6.18.

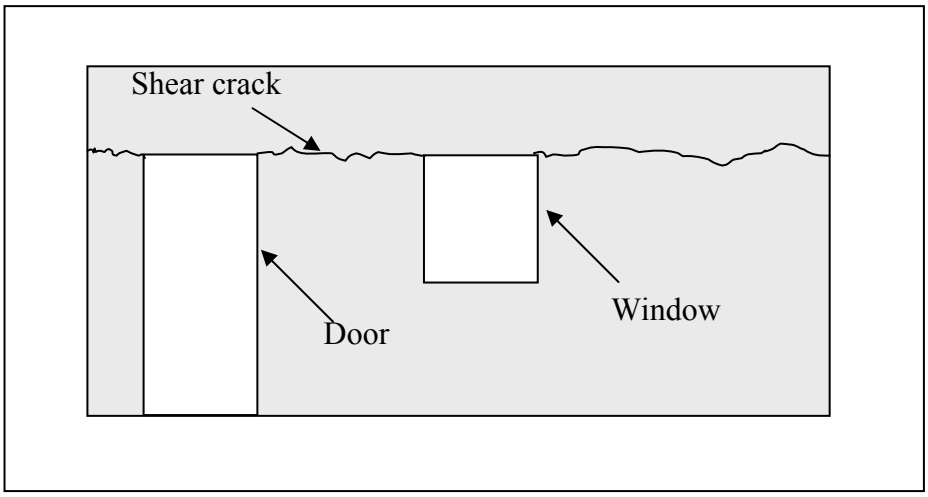

Figure 6.18: First floor masonry front wall with openings.

Figure 6.18 shows that the length of the failure crack is equal to the total wall length minus those of openings. The average sum of the lengths of door and window is near the 30% of the wall length (in some cases, the length of the window can be bigger, as shown by Figure 6.19). For upper floors, in some cases there are balconies (building B3-b) while in other cases there are only windows (building B3-c); anyway, the situation of the cladding walls is similar to the one in the first floor (Figure 6.18). About the partitioning walls, the situation is similar even though the percentage of openings is smaller as there are no inner windows.

The shear strength F_{Rws} of the coplanar walls is given by the Mohr-Coulomb criterion:

$$F_{Rws} = L_w \times t_w \times \tau_{wk} + \mu \times R_s \times \sin\theta \qquad \text{eq. 6.7}$$

In cantilevered walls only the first term ($L_w \times t_w \times \tau_{wk}$) can be considered.

After the first failure, only the second term can be relied on (residual strength).

In 6.7 L_w is the wall length (subtracting the lengths of the major openings), t_w is its width, τ_{wk} is the characteristic value of the shear stress strength of the wall, μ is the friction coefficient, R_s is the diagonal force and is θ the diagonal angle (see Figure 6.16).

R_s force is given by

$$R_s = (\tau_{wk} \times d_m \times t_w) / [1 - \mu\,(h / L_w)] \qquad \text{eq. 6.8}$$

In equation 6.8 d_m is the diagonal length and h is the column height (see Figure 6.16).

For walls with openings (front, rear and partitioning) this mode is possible but the vertical component of the diagonal compression can not be completely accounted for. Figure 6.19, Figure 6.20, Figure 6.21 and Figure 6.22 show that other diagonal struts are possible. Given the variability of the openings and of failure mechanisms it is grossly estimated that the value of the R_s force is halved.

It is remarkable that in cantilevered walls this mode, as discussed previously, such vertical component can not be absolutely relied on also because of the lack of side columns.

The friction coefficient is taken as $\mu = 0.4$ [ENV-1996].

The average value of the diagonal angle θ in the *x* direction is given by tan θ = 2.8 / 6 = 0.46; hence θ = 25 º. In the *y* direction is given by tan θ = 2.8 / 5 = 0.56; hence θ = 29.25 º.

The values of R_s and of F_{Rws} in both directions are computed next (according to equations 6.7 and 6.8).

***y* direction.** One wall without openings L_w = 4.80 m.

$R_s = (80 \times 5.46 \times 0.15) / [1 - 0.4\ (2.8 / 5)] = 84.43$ kN

$F_{Rws} = 4.80 \times 0.15 \times 80 + 0.4 \times 84.43 \times \sin 29.25º = 74.10$ kN

The residual strength is:

$F_{Rws} = 0.4 \times 84.43 \times \sin 29.25º = 16.50$ kN

***x* direction.** One wall (coplanar or cantilevered) with 30% openings $L_w = 5.80 \times 0.70 = 4.06$ m.

$R_s = (80 \times 6.44 \times 0.15) / [1 - 0.4\ (2.8 / 6)] = 95.02$ kN

Coplanar wall: $F_{Rws} = 5.80 \times 0.70 \times 0.15 \times 80 + 0.5 \times 0.4 \times 95.02 \times \sin 25º = 56.75$ kN

Cantilevered wall: $F_{Rws} = 5.80 \times 0.70 \times 0.15 \times 80 = 48.72$ kN

The residual strength of the cantilever wall is zero because of the lack of reliability of the vertical compressive force; on the other hand, the residual strength of the coplanar wall is:

$F_{Rws} = 0.5 \times 0.4 \times 95.02 \times \sin 25º = 8.03$ kN

The resulting strengths for this mode per unit (effective) wall length are shown by Table 6.9.

Wall type	Initial strength	Residual strength
x direction. Coplanar	13.98	1.98
x direction. Cantilever	12.00	-
y direction	15.44	3.44

Table 6.9: Horizontal wall strength. Shear failure mode (kN/m).

6.3.5.3 Diagonal compression failure of the coplanar walls

Generally, at low levels of in-plane lateral force, the frame and infill walls act jointly, and behave as a structural wall with boundary elements (confined masonry); at higher lateral deformations, the behavior of the system becomes complex, as the frame deforms in a flexural mode while the walls do so in a shear mode (Figure 6.16). This results in a separation between the frame and the panel at the corners of the tension diagonal, and the development of a compression strut in the compression diagonal (bracing action of masonry infill), with a contact zone between the frame and the infill panel with a length denoted as *z*, and a diagonal strut width (*w*) smaller than that of the full panel. The strut width may conservatively be taken as: $w = 0.25 \times d_m$, where d_m is the diagonal length.

This mode is different for side (longitudinal, y) and transversal (x) walls since these last (front, rear and partitioning) possess openings (doors and windows) which obviously interrupt the diagonal strut.

For walls without openings, Paulay and Priestley recommend using the following conservative semi-empirical expression for the diagonal compression strength of the wall:

$$F_{Rwd} = w \times t_w \times f_{wck} / (3 \times \sin\theta \times \cos\theta) \qquad \text{eq. 6.9}$$

Figure 6.16 shows that the strength of this mode is obviously bounded by the shear strength of the columns.

***y* direction.** One wall without openings $L_w = 4.80$ m.

$F_{Rwd} = 0.25 \times 5.46 \times 0.15 \times 350 / (3 \times \sin 29.25º \times \cos 29.25º) = 56$ kN

For walls with openings, the strength is, obviously, smaller and depends on the position and size of the openings.

Figure 6.19 and Figure 6.20 present possible failure mechanisms for a cladding wall pushed by lateral forces. It is remarkable that the percentage of openings has been conservatively assumed as significantly bigger than the 30% considered in the estimation of the shear strength.

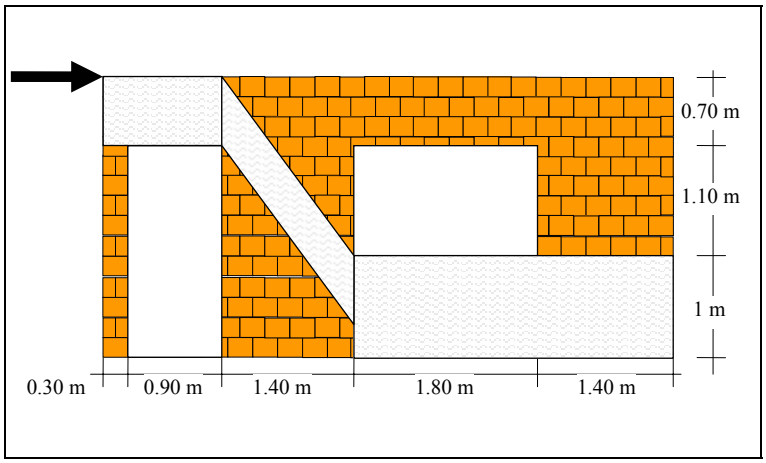

Figure 6.19: Failure mechanism for cladding wall and left force.

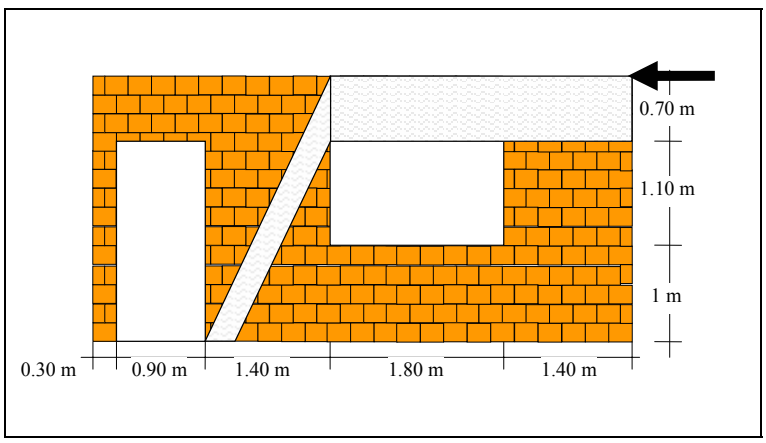

Figure 6.20: Failure mechanism for cladding wall and right force.

Figure 6.21 and Figure 6.22 present similar possible failure mechanisms for a partitioning wall pushed by lateral forces.

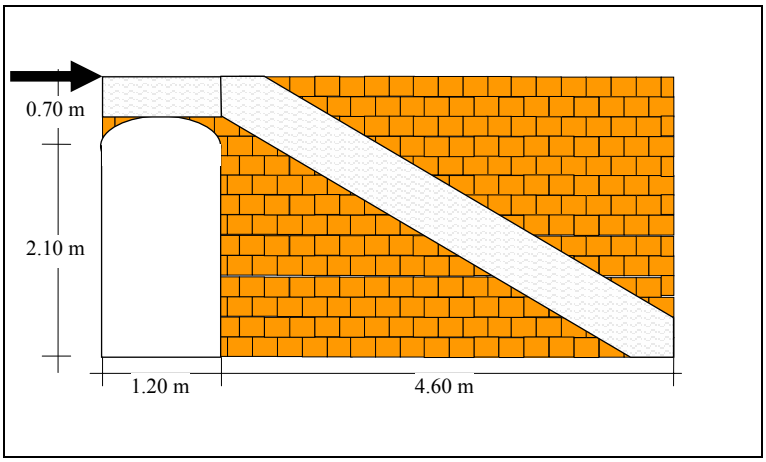

Figure 6.21: Failure mechanism for partitioning wall and left force.

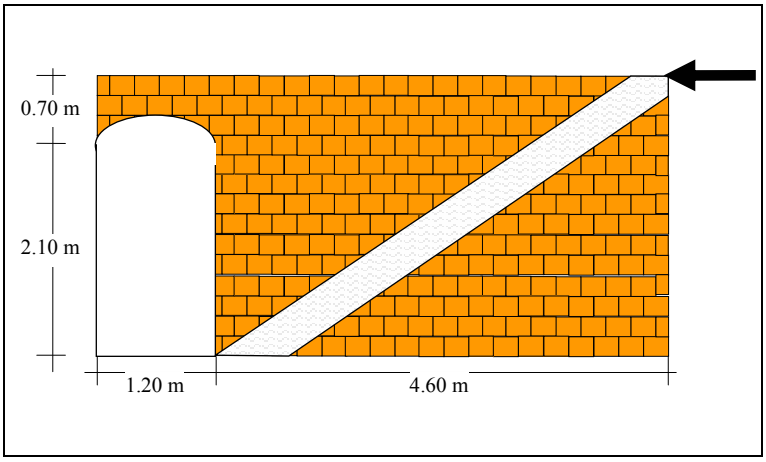

Figure 6.22: Failure mechanism for partitioning wall and right force.

The four previous Figures show that the strength is significantly smaller than in the longitudinal walls as the struts are more vertical. Moreover, Figure 6.20 and Figure 6.22 show that these struts are not reliable enough since the lower (left) end (wall toe) might slide on the floor base and, in any case, high stress concentrations would arise (while the rather brittle bricks would not resist them). Hence, this strength is grossly estimated as one fourth of the one without openings:

***x* direction.** One (coplanar) wall with 30% openings L_w = 4.06 m.

F_{Rws} = 0.25 × 0.25 × 6.44 × 0.15 × 350 / (3 × sin 25º × cos 25º) = 18.39 kN

In static loading this mode is rather ductile, i.e. residual strength after the initial failure exists. However, on inelastic cycling the capacity of the diagonal strut will degrade. It can be conservatively assumed that the remaining resistance is zero.

The resulting strengths for this mode per unit (effective) wall length are shown by Table 6.10.

Wall type	Initial strength	Residual strength
x direction. Coplanar	3.17	-
y direction	11.67	-

Table 6.10: Horizontal wall strength. Diagonal compression mode (kN/m).

6.3.5.4 Shear failure of the columns

Instructions from the ACI 318 [American Concrete Institute, 2002] recommend estimating the shear resistance V_n for reinforced concrete members using the expression:

$$V_n = V_c + V_s \qquad \text{eq. 6.10}$$

where V_c is the concrete contribution and V_s is the shear strength due to the stirrups action. This last resistance is neglected as the spacing between stirrups is excessive ($s_2 \geq 200$ mm, so allowing the formation of transversal 45º cracks), the diameter is small ($\phi = 3.175$ mm) and the steel yielding point is extremely low:

$$V_s = 0$$

For members under axial compression and with potential plastic hinges, Paulay and Priestley (1992) recommend the following expression for the concrete shear strength:

$$V_c = 4\, v_b\, b_w\, d\, (N_u / A_g f_{ck})^{½} \qquad \text{eq. 6.11}$$

where b_w is the web width, d is the effective depth (distance from the extreme fiber to the tensioned steel), N_u is the axial force in the member, A_g is the gross area of the section, f_{ck} is the characteristic compressive strength of the concrete and v_b is given by

$$v_b = (0.07 + 10\, \rho_w)\, (f_{ck})^{½} \leq 0.2\, (f_{ck})^{½} \qquad \text{eq. 6.12}$$

where ρ_w is the reinforcement amount

$$\rho_w = A_s / b_w\, d \qquad \text{eq. 6.13}$$

where A_s is the area of the tensioned reinforcement.

Equation 6.11 shows that the effect of axial compression is beneficial; therefore the axial forces in the columns have to be evaluated conservatively. It has been considered that it incorporates the self weight of the frame (beams and columns belonging to upper levels) plus half of the weight of the slabs (the remaining part is withstood by the walls via concrete creep). The live load and the walls are mainly supported by the walls themselves, as they are much stiffer (in the vertical direction) than the frame.

The axial forces for the columns are computed next. There are two types of columns, the outer (corner) and the inner ones (side, which carry the double of slab tributary area than the outer columns).

Building B1

Outer columns slab and beam weight:

$0.5 \times 1.832 \times 3 \times 2.5$ (slab) + $0.2 \times 0.2 \times 5.1 \times 24$ (beams) = 11.77 kN

Inner columns slab weight:

$0.5 \times 1.832 \times 3 \times 5$ (slab) + $0.2 \times 0.2 \times 7.6 \times 24$ (beams) = 21.04 kN

Building B2

First level outer columns. Slab and self weight of frame:

11.77 kN + $0.2 \times 0.2 \times 2.8 \times 24$ (columns) = 14.46 kN

First level inner columns. Slab and self weight of frame:

21.04 kN + $0.2 \times 0.2 \times 2.8 \times 24$ (columns) = 23.73 kN

Buildings B3-b and B3-c

Second level outer columns. Slab and self weight of frame:

11.77 kN + $0.2 \times 0.2 \times 2.8 \times 24$ (columns) = 14.46 kN

Second level inner columns. Slab and self weight of frame:

21.04 kN + $0.2 \times 0.2 \times 2.8 \times 24$ (columns) = 23.73 kN

First level outer columns. Slab and self weight of frame:

$2 \times$ (11.77 kN + $0.2 \times 0.2 \times 2.8 \times 24$) (columns) = 28.92 kN

First level inner columns. Slab and self weight of frame:

$2 \times$ (21.04 kN + $0.2 \times 0.2 \times 2.8 \times 24$) (columns) = 47.46 kN

	B1		B2		B3-b and B3-c	
	Inner	Outer	Inner	Outer	Inner	Outer
Levels	N_u (kN)	N_u (kN)	N_u (kN)	N_u (kN)	N_u (kN)	N_u (kN)
1	21.04	11.77	23.73	14.46	47.46	28.92
2	-	-	0	0	23.73	14.46
3	-	-	-	-	0	0

Table 6.11: Axial forces in one column.

The reinforcement ρ_w amount is

$$\rho_w = 2\ \pi\ (2.54 / 4)^2 / 20 \times 18 = 0.007$$

v_b is given by

$$v_b = (0.07 + 10 \times 0.007)\ (10)^{½} = 0.443\ \text{MPa}$$

V_c is given by

$$V_c = 4 \times 0.443 \times 200 \times 180\ (N_u / 200 \times 200 \times 10)^{½}\ \text{N}$$

The seismic strength F_{Rcs} (= V_c) to shear failure of a given column is listed at Table 6.12.

	B1		B2		B3-b and B3-c	
	Inner	Outer	Inner	Outer	Inner	Outer
Levels	F_{Rcs} (kN)	F_{Rcs} (kN)	F_{Rcs} (kN)	F_{Rcs} (kN)	F_{Rcs} (kN)	F_{Rcs} (kN)
1	14.63	10.94	15.54	12.13	21.97	17.15
2	-	-	0	0	15.54	12.13
3	-	-	-	-	0	0

Table 6.12: Shear strength in one column.

As the columns are square and equally reinforced in both directions, these values are the same in *x* and *y* directions.

6.3.5.5 Bending failure of the columns or beams

The collapse mechanisms of the 2-D frames described by Figure 6.24 are composed by four and six hinges, respectively. The lateral forces required to generate such mechanism can be obtained by a classical push-over analysis. This analysis consists of applying growing horizontal forces on the beams until (progressive) collapse. It is assumed that the hinges form at the ends of beams or columns; this assumption is conservative as it would more costly (in terms of horizontal force) to generate other mechanisms with closer plastic hinges. It should be kept in mind that most of the experts in earthquake engineering recommend do not trust in plastic hinges if the transversal reinforcement does not provide enough confinement; this question can be only clarified by experimental analysis (see 6.3.5.10).

The plastic moment is obtained by a section analysis using the SAP2000 software [Wilson, 2002] neglecting the contribution of the axial force (this assumption is acceptable because the axial forces are rather low). Figure 6.23 shows the computed moment-curvature plot.

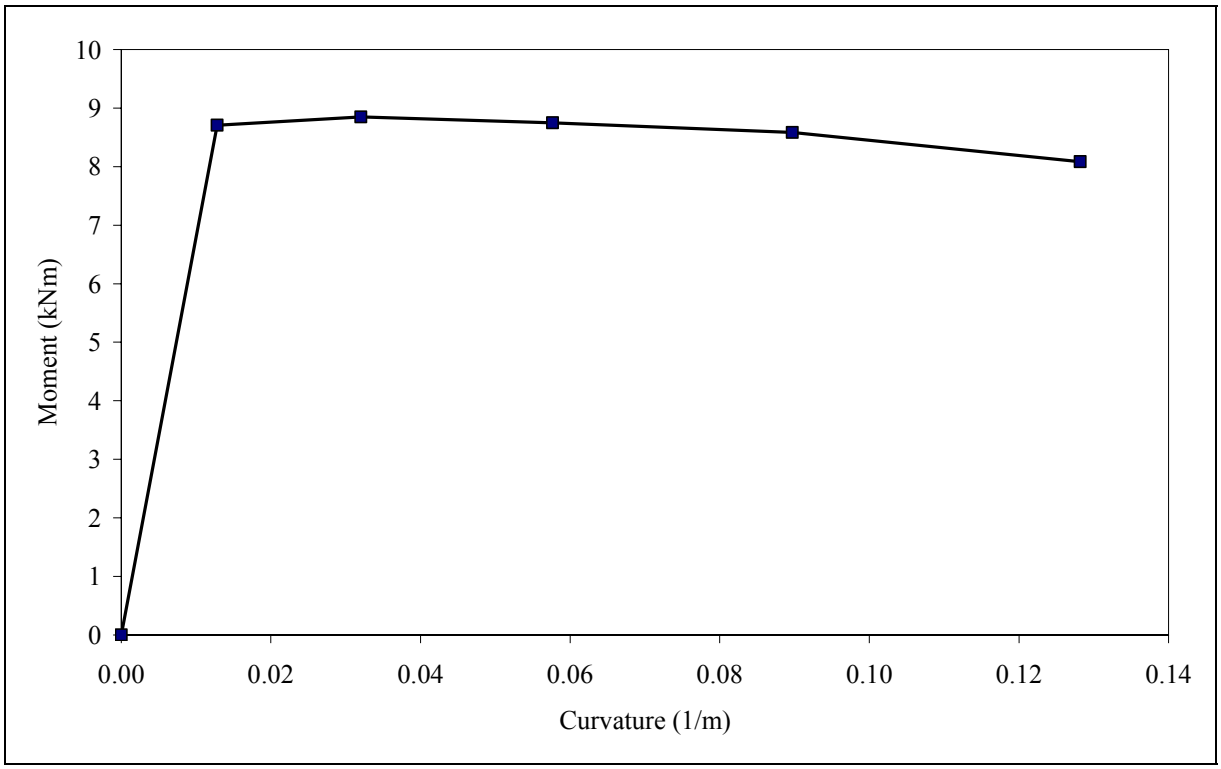

Figure 6.23: Moment-curvature law.

Figure 6.23 shows that the maximum moment (about 8.85 kN/m) is bigger than the previously computed value (6 kN/m). This difference can be explained by the conservative hypothesis considered there. The moment in the plastic hinge is conservatively estimated as M_{pl} = 6 kNm.

As discussed previously, under serviceability conditions, the columns are scarcely bent and their behavior is mostly compressive. It leads to assume that the initial values of the bending moments are zero.

For the frame of buildings B2 and B1, the first pair of plastic hinges are formed at the columns bases for a lateral load F_1 = 7.01 kN. The second pair of plastic hinges are formed at the beam-column joints for an additional lateral load F_2 = 1.86 kN. Hence, the total collapse load is $F_{Rcb} = F_1 + F_2 = 8.87$ kN. As the ductility (rotation capacity) of the hinges is not reliable (mainly because of the lack of splice length and of enough transversal reinforcement, as discussed previously), it is conservatively assumed that only the first value can be relied on: $F_{Rcb} = F_1 = 7.01$ kN.

For the frame of building B3, the two lateral loads on the first and second floors should follow the pattern F (1st floor) and $2.826F$ (2nd floor) as described by Table 6.17 (Vertical distribution of base shear for prototype buildings). The first pair of plastic hinges are formed at the lower columns bases for a lateral load F_1 = 1.627 kN. The second set of plastic hinges

are formed at the ends of the first floor beams for an additional lateral load $F_2 = 0.164$ kN. The third set of plastic hinges are formed at the ends of the second floor beams for an additional lateral load $F_3 = 0.216$ kN. Hence, the total collapse load (i.e. the base shear, applied to the first floor) is $F_{Rcb} = F_1 + F_2 + F_3 = 2.01$ kN. The value for all the frame is $2.01 + 2.826 \times 2.01 = 7.68$ kN. As the ductility (rotation capacity) of the hinges is not confiable, it is conservatively assumed that only the first value can be relied on: $F_{Rcb} = F_1 = 1.627$ kN; in terms of the base shear it corresponds to $1.627 \times 3.826 = 5.453$ kN.

Figure 6.24 shows the frames with the progressive formation of plastic hinges.

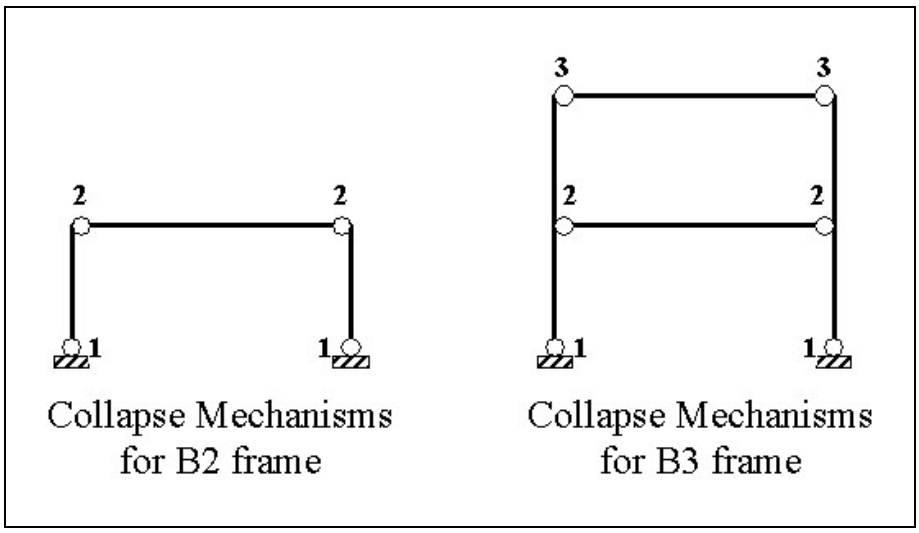

Figure 6.24: Collapse mechanisms.

For the *y* direction, the results per column are roughly the same.

The cantilever columns in the upper floor of buildings B2 and B3 are not considered as it has been concluded that their shear strengths are not reliable and, hence, such failure mode will be always more critical than the bending one.

These numerical results are described by Table 6.13.

Ductility	Buildings B1 and B2	Buildings B3
Yes	4.44	3.84
No	3.50	2.726

Table 6.13: Horizontal base shear strength per column (kN). Bending failure.

6.3.5.6 Combined failure of walls and frame

As a conservative criterion, it can be assumed that any of the two aforementioned failure mechanisms of the walls (horizontal shear or diagonal compression) can be combined with any of these two failure modes of the frames (shear or bending) to form overall collapse mechanisms of the whole building.

As shown by Figure 6.16 the shear failure of the walls is followed by shear or bending failure of the frame columns. The initial shear strength of the walls is given by the classical Mohr-Coulomb criterion [Paulay and Priestley, 1992]; after the yielding of the frame initiates, the

cohesion vanishes and only the friction term can be considered. Consequently, the maximum strength in this mode is given by the lowest of (1) the initial shear strength of the walls (but no more than the shear strength of the columns) and (2) the remaining shear strength of the walls plus the shear or bending strength of the columns.

To analyze the global failure modes for buildings B2 and B3, it is necessary to consider the distribution of the equivalent lateral seismic forces along the height of the building given by Table 6.17 (Vertical distribution of base shear for prototype buildings). The derived conclusions are given next to that Table.

The joint horizontal behavior of un-coplanar walls and frames is guaranteed by the transmission of the shear force via horizontal shear forces in the slabs. This arises mainly in two cases: cantilever cladding wall for building B3-c and vertically unaligned partition walls.

6.3.5.7 Out of plane failure of the walls

The resistance of the upper walls to this type of failure is hard to estimate but its reliability is low given the poor quality of the mortar and the lack of upper collar beams and of reliable ties (the roofs are light and weak). This failure mode is dangerous as can kill people, both inside and outside the building.

The Venezuelan code [MINDUR and FUNVISIS, 1998] states that the vertical cantilever walls are designed to withstand a significant top horizontal force.

6.3.5.8 Detachment of the roofs

The roofs, yet light, are not rigidly connected to the supporting members (walls and columns) and, hence, are in serious risk (hard to estimate) of falling. This might have fatal consequences.

6.3.5.9 Collapse of vertical propless elements

Due to the vertical component of the seismic action, some vertically unsupported elements (cantilevered walls in building B3-c and vertically discontinuous walls in buildings B2 and B3) can undergo vertical accelerations that might lead to their collapse. This risk is serious as the supporting frame and slabs are already highly demanded by the gravity loads (beyond their capacities, according the calculations in the previous subsection). Moreover, the walls carry more weight than expected, further increasing the risk.

6.3.5.10 Required tests

As discussed at the beginning of this subsection, these conclusions are not fully reliable and further tests are strongly recommended. Their main features are described next.

The approach consists of the two consecutive steps:

- To perform testing about laboratory models of existing constructions in order to confirm or to modify the theoretical conclusions drawn here and the construction and retrofit recommendations described at chapter 7.
- To implement such recommendations in similar models and to perform additional testing.

General conditions:

- All the experiments should be full scale.

- The characteristics of the constructions should be faithfully reproduced. A comprehensive survey about the actual construction techniques have to be performed, the order among the different operations is relevant (e.g. the walls are erected after the columns and the upper beam are cast).
- Even those elements without apparent relevant influence in the seismic behavior (e.g. stairs, heavy furniture and appliances, roofing elements, minor openings and grooves in the walls) should be introduced in order to reveal unexpected failure modes.

Two types of tests are needed:

- The prototype buildings B1, B2, B3-b and B3-c have to be built; if not possible, at least a span (with four columns) with the cantilever (for building B3-c). Dynamic 3-D shaking table tests should be carried out; if not possible, at least horizontal pseudo-dynamic tests at a reaction wall (it is remarkable that, since the buildings are quite flexible in the horizontal direction, not a very stiff wall is required).
- Relevant parts of the buildings (beam-column joints, column or beam stretches, wall portions, among others) can undergo cyclic testing until failure.

The sought information is the most critical mode failure and the strength and ductility for such mode.

For both types of tests the structural parameters of the materials (cement, aggregates, concrete, steel, mortar and wall and slab bricks) have to be measured.

6.3.6 Analysis by the Venezuelan code

A code-type analysis for the representative buildings B1, B2 and B3, is performed. The base shear demand for the entire building is estimated using the Venezuelan code instructions [MINDUR and FUNVISIS, 1998]. As in the previous subsection, no safety factors have been considered. The design is based in the so-called "Equivalent Static Method" assuming that the buildings have mostly plan symmetry and vertical regularity.

6.3.6.1 Design spectrum

The values of the parameters characterizing the response spectrum are given next.

- The maximum horizontal acceleration coefficient is A_0 = 0.3 g (seismic zone 5, termed "high seismic risk").
- The correction factor (accounting for the soil type) ranges in between φ = 0.7 (corresponding to spectral shape S2) for extremely soft soils, and φ = 1 for rock or very stiff soils (corresponding to spectral shape S1). In the "La Milagrosa" settlement the soil type can be classified as "stiff or dense" soil (see Subsection 5.4.3.1). Hence, φ = 0.9 and the spectral shape is S2.
- The importance factor is α = 1 as the housings belong to building group B2 (housing units).
- The period T^* initiating the descendant branch of the spectrum is T^* = 0.7 s.
- The average amplification factor is β = 2.6.
- The exponent of the descendant branch is p = 1.
- The reduction factor (because of the structural ductility) depends on the type of structure and on the design level which ranges in between level 1 (design for gravity loads only) and 3 (code-compliant earthquake-resistant design). In the "La Milagrosa" settlement, the

poor detailing of concrete members (which are characteristic of non-ductile RC structures) leads to assume the reduction factor as $R = 1$ (no ductility). This non-ductile feature of the buildings, locates them in the non-compliant side of the code; however, the conservative decision taken is to use no reduction factor for the estimation of the design spectra. When a given building does not have ductility, the earthquake demand is expected to be taken in the elastic domain; although this is very difficult to achieve in practice, it serves in this case, as assessment procedure.

The spectrum is drawn at Figure 6.25 by assuming linear interpolation between the values of $T = 0$ and $T = T^* / 4$.

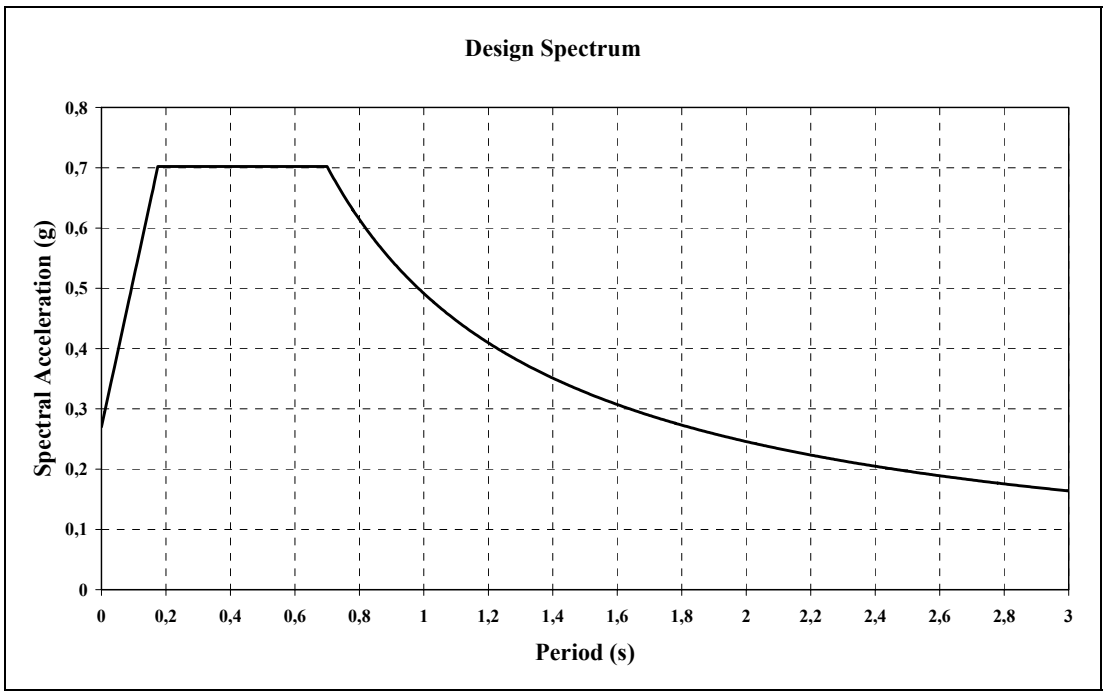

Figure 6.25: Elastic Design Spectrum in the Venezuelan Seismic Code.

6.3.6.2 Fundamental periods

The fundamental periods T of the buildings are computed from the semi-empirical expressions included in the article 9.3.2 of the Venezuelan code [MINDUR and FUNVISIS, 1998]: for type I buildings (frames) $T = C_t (h_n)^{0.75}$, where $C_t = 0.07$ for reinforced concrete and for shear wall buildings $T = 0.05 (h_n)^{0.75}$. h_n is the height of the building in m. Table 6.14 contains the results of applying such expressions to buildings B1, B2 and B3.

Number of floors	Height (h_n) (m)	Frame model	Shear wall model
1	2.8	0.151	0.108
2	5.6	0.254	0.182
3	8.4	0.345	0.246

Table 6.14: Fundamental periods *T* (s) according to the Venezuelan code.

Results from Table 6.14 show that most of the periods computed according the Venezuelan code [MINDUR and FUNVISIS, 1998] lie inside the plateau of the above design spectra. Consequently, it is useless to try to obtain more accurate estimates of such periods. For building B1, some of the computed periods lie slightly left to the plateau; however, this fact is considered irrelevant and is disregarded (both for safety and simplicity reasons).

6.3.6.3 Base shear

The weight of the prototype buildings is calculated by assuming that the masses are concentrated (lumped) at the floors. Only half of the first level walls and columns are included in the mass. According to the Venezuelan code [MINDUR and FUNVISIS, 1998] the weight includes the dead load and a percentage (25%) of the live one. The live load for the slabs is chosen as $L = 1.5$ kN/m^2, as this value (prescribed by the Venezuelan regulations) is considered quite representative of the actual figures. The live load for the light roofs (B2 and B3) is taken as zero while for the roof at B1 is $L = 1$ kN/m^2. The self-weight of the slabs is 1.832 kN/m^2. The apparent unit weight for the masonry is $\gamma = 12$ kN/m^3; the weight per square meter is 1.8 kN/m^2. The weight of the light roof is 0.4 kN/m^2.

Building B1

Walls and slab weight:

$54 \times 1.4 \times 1.8 + 1.832 \times 15 \times 6 = 300.96$ kN

Frame self-weight:

$(0.2 \times 0.2 \times 1.4 \times 8 + 0.2 \times 0.2 \times 28.4 + 0.2 \times 0.2 \times 22.4) \times 24$ kN/m^3 $= 59.52$ kN

Live load:

$0.25 \times 1 \times 15 \times 6 = 22.5$ kN

Total weight:

$300.96 + 59.52 + 22.5 = 382.98$ kN

Building B2

First floor:

$54 \times 2.80 \times 1.8$ (walls) + [$59.52 + (0.2 \times 0.2 \times 1.4 \times 8) \times 24$] (frame) + $1.832 \times 15 \times 6$ (slab) + $0.25 \times 1.5 \times 15 \times 6$ (live) = 541.06 kN

Second floor:

$54 \times 1.40 \times 1.8$ (walls) + $(0.2 \times 0.2 \times 1.4 \times 8) \times 24$ (frame) + $0.4 \times 15 \times 6$ (roof) = 182.83 kN

Total weight:

$541.06 + 182.83 = 723.89$ kN

Buildings B3-b and B3-c

First and second floors:

54 × 2.80 × 1.8 (walls) + [59.52 + (0.2 × 0.2 × 1.4 × 8) × 24] (frame) + 1.832 × 15 × 6 (slab) + 0.25 × 1.5 × 15 × 6 (live) = 541.06 kN

Third floor:

54 × 1.40 × 1.8 (walls) + (0.2 × 0.2 × 1.4 × 8) × 24 (frame) + 0.4 × 15 × 6 (roof) = 182.83 kN

Total weight:

541.06 + 541.06 + 182.83 = 1264.95 kN

These results are summarized in Table 6.15

Building type		
B1	B2	B3-b and B3-c
382.98	723.89	1264.95

Table 6.15: Total Weight of the prototype buildings (kN).

The base shear (at both directions) is given by $V_0 = \mu A_d W$, where A_d is the response spectral ordinate for the fundamental period of the considered building, W is its total weight, and μ is the greater of the values given by:

$$\mu = 1.4\left[\frac{N+9}{2N+12}\right] \qquad \text{eq. 6.14}$$

or

$$\mu = 0.80 + \frac{1}{20}\left[\frac{T}{T^*} - 1\right] \qquad \text{eq. 6.15}$$

where N is the storey number, T is the fundamental period and T^* is the period initiating the descendant branch in the response spectrum. This last equation is computed by using T for frames (Table 6.14) as they are more conservative since yield bigger results for μ. The greater values of μ are obtained from the first expression. Table 6.16 shows the results of μ and V_0.

Prototype	μ	V_0 (kN)
B1	1	1 × 0.702 × 382.98 = 268.85
B2	0.962	0.962 × 0.702 × 723.89 = 488.86
B3-b and B3-c	0.933	0.933 × 0.702 × 1264.95 = 828.50

Table 6.16: Base shear for the prototypes studied.

6.3.6.4 Lateral forces

The vertical distribution of the base shear along the height of the building is performed according to the Venezuelan seismic code [MINDUR and FUNVISIS, 1998]:

$$V_0 = F_t + \sum_{i=1}^{N} F_i \qquad \text{eq. 6.16}$$

where N is the number of floors, F_t is the lateral force at the upper level (N):

$$F_t = \left(0.06 \frac{T}{T^*} - 0.02 \right) V_0 \qquad \text{eq. 6.17}$$

the acceptable range for F_t is:

$$0.04 V_0 \le F_t \le 0.10 V_0$$

and F_i is the lateral force corresponding to level i calculated by the expression:

$$F_i = (V_0 - F_t) \frac{W_i \, h_i}{\sum_{j=1}^{N} W_j \, h_j} \qquad \text{eq. 6.18}$$

where W_j is the weight of the j^{th} storey of the building, and h_j is its height (measured from the base). This equation represents a distribution according to an assumed linear first mode shape.

Neglecting the influence of the constant term F_t in the distribution of the base shear among all the floors (as it can be at most the 10% of the base shear), the patterns for the lateral forces are:

- For building B1: F.
- For building B2: F, ξ 2 F.
- For buildings B3-b and B3-c: F, 2 F, ξ 3 F.

The value of ξ depends on the ratio between the masses of the roof and of the lower slabs. For the four considered prototype buildings: ξ = 182.83 / 541.06 = 0.3379. The lateral forces (F_i) in the prototypes are shown in Table 6.17.

Prototype Building	F_1 (kN)	F_2 (kN)	F_3 (kN)
B1	268.85	-	-
B2	291.71	197.15	-
B3-b and B3-c	206.41	412.84	209.25

Table 6.17: Vertical distribution of base shear for prototype buildings.

The torsion effects generated by accidental eccentricities between the centers of mass and of rigidity are conservatively represented by multiplying the demands (equivalent lateral forces) by 1.15. This value has been selected as an average between the forces corresponding to the outer frames or walls (increased by a factor of 1.3) and those for the center positions. The simultaneity among the seismic inputs in both directions has been represented by the combination of the seismic forces in one direction with the 30% of the forces in the orthogonal one [MINDUR and FUNVISIS, 1998]; however, this is rather irrelevant as the

elements intended to resists the forces in both directions are not the same. The resulting forces are shown in Table 6.18.

Prototype Building	F_1 (kN)	F_2 (kN)	F_3 (kN)
B1	309.18	-	-
B2	335.47	226.72	-
B3-b and B3-c	237.37	474.77	240.64

Table 6.18: Lateral seismic forces.

These lateral forces (Table 6.18) are the demands imposed for the worst expected event for the city of Mérida considered in the Venezuelan seismic code [MINDUR and FUNVISIS, 1998] and are used next to estimate the possible failure modes of the prototype buildings.

6.3.6.5 Vertical forces

The Venezuelan seismic code [MINDUR and FUNVISIS, 1998] states that in cantilevers, the effects of the vertical component of the seismic input can be represented by an increment of the gravity load obtained multiplying it by the factor

$$1 + 0.25\ \alpha\ \beta\ \phi\ A_0 = 1 + 0.25 \times 1 \times 2.6 \times 0.9 \times 0.3 = 1.1755$$

This applies to the vertically cantilevered walls (building B3-c) and to the vertically discontinuous partitioning walls. Since the demands for ordinary gravity loads exceed the resistances, it is clear that the risk of collapse even in case of moderate earthquake is high.

6.3.7 Expected failure modes

This subsection combines the calculations of the strengths of the buildings with their respective demands to derive the likely failure modes and levels of safety.

6.3.7.1 Building B1

Frames. In both directions, the shear strength is $14.63 \times 4 + 10.94 \times 4 = 102.28$ kN and the bending resistance is $4.44 \times 8 = 35.52$ kN (assuming enough rotation capacity in the hinges). Hence, the frames fail by plastic hinges formation as its strength is lower than the one of the shear failure.

Walls in *x* direction. The total lengths of the cladding and partitioning walls are 8.12 and 15 m, respectively. The shear strength of the cladding walls is $13.98 \times 8.12 = 113.32$ kN while the residual value is $1.98 \times 8.12 = 16.08$ kN. The strength to the diagonal compression mode is $3.17 \times 8.12 = 25.74$ kN; it is lower than the shear resistance of the frame. The shear strength of the partitioning walls is $12.00 \times 15 = 180.00$ kN while the residual value is 0. The resistance of the diagonal compression mode is $3.17 \times 15 = 47.55$ kN.

Walls & frames in *x* direction. The failure mode is by shear of the cladding walls and of the partitioning ones. The initial strength is $113.32 + 180 = 293.32$ kN and the residual resistance

is obtained adding the shear remaining strength of the wall to the resitance of the frames to bending: 16.08 + 35.52 = 51.60 kN; hence, this failure mode is brittle.

Walls in *y* direction. The total lengths of the cladding and partitioning walls are 28.8 and 6 m, respectively. The shear strength of the cladding walls is 15.44 × 28.8 = 444.67 kN while the residual value is 3.44 × 28.8 = 99.07 kN. The strength to the diagonal compression mode is 11.67 × 28.8 = 336.10 kN; it is bigger than the shear resistance of the frame and it should be limited to 102.28 kN. The shear strength of the partitioning walls is 12.00 × 6 = 72.00 kN while the residual value is 0. The diagonal compression mode is not possible.

Walls & frames in *y* direction. The failure would arise by shear of the columns due to the diagonal strut compression force and by shear failure of the partitioning walls. The strength is 102.28 + 72 = 174.28 kN. This failure mode is brittle -no residual strength-.

Strengths & demands. Table 6.19 shows, for each direction, the most critical failure modes, the corresponding base shear strengths and the demands.

Direction	Failure mode	Strength (kN)	Demand (kN)
x (transversal)	Shear of the cladding and partitioning walls (brittle)	293.32	309.18
y (longitudinal)	Shear of the columns and of partitioning walls (brittle)	174.28	309.18

Table 6.19: Seismic behavior of building B1.

Results from the last two columns in Table 6.19 show that the demands exceed the strengths. It might mean that the risk of collapse exists not only in case of intense earthquakes but also for less intense ones.

6.3.7.2 Building B2

For building B2, the demanding shear force is bigger than for building B1; hence, the differences among the demands and the strengths will be also bigger.

Table 6.20 shows, for each direction, the most critical failure modes, the corresponding base shear strengths and the demands.

Direction	Failure mode	Strength (kN)	Demand (kN)
x (transversal)	Shear of the cladding and partitioning walls (brittle)	293.32	562.18
y (longitudinal)	Shear of the columns and of partitioning walls (brittle)	174.28	562.18

Table 6.20: Seismic behavior of building B2.

Results from the last two columns in Table 6.20 show that the demands largely exceed the strengths. It might mean that the risk of collapse exists not only in case of intense earthquakes but also for less intense ones.

6.3.7.3 Buildings B3

For buildings B3, the demanding shear force is bigger than for buildings B1 and B2; hence, the differences among the demands and the strengths will be also bigger.

Table 6.21 shows, for each direction, the most critical failure modes, the corresponding base shear strengths and the demands.

Direction	Failure mode	Strength (kN)	Demand (kN)
x (transversal)	Shear of the cladding and partitioning walls (brittle)	293.32	952.76
y (longitudinal)	Shear of the columns and of partitioning walls (brittle)	174.28	952.76

Table 6.21: Seismic behavior of building B3.

Results from the last two columns in Table 6.21 show that the demands largely exceed the strengths. It might mean that the risk of collapse exists not only in case of intense earthquakes but also for less intense ones.

6.3.8 Observed damage in similar situations

Observing the behavior to seismic action for the building type or similar ones (non-engineered housing with RC frame and hollow clay block infill walls) in several earthquakes, information about the deficiencies of the building type and the possible damage and/or damage patterns may be identified.

For this purpose, four reconnaissance post-earthquake studies are used: two, for the building damage observed in the El Quindío, Colombia, 1999 earthquake: [Yoshimura et. al, 1999; Pujol et. al, 1999], and other two for the building damage observed in the Izmit, Turkey, 1999 earthquake: [PEER, 2000], and a USGS circular [USGS, 2000].

The maximum ground motion parameters in the studies are shown in Table 6.22; both earthquakes generated great amounts of damage in a much extended zone, reaching many cities. The reports describe the damage in the most affected locations, which for Colombia corresponds to the cities of Armenia and Pereira, and for Turkey, to the city of Izmit in the Kocaeli region.

The studies from the Colombian earthquake describe the damage generated by strong motion in a building type very similar to those in La Milagrosa (Mérida) as this typology is common for several countries in South America (as for example: Colombia, Brazil, and Venezuela), where such informal settlements are mostly located surrounding or inside important cities. The damage observations for the Turkish earthquake describes, in general, how RC frame buildings undergo severe damage for a strong earthquake, and identifies the deficiencies found with respect to the structural system and other particular characteristics.

Location	Magnitude	Depth (km)	Distance to epicenter (km)	Horizontal Acceleration (g)	Vertical Acceleration (g)
Pereira	$m_b = 5.9$	5 - 10	50	0.08 (rock) 0.3 (fills)	-
Armenia	$m_b = 5.9$	5 -10	15	0.528 (E-W) (fills) 0.584 (N-S) (fills)	0.479
Izmit	$M_W = 7.4$	15.9	8	0.171 (N-S) (rock) 0.225 (E-W) (rock)	0.146

Table 6.22: Ground motion parameters describing earthquakes.

The reports from both earthquakes describe the general damage inflicted upon the cities, the building seismic damage and the casualties generated. The descriptions are presented next separately for each country.

6.3.8.1 The El Quindío (Colombia) Earthquake

The El Quindío, January 25th 1999 earthquake affected 35 cities in the region [Pujol et. al, 1999], where the effects accounted for 1,171 people dead and 4,795 people injured, damage in buildings rose up to 21,178 dwelling and non-dwelling buildings totally collapsed, and more than 32,000 buildings partially collapsed [Yoshimura et. al, 1999]. The most affected cities by the earthquake are Armenia and Pereira, concentrating between both around 73% of all deaths, 62% of all injured and 52% of all collapsed buildings; the distribution of effects are shown in Table 6.23, where it may be seen how the city of Armenia suffered most of the disastrous effects of the earthquake.

The three following building types: Confined Masonry Wall Structures and Masonry Filled Slender RC Frame Structures (less than five stories) in [Yoshimura et. al, 1999], and Low-rise Reinforced Concrete buildings in [Pujol et. al, 1999], are equivalent to the type RC frames with hollow clay block infill walls described in this research. In both reports, the observed building types concentrated great amounts of damage (near collapse), and even though [Yoshimura et. al, 1999] establishes differences between the two building types exposed (by the different construction practices in each one of them) the described damage is similar for both. General failure mechanisms are related to the performance of the infill walls, and a lack of adequate sizing and detailing of beams, columns, and beam-column joints.

City	Effects	
	People	Buildings
Armenia	800 deaths 2,300 injured	> 10,000 collapsed buildings
Pereira	50 deaths 650 injured	925 collapsed buildings
Total	850 deaths 2,950 injured	> 10,925 collapsed buildings

Table 6.23: Effects of the earthquake in Armenia and Pereira, after [Yoshimura et. al, 1999].

The observed damage and its possible reasons in the (severely) damaged RC building structures (low-rise) are described next:

- The observed damage in the infill walls (most of them with diagonal cracks over its entire geometry, and out-of-plane failure with collapse of -parts of- or -entire- walls) leads to presume a low strength and a great fragility (brittleness) of the walls, consequently, the lateral resisting capacity of the system is rather responsibility of the RC frame (see Picture 6). This wall fragility is mainly produced by the poor connections between the masonry units within themselves and with the surrounding RC frame, where neither horizontal reinforcements of the walls nor special attachment elements from the walls to the frames were present (see Picture 7).

Picture 6: Damage in masonry wall (3rd floor), building in Pereira, Colombia [Pujol et. al, 1999].

- As a result of wall damage and partial collapse, the remaining RC columns became slender independent ones (see Picture 7), where the damage observed verified column buckling and crushing in some cases, with the consequent loss of lateral and gravity load-carrying capacity with total or partial collapse of the buildings. This effects are the result of relatively small-sized members with inadequate reinforcing practices (poor reinforcement details), such as:
    - Longitudinal reinforcement amount below the required one (usually four steel bars with diameters Φ = ½").
    - Excessive distance in between consecutive transverse reinforcement bars (stirrups), usually such distance is equal to the greater size of the cross section (see Picture 8, Left). Moreover, there are deficiencies in stirrup detailing, such as 90º hooks (instead of 135º ones).
    - Lack of adequate stirrup location in beam-column joints, with stirrup hooks at 90º.
    - Short lap splicing of longitudinal reinforcement at the column's base, with high probabilities of hinging mechanisms occurrence.
- Shear failure of columns was also observed as result of short column (captive column) configurations (see Picture 8, Right).

Picture 7: Damage to a RC a column, building in Armenia, Colombia [Yoshimura et. al, 1999].

A summary is presented next. Extensive earthquake damage to structural or non-structural elements was observed in buildings with deficiencies identified as: (1) inadequate structural design (poor member sizing and detailing, and low strength and fragility of unreinforced walls), (2) buildings extremely irregular (asymmetric plan layout, uneven elevation configuration, and abrupt changes in lateral resistance), and, (3) buildings founded on steep hillsides or soft soils (see Picture 9). It is remarkable that these three deficiencies are not exclusive each other; even some buildings may undergo the concomitance of all of them.

Picture 8: Damage in columns. Left: buckling of longitudinal reinforcement due to the lack of adequate transverse reinforcement. Right: Short-column effect. Both buildings in Armenia, Colombia. After [Pujol et. al, 1999].

Picture 9: Damage in building due to steeped soft soil. Building in Armenia, Colombia. [Yoshimura et. al, 1999].

6.3.8.2 The Izmit (Turkey) earthquake

The Izmit (Kocaeli region) earthquake occurred in August 17, 1999, it caused a death toll of 17,121 people, and 43,953 persons injured, leaving more than 250,000 people homeless. Around 77,000 housing units were heavily damaged, more than 77,000 dwellings were moderately damaged, and about 90,000 were lightly damaged. Most of the residential buildings affected in the region were RC frame with masonry infill type (more than 20,000 collapsed and many more suffered moderate to severe damage); this structural type is present not only in the multistory residential buildings (usually four to eight stories high), but also in the combined ground-floor commercial and upper levels residential buildings in the region (from three to eight stories in height). The region with heavy damage in buildings extended from the city of Yalova (50 km west of the epicenter) to the city of Düzce (100 km east of the epicenter) [USGS, 2000].

Most of the cases of building collapse showed no evidence of shear walls, thus, lateral resistance was provided by frame action exclusively. Concrete compression strength was not measured, but honeycombing was observed in similar new construction that did not collapse, this suggests poor concrete placement practices with the consequent reduction in resistance. Smooth (undeformed) reinforcing bars were widely used in longitudinal and transverse reinforcement. Most of the RC frame buildings may be characterized as having a very little ductility or no ductility at all [PEER, 2000; USGS, 2000].

The damage observed in the Residential and Commercial RC construction types in Turkey, is described and discriminated in [PEER, 2000]. The scope of this research is oriented towards a definition of performance states (Performance Based Earthquake Engineering), concentrating in the performance level of collapse prevention; thus, the buildings analyzed were those with partial or total downfall, in search for the generated collapse mechanisms. Generally, the inferred collapse mechanisms involved severe damage to the (moment-resisting frame system), mostly in the first level columns forming a soft-story collapse mechanism; this might be due to the differences in framing and infill wall geometry between the first and second stories and the use of non-ductile details in the RC frame with a poor quality construction. Damage to infill walls was also concentrated in the lower stories of the buildings, probably because of higher strength demands of the frame/infill-wall system. The lateral stiffness of the

masonry infill walls was found likely of the same order or greater than that of the moment-resisting frame; consequently, the (brittle) fracture of the first and second story masonry infill walls would have significantly overloaded the non-ductile first and second story columns. Also, some columns failed due to the impact of adjacent buildings (pounding effect).

The deficiencies observed as the principal cause of damage might be discriminated, for the frame system, by means of its components: beams, columns, and beam-column joints.

- Damage in beams. Little damage was generated to the beams, perhaps because columns were generally weaker and less ductile than them. However, where damage was observed, the detected deficiencies were: smooth rebars (allowing slippage) and beam bottom rebar inadequately anchored in the beam-column joints (allowing the slippage from the joints when the bending moments invert their signs) (see Picture 10).

Picture 10: Beam damage, longitudinal reinforcement slippage. Building in Adapazari, Turkey [PEER, 2000].

- Damage in columns. The typical verified damage states were: (1) shear and axial failure with buckling of longitudinal rebars and loss of concrete confinement (see Picture 11, Left), (2) shear failure in short-columns (captive columns) (see Picture 11, Right), and (3) large rotations at the ends of the columns with severe cracking and loss of concrete (see Picture 12). The detected deficiencies are:
  - Excessive beam strength compared to the one of columns.
  - Non-ductile detailing as unconfined lap splices (smooth rebars and excessive stirrup spacing) and lap splicing location at floor level without adequate confinement due to the transverse reinforcement.
  - Interaction between the columns and the infill masonry walls (lateral stiffness of the masonry greater or equal than that of the moment frame).
- Damage in beam-column joints. Rotation of the joints and beam slippage was observed, mainly due to the inadequate confinement of the joints (absence of transverse reinforcement in beam-column connection), the use of smooth rebars, and insufficient or inexistent beam rebar anchorage.

Picture 11: Damage in columns. Left: Shear an axial failure due to excessive stirrup spacing. Right: shear failure in captive column. Building in Adapazari, Turkey [PEER, 2000].

Picture 12: Damage to beam-column joint, large rotations at the end of the columns. Building in Adapazari, Turkey [PEER, 2000].

Summarizing, close RC building types with common deficiencies, in reports from Colombia and Turkey, exhibited similar damage patterns: the unreinforced masonry walls (mostly brittle) play a critical role in the mechanisms of lateral load resistance, which once overloaded, undergo considerable damage and leave the non-ductile RC frame the responsibility to resist the seismic action. Wall damage concentration is found in the lower levels of buildings, where the seismic stresses build-up considerably over the (non-ductile) RC frame easily overloading their members (beams, columns, and beam-column joints), and generating the described damage. Ellul and D'Ayala (2004) identify the seismic deficiencies

in buildings belonging to a certain type (low engineered masonry infilled reinforced concrete frame, which are found to be similar to those in the typology studied), and with similar response to seismic action (the above mentioned damage patters); the most relevant highlights of the research include considerations over the characteristics (construction quality and position) of the masonry infills and their role in seismic resistance, which "… *act as a first line of seismic defense in a building* …". Consequently, the interaction between RC frame and infills is determinant in the seismic performance of the buildings.

The latter accounts for deficiencies describing the inadequate lateral load resisting system (RC frame-infill walls) detected in the building types. Other defects are observed, such as: irregular framing, adjacency problems, and steep slope and/or soft soil sited buildings. In these cases the damage patterns may be identified if a predominant deficiency is detected, otherwise, the identification of a probable damage pattern becomes a complicated task.

6.3.9 Vulnerability Assessment

6.3.9.1 The Italian Vulnerability Index Method (IVIM)

The IVIM methodology considers two main construction typologies: masonry and reinforced concrete. As discussed previously, the non-engineered buildings at "La Milagrosa" have been conceived as moment-resisting reinforced-concrete frames; however, for strong seismic inputs their horizontal behavior is mainly governed by the shear strength of the infill walls and also the serviceability gravity loads are rather resisted by such walls. In spite of this unexpected performance, the buildings are considered inside the IVIM approach as reinforced concrete because the vulnerability methodology for masonry constructions is clearly inadequate to represent the properties of such constructions.

The "Second Level Assessment Form" [GNDT, 2001b] is applied to the buildings in the settlement; the modified version described in ANNEX C is used to carry out a visual inspection of the buildings complying with the type (506 buildings out of 533). A brief description of the building typology is addressed, linked to each of the eleven parameters, in order to explain the chosen qualifications.

1. **Resisting System Type and Organization**: as the walls are expected to collaborate with the frames in the resistance to lateral actions, a complete confinement of the walls in all levels must exist. In the buildings under observation this characteristic is absent in all the buildings with two or more levels, as the upper walls are not topped by beams joining the columns (absence of collar-beam), and do not produce enough confinement. The roofing structure (usually metallic) is supported directly over the walls and columns, with no special detailing in the superior border of the walls. In the case of one level building with slab roofing, confinement is verified, but none of the buildings comply with instruction *iv* (minimum vertical separation between the beam top and the wall top) in qualifications A or B. All the buildings in the survey are qualified as "**C**".
2. **Resisting System Quality**: the structure is a reinforced concrete frame but the resisting system (to lateral actions) involves also hollow clay tile infill walls. The RC frame, presents almost identical column-beam sections of an average dimension of 20 cm by 20 cm (400 cm^2), where the detailing of reinforcing bars is poor, not only in the diameters used (1/2" or 3/8" for longitudinal and 1/4" or 3/8" for transverse reinforcing steel) but also in the excessive stirrup separation (equal to the section total depth) and in the inadequate tie anchorage (90º instead of the 135º recommended by

seismic codes). The poor detailing in beams and columns does not guarantee continuity in the connection and may have, consequently a poor seismic performance. Also, lap splicing in longitudinal reinforcement for the columns in consecutive levels is produced at the bottom of the columns (as the building type usually grows progressively in the vertical direction according to the increasing needs of the occupants) instead of at the mid-height of the column as recommended in seismic codes (see Picture 13). These characteristics are typical of non-ductile RC frames. With respect to the walls, field observations show deficiencies in the quality of the materials (broken bricks, low quality mortar which is easily scratched) and also a low quality workmanship (see Picture 14). It is important to remark that the observations are performed not only in the "La Milagrosa" Barrio, but also in other similar settlements in Mérida, where some buildings were in the construction process and the details could be easily observed. As the methodology relies on the qualification in the expertise of the surveyor, the decision is to qualify this parameter as "**C**" for all buildings in the survey, based in the observed deficiencies.

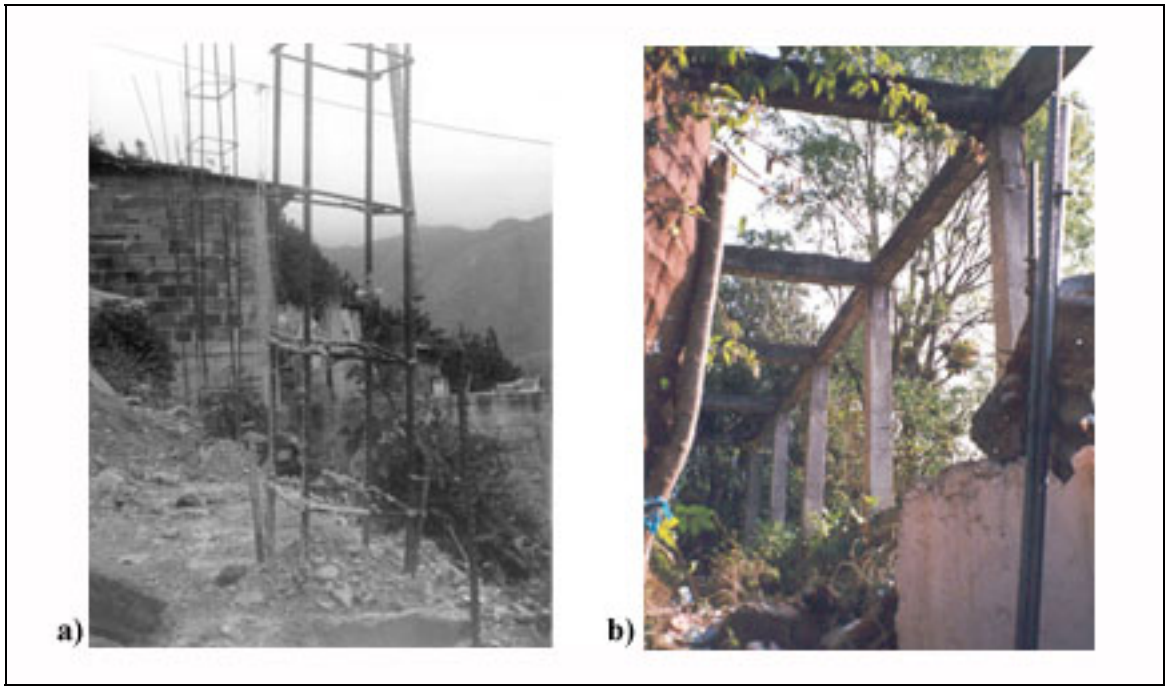

Picture 13: Resisting system quality details. a) Lap splicing in column base is observed, and the excessive spacing of stirrups. b) Structure for the first phase of growth, showing identical dimensions for columns and beams, also the excessive stirrup spacing is noticed and an insufficient concrete covering of the reinforcing steel (this structure is in an abandoned state due to its construction in forbidden lands and a consequent restriction to occupation).

Picture 14: Alley in the Cristo Rey Sector showing four houses, the low quality of workmanship and materials in the walls and the absence of collar beams is observed.

3. **Conventional Resistance**: For the "La Milagrosa" buildings a deeper study to calculate the shear demands and strengths is performed in subsection 6.3.6 according to Venezuelan seismic design code [Mindur and Funvisis 1998]. The values of coefficient α are given at Table 6.19, Table 6.20 and Table 6.21 for buildings B1, B2 and B3, respectively.

Building	Direction	Coefficient α
B1	*x*	0.68
B1	*y*	0.83
B2	*x*	0.37
B2	*y*	0.46
B3	*x*	0.22
B3	*y*	0.27

Table 6.24: Shear strength-demand ratio.

Values from Table 6.24 show that building B1 can be qualified as B while buildings B2 and B3 have to be clearly scored as C.

4. **Location and Soil Condition**: this parameter distribution responds to the slope of the terrain in the building site, in the three categorizations established in the 2nd level assessment form. The (greater) percentage of site slopes lower than 15% is around 63%, which are qualified as "A", followed by slopes bigger than 15% and lower or equal than 30%, representing around 26% of all the sites and qualified as "B"; and finally, slopes greater than 30% with a 10% of total building's site being qualified as "C".
5. **Diaphragms**: this parameter depends on the characteristics of the slabs and the roofing type. Buildings with two or more levels have slabs built with "I" shaped hot

rolled (secondary) steel beams with hollow clay tiles, supported directly by RC (main) beams (see Picture 15, Picture 16 and Picture 17). The support conditions in such diaphragms are poor, where in some places no apparent connections other than the gravitational, seem to be operating. The steel beams are usually IPN 80 mm in height and not all of them are connected to the RC main beams. The (hollow) clay tiles are normally 60 or 80 cm in length, 20 cm wide, and 6 cm in height. Over this arrangement, a steel wire mesh (usually 15 by 15 cm) and a cement mortar (4 cm in height) constitute the floor base. Respect to the roofing, three types of roofs are observed (in one level and in two or more levels buildings):

a. Metal sheeting supported over an array of "I" shaped steel beams or rectangular steel beams, resting directly over walls and columns.
b. Slab (as the type described previously) supported over the RC beams (one or two level buildings, see Picture 16).
c. Tile supported over wooden deck with "I" shaped steel beams as main structure, directly supported over walls and columns (two or more levels).

In spite three types of roofing are observed, none of them is adequately connected to the frame structure. In buildings with one level, the roofing system does not guarantee the lateral load transmission to and between the vertical resisting elements, being the worst case the horizontal slab, due to its greater weigh respect to the other two types of roof. Hence, in two or more levels buildings, the slabs do not configure efficient diaphragms. , The roofs do not guarantee the lateral load transmission to and between the vertical resisting elements, due to the inadequate (poor) connections. The qualification for all the assessed buildings is "**C**".

6. **Plan Configuration**: in the assessment of the buildings, plan configurations are considered as regular or irregular:
    a. Regular plan configuration: rectangular or quasi-rectangular in plan shape, where structural axis are at regular distances ranging from 4.0 to 6.0 m, with a simple bay in the shortest direction and several bays (from two to five) in the longest one; this implies a regular column distribution in the plan. The plan width/length proportions of the buildings range from 1.0 to 0.12. Based in the observations, three qualifications, depending only on the width/length ratio, may be established for these (regular) buildings:
        i. The ratio width/length is greater than 0.4, with an "A" qualification. This category accounts for 227 buildings, representing a 44.86%.
        ii. The ratio width/length is lower or equal than 0.4 and greater or equal than 0.2, with a "B" qualification. The number of buildings with this category is 182, the 35.97%.
        iii. The ratio width/length is lower than 0.2, with a "C" qualification. The number of these buildings is reduced, only 10 representing the 2% of all the buildings.
    b. Irregular plan configuration: compounds and complex plan shapes, such as "T", "C", or "L", as well as other irregular shapes. The assessments of these buildings through the instructions in the form do not allow establishing a qualification other than "C". These groups sum a total of 87 buildings, which accounts for the 17.2% of all the buildings.

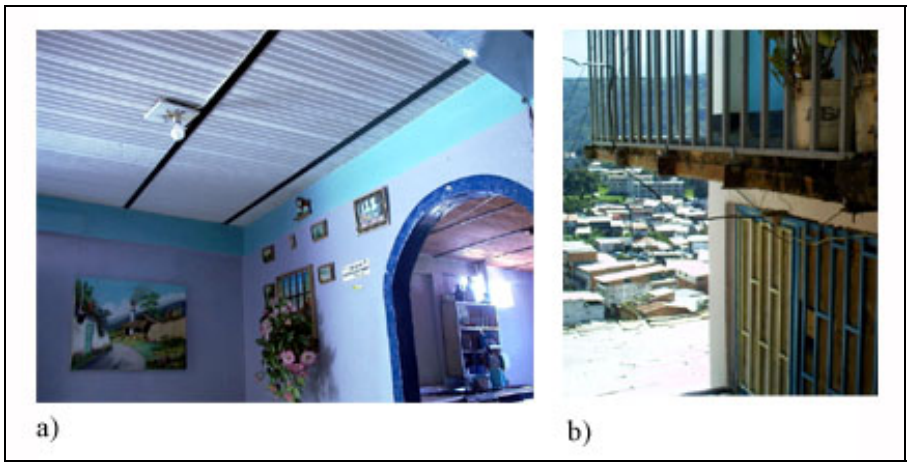

Picture 15: Typical slabs in the building type assessed. a) Inside a two level building, the "I" shaped steel girders slide into the hollow clay tiles. b) Detail of the slab in a balcony perimeter.

7. **Vertical Configuration**: *T/H* (*T* being the height of any top prominence and *H* being the total height of the building) ratio is observed to be inside the limits of "A" qualification for almost all the buildings. However, as the resisting system is not completely regular (lower number of columns in consecutive levels), a great quantity of the buildings are qualified as "B" (440 buildings, representing 87%). The regularity in frame and wall throughout all the building height is observed in 62 buildings, representing the 12.25% of all the buildings, qualified as "A". Finally only four buildings (0.75%) may be qualified as "C" because of the significant variation of the resisting system between two consecutive levels.

Picture 16: Roof Types in Barrios. a) Slab roof in one or more levels, and metal sheeting roof in two levels. b) Tile roofing supported over wooden deck and "I" shaped steel beams.

8. **Connectivity between elements**: although the connectivity observed presents adequate ratios (as connections are mostly produced with the characteristics of "A" qualification respect to the, γ_1, γ_2, and γ_3 ratios) the least dimension of the columns is lower than 25 cm, but with an average dimension of 20 cm, not qualifying neither as "A" nor as "C", but as "**B**". This qualification is used for all the assessed buildings.
9. **Low Ductility Structural Members**: for buildings in flat terrain, no low-ductility elements are observed; the stairways are mostly produced in steel (as it is cheaper and

simpler to built than the RC stairways). Conversely, low-ductility elements appear in the buildings over high slope sites (see Picture 17). The distribution of this parameter in the buildings observed accounts for 394 buildings (77.87%) qualified as "A", 78 buildings (15.42%) with "B" qualification, and 34 buildings (6.71%) qualified as "C". No short column configurations are detected in the buildings surveyed.

10. **Non-structural Elements**: mostly external elements such as parapets delimiting balconies or parapets in the perimeter of the upper level's slab are observed; the connections between these elements and the structure are poor; only mortar is used to connect the parapets. However, almost a fifth part of the buildings (19.76%, 100 buildings) is found to qualify as "A"; and a small percentage qualifies as "B" (0.6%, 3 buildings). The rest of the buildings present characteristics as the described previously, accounting for a 79.64% of all the buildings (404 buildings).
11. **Preservation State**: although the constructions evaluated present precarious building detailing and low quality of workmanship, no damages (such as fissures in elements and/or foundation settlements) are observed in the assessed structures. Qualification for all evaluated buildings is assumed as "**A**".

Results from the survey, expressed as the percentages of the eleven parameters respect to the total number of buildings assessed (506 buildings in total) is shown in Figure 6.26, where the different qualifications are described as: *KiA* for "A" qualification, *KiB*, for "B" qualification, and *KiC* for "C" qualification of parameters.

Picture 17: High-slope site for housing unit, structural members are observed in different lengths, with low-ductility elements in the middle structural axis, see columns over the foundations.

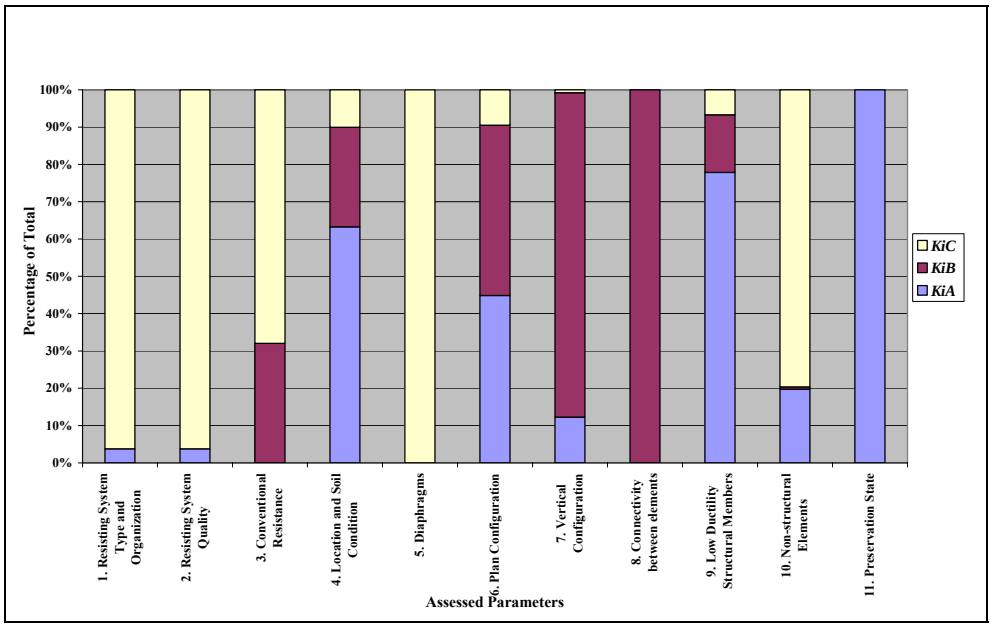

Figure 6.26: Vulnerability Parameters distribution (by percentages) in the buildings assessed.

The quantification of the vulnerability index I_v for each of the buildings in the survey is performed, by means of the expression:

$$I_v = 1 + \frac{\sum_{i=1}^{11} K_i W_i}{\sum_{i=1}^{11} K_{iC} W_i} \qquad \text{eq. 6.19}$$

Where, K_i is the qualification (quantified as shown in Table 3.2) of the parameter and W_i is its weigh.

The vulnerability indices obtained through this operation range from 0.42 to 0.76. The distribution for the index values are shown in Table 6.25 and Figure 6.27. The most common index is 0.61 with about 25% of all buildings in the survey, and around 63% of the buildings have indices within the values I_v = 0.58 and I_v = 0.64. The superior index values I_v = 0.73 and I_v = 0.76, account for around a 1.5% of the buildings in the survey.

Order	Vulnerability Index	Nº of Buildings	Percentage of Total
1	0.42	7	1.38
2	0.45	28	5.53
3	0.48	19	3.75
4	0.52	21	4.15
5	0.55	44	8.7
6	0.58	115	22.73
7	0.61	128	25.3
8	0.64	77	15.22
9	0.67	32	6.32
10	0.7	27	5.34
11	0.73	7	1.38
12	0.76	1	0.2
	Total	**506 Buildings**	**100 %**

Table 6.25: Vulnerability Indices distribution in survey.

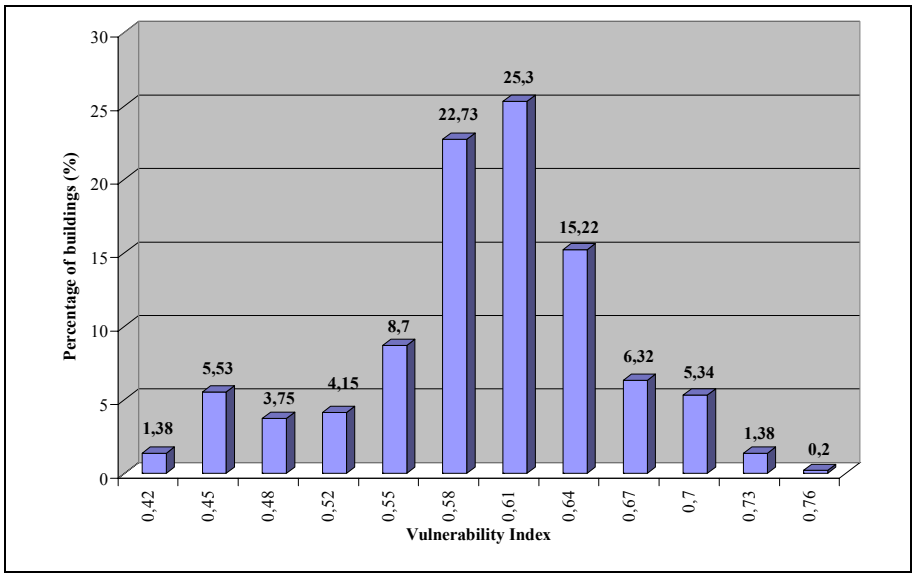

Figure 6.27: Vulnerability Index distribution

The index distribution by sectors (Figure 6.28) shows the number of buildings with a certain vulnerability index for each of the four different sectors. The most common indices by sectors are: $I_v = 0.61$ for the Miranda and Los Molinos sectors, $I_v = 0.58$ for the La Milagrosa sector, and $I_v = 0.64$ for the Cristo Rey sector. Indices concentrate in the range from $I_v = 0.58$ to $I_v = 0.64$, (around a 63% of the total buildings). Vulnerability index $I_v = 0.67$ is observed in the Cristo Rey and La Milagrosa sectors accounting for about 6%, and indices greater than 0.67 are observed mostly in the Cristo Rey sector, accounting for more than a 1% of all the buildings in the survey, the remaining 23.5% of the buildings account for the lower values ranging from 0.42 to 0.55.

Results of the vulnerability index distribution are shown in Map 6.13, where the most relevant characteristic is the greater concentration of higher indices in the Cristo Rey Sector (darker buildings at the northwestern side of the map), which is settled over high slope terrain (30% to 60% slopes). This representation shows again, how the higher contents of the highest indices appear in this sector.

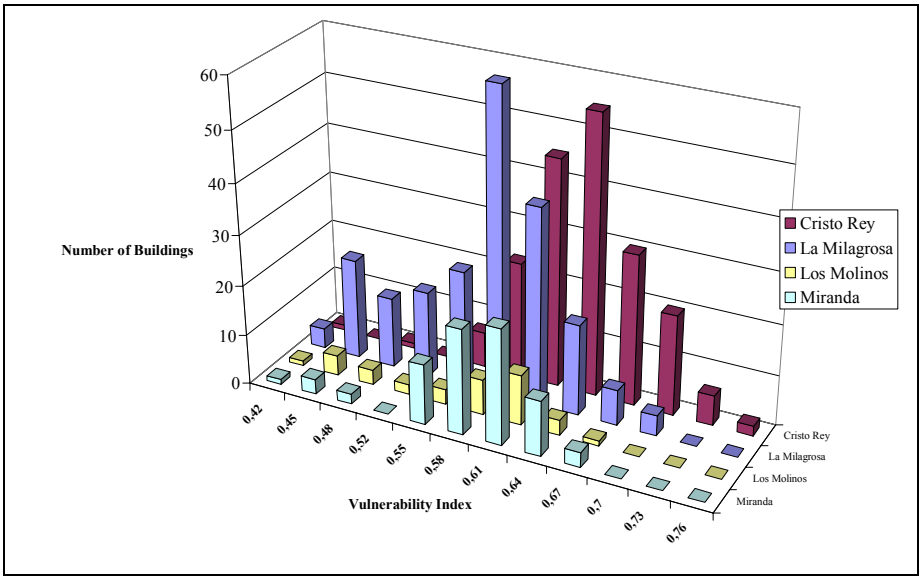

Figure 6.28: Vulnerability Index distribution by sectors (in buildings number).

The Italian Vulnerability Index Method (IVIM) has shown utility in building classification, establishing 12 categories for the buildings in La Milagrosa, starting at index value $I_V = 0.42$ (least vulnerable buildings of the group) and ending at value $I_V = 0.76$ (most vulnerable buildings of the group), with eleven steps at a change rate of $\Delta I_V = 0.03$ representing the eleven intermediate classes between the extreme values. This classification may be used to assign vulnerability indices through the LM1 method, where this approach, apart from being applicable for building classification, offers the possibility to forecast damage by means of the Probability Damage Matrices for each of the vulnerability indexes considered in classification.

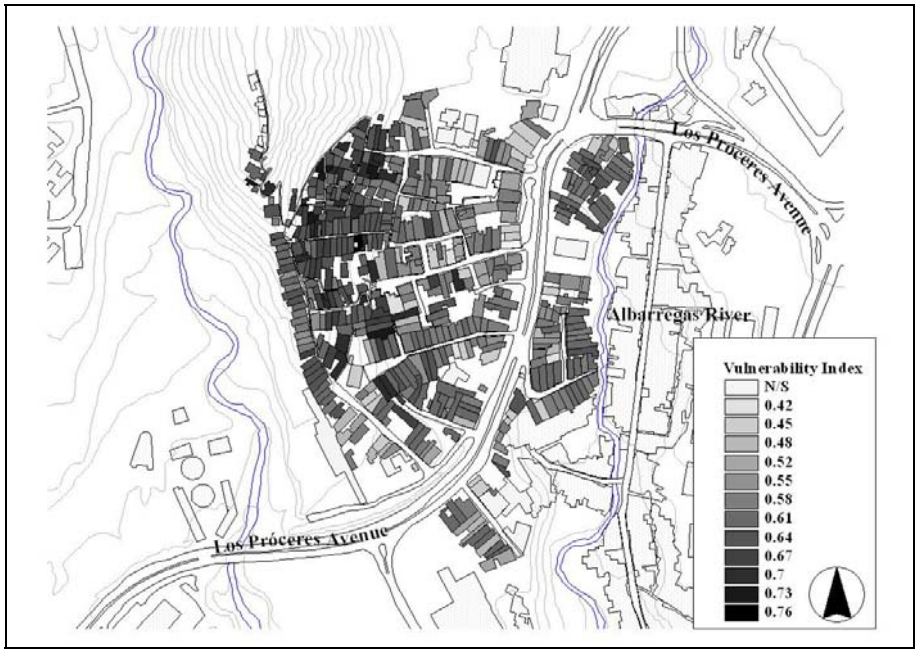

Map 6.13: Vulnerability Index distribution in La Milagrosa Barrio (N/S: Not studied).

The vulnerability index methodology (IVIM) exposed offers a very complete assessment suite for three out of the four major deficiencies observed in the reports (see Subsection 6.3.8) (inadequate structural design, irregular framing systems, and steep slope and/or soft soil sited buildings), not taking into account the adjacency problems. This lack may be due to particular characteristics of building site in Italian settlements, as the adjacency problems have proven important, and sometimes determinant, in seismic damage.

The parameters list does not account for the pounding effect in close-neighboring buildings. A new parameter is then proposed at Table 6.26.

Number	Parameter	Qualification K_i			Weight W_i
		A	*B*	*C*	
1	Resisting System Type and Organization	0	1	2	4
2	Resisting System Quality	0	1	2	1
3	Conventional Resistance	-1	0	1	1
4	Location and Soil Condition	0	1	2	1
5	Diaphragms	0	1	2	1
6	Plan Configuration	0	1	2	1
7	Vertical Configuration	0	1	3	2
8	Connectivity between elements	0	1	2	1
9	Low Ductility Structural Members	0	1	2	1
10	Non-structural Elements	0	1	2	1
11	Preservation State	0	1	2	1
12	Adjacency	0	1	3	2

Table 6.26: IVIM parameters with the proposed 12th parameter (adjacency).

The twelfth parameter in Table 6.26 is qualified with 0 (A, no added vulnerability), 1 (B, low increment of vulnerability) and 3 (C, highest vulnerability growth). Qualification C is scored with 3 because the increment of vulnerability compared to B is greater than the one of B with respect to A. The weighting coefficient is selected as $W_{12} = 2$ since the risk of collapse due to pounding is considered serious. A draft qualification for this parameter is proposed in the following.

Adjacency. This parameter accounts for the risk of pounding due to the vicinity of adjacent buildings. The qualification is described next following the same indicators (from A -not vulnerable- to C -most vulnerable-).

A. The distance to the nearby building is enough to prevent hammering during strong inputs.
B. There are adjacent buildings with the same number of floors than the considered one and whose slabs are roughly at the same level.
C. There are adjacent buildings whose slabs are not at the same level than those of the considered one or whose number of floors is different.

The expression for the vulnerability index is modified as it keeps ranging in between 0 and 1:

$$I_V = 1 + \frac{\sum_{i=1}^{12} K_i W_i}{\sum_{i=1}^{12} K_{iC} W_i} \qquad \text{eq. 6.20}$$

The distribution of the indices in the Barrio is shown in Figure 6.29, where the categories are now 18 instead of the 12 without considering the adjacency parameter. The result of including this parameter is more resolution in the vulnerability indices, as it may be seen in Map 6.14, where the highest indexes concentrate where adjacency problems are expected to be most probable.

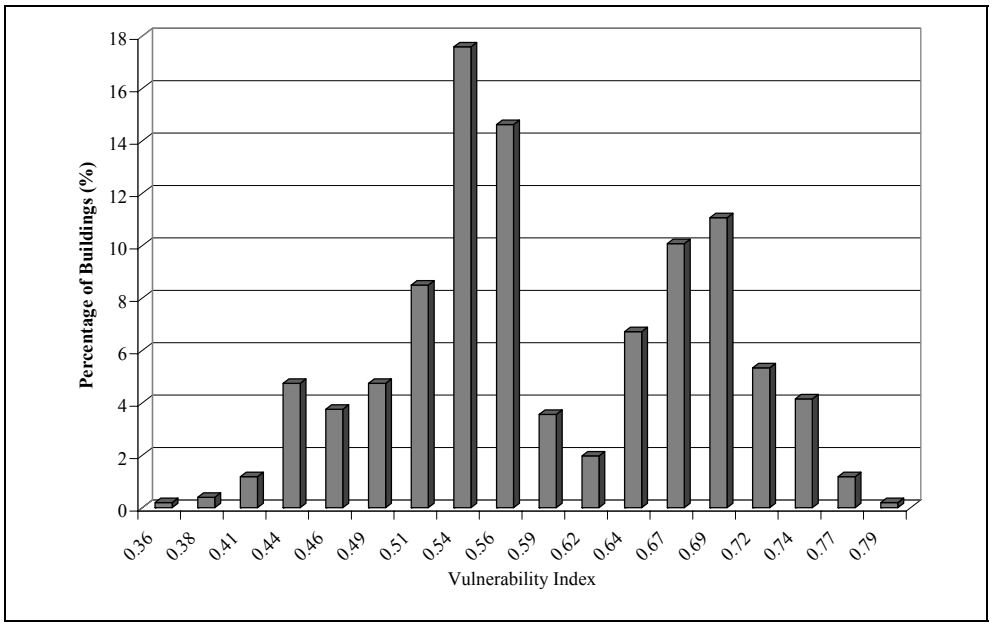

Figure 6.29: New vulnerability index distribution considering the adjacency parameter.

The use of this 12th parameter requires a calibration with observed damage (as performed originally in the IVIM method), or by means of numerical modeling (as performed by [Yépez, 1996]). In this research, the resulting vulnerability indices including the adjacency parameter are used only to compare the resolution with the original method, as the values for the qualifications, as well as the weight of the parameter have been considered based in the opinion of the author.

Map 6.14: New vulnerability index distribution in La Milagrosa Barrio, considering the adjacency parameter (N/S: Not studied).

6.3.9.2 The LM1 Methodology

With the IVIM classification, a starting point for the application of the LM1 methodology is already available, as the classification offers a detailed description of the different seismic deficiencies of the buildings through the vulnerability indices. Following the applicability

protocol of the LM1 methodology, a Typological Vulnerability Index (V_I*) must be sought within the Building Typology Matrix (Table 6.3), and then adequated (Equation 6.1) through the consideration of the seismic behavior modifiers (Table 3.9) and the Regional Vulnerability Factor. In the study case, no regional vulnerability factor is available, thus, it is not considered for the adequation of the typological vulnerability index.

The building typology studied in La Milagrosa corresponds to a reinforced concrete moment resisting frame typology, without seismic features, which corresponds to the RC1 typology in the BTM. The typological vulnerability index chosen is V_I* = 0.442, which is adequated by means of the seismic behavior modifiers in Table 3.9, to obtain the two extreme values in the IVIM classification (least and most vulnerable buildings of the category). The lower value for the index is considered as a pre-code building with regular configuration in plan and elevation, one level in height, mostly aggregated (buildings very close one to another, i.e. very small building-adjacency distances), and with isolated footings as foundations. The upper value of the index is considered as a pre-code building with irregular plan and elevation configuration, three levels in height, mostly aggregated, with isolated footings as foundations and founded over a pronounced slope. The extreme values for the vulnerability indices in the survey are shown in Table 6.27, displaying both the existing IVIM classification and the proposed LM1 one with the V_I representative values considering the behavior modifiers.

		V_I representative values				
	IVIM Class	$V^{min}_{I,BTM}$	$V^{-}_{I,BTM}$	$V^{*}_{I,BTM}$	$V^{+}_{I,BTM}$	$V^{max}_{I,BTM}$
Lower value	**0.42**	0.18	0.247	**0.642**	1	1.22
Upper value	**0.76**	0.34	0.407	**0.802**	1.16	1.38

Table 6.27: Lower and Upper values of LM1 vulnerability index, in the La Milagrosa survey.

The IVIM classification shows, between the extreme values (lower and upper values of the index), a uniform change from one index value to the next (in 11 steps with step value $\Delta I_V = 0.03$), the same behavior is proposed for the application of the LM1 classification, based in the two extreme values obtained. Thus, in order to estimate the rest of the indices in the survey, the difference between the upper and lower value is calculated and distributed uniformly in a 12 category classification with a constant step between the increasing values. In this fashion, the LM1 indices for the La Milagrosa Barrio survey are those shown in Table 6.28, with the corresponding equivalence to the IVIM classification.

The mean damage grade expression (equation 3.14), is used for estimating the mean semi-empirical vulnerability functions for each of the vulnerability indices in the classification, considering macroseismic intensities from I = VI to I = XII (Figure 6.30), where the regular spacing of the different curves denote the regular steps between the index values. These semi-empirical functions allow estimating the probable damage distribution according to the La Milagrosa survey, so to relate this damage with the IVIM classification and to obtain a preliminary distribution of damage in the settlement.

Category	IVIM Indices	V_I representative values				
		$V_{I,BTM}^{min}$	$V_{I,BTM}^{-}$	$V_{I,BTM}^{*}$	$V_{I,BTM}^{+}$	$V_{I,BTM}^{max}$
1	**0.42**	0.18	0.247	**0.642**	1	1.22
2	**0.45**	0.19	0.26	**0.656**	1.01	1.23
3	**0.48**	0.2	0.27	**0.671**	1.02	1.24
4	**0.52**	0.21	0.28	**0.685**	1.03	1.25
5	**0.55**	0.22	0.29	**0.7**	1.04	1.26
6	**0.58**	0.23	0.3	**0.714**	1.05	1.27
7	**0.61**	0.24	0.31	**0.729**	1.06	1.28
8	**0.64**	0.25	0.32	**0.743**	1.07	1.29
9	**0.67**	0.26	0.33	**0.758**	1.08	1.3
10	**0.7**	0.27	0.34	**0.772**	1.09	1.31
11	**0.73**	0.28	0.35	**0.786**	1.1	1.32
12	**0.76**	0.29	0.36	**0.802**	1.11	1.33

Table 6.28: Values for the LM1 vulnerability index, in the La Milagrosa survey.

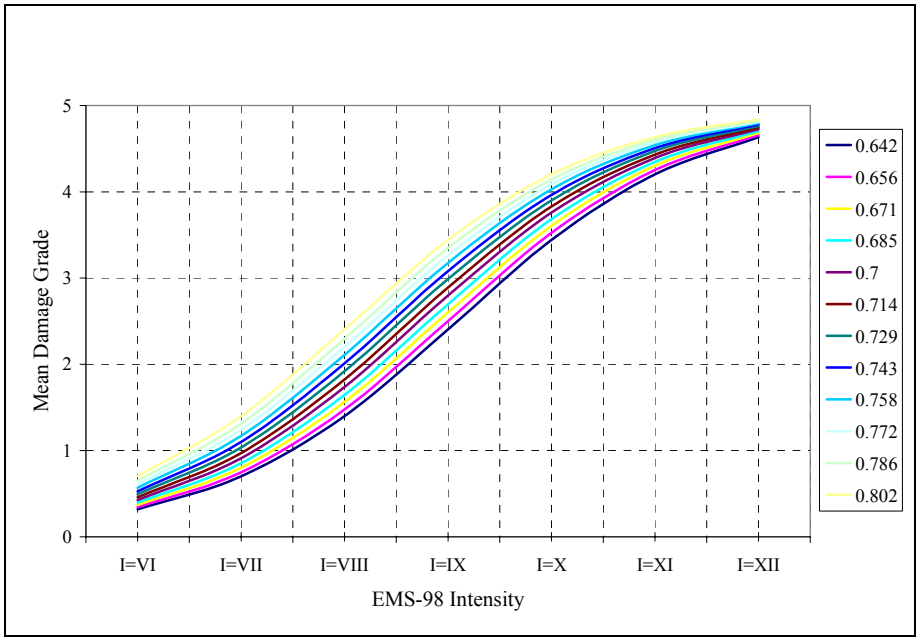

Figure 6.30: Mean semi-empirical vulnerability functions for LM1 classification.

6.3.9.3 Expected damage in the La Milagrosa Barrio.

Through the application of the LM1 approach to the studied building typology (non-engineered RC frame with hollow clay block infill walls) in the La Milagrosa Barrio, the damage forecast for the expected scenario events is performed, based in the Damage Probability Matrices for the 12 vulnerability classes considered (see Table 6.28). The procedure is very similar to the one performed in the damage forecast for the city of Mérida, but applying the DPM's to building groups belonging to the corresponding vulnerability classes considered inside the survey.

The results of the damage distribution in the La Milagrosa Barrio are shown in Figure 6.31 (by percentage of buildings with respect to the total number of buildings belonging to the

typology), for the four considered scenario events. The damage classification is the one of the EMS-98 (Table 2.1), including Damage Grade 0 (no damage). In the distribution, the mean damage grades for each of the EMS intensities (see Figure 6.30) are clearly identified. For I = VI the predominating damage grade is 0, with a 72% of all the buildings belonging to the typology, for I = VII the greater percentage of buildings (40%) undergoes Damage Grade 1, for I = VIII a 35% of the buildings suffer Damage Grade 2, and finally, for I = IX, Damage Grade 3 concentrates a 35% of the buildings in that typology. Important damage appears at intensity I = VIII, where the superior damage grades 4 (very heavy damage) and 5 (destruction) accumulate a 7% of the buildings, Damage Grade 3 (substantial to heavy damage) accounts for a 21% of the buildings belonging to the typology. In the last scenario event, I = IX, the superior Damage Grade 4 concentrates around a 25% of the buildings, while Damage Grade 5 (destruction) accounts for a 5% of the buildings.

A discrimination of the damage distribution for the twelve vulnerability classes for each of the considered scenario events is shown in Figure 6.32. This figure has a double purpose: the description of the percentage of buildings belonging to a vulnerability class (similar to that in Figure 6.27), and the percentage of buildings from that vulnerability class undergoing a certain damage grade, all respect to the total number of buildings belonging to the typology.

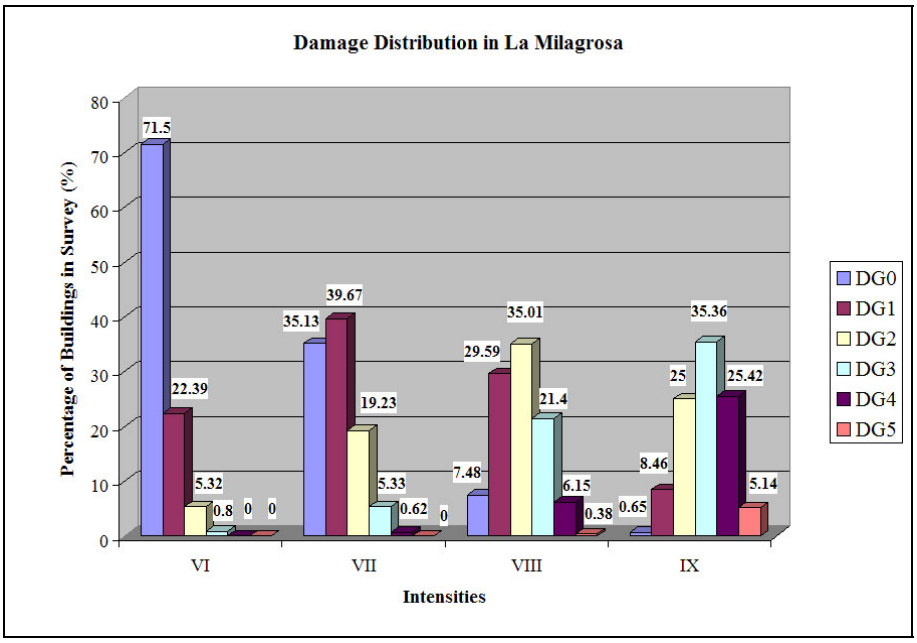

Figure 6.31: Damage distribution in the La Milagrosa Barrio.

For the case of scenario event I = VI, the damage grade 0 (no damage) is predominant in this distribution with more than a half of the buildings belonging to the vulnerability class, damage grade 1 represents around a fourth part of the undamaged buildings. The damage grade 2 occur in a small percentage of the buildings, and damage grade 3 only occurs in vulnerability classes 0.714, 0.729 and 0.743 which are the most common in the distribution. The superior damage grades 4 and 5 are not present in the distribution.

The distribution for I = VII shows an incremental evolution of the damage grades 1, 2, 3, with the occurrence of damage grade 4 (in small percentages) in the most populated vulnerability classes and damage grade 5 does not occur at this intensity. The damaged buildings (from damage grade 1 to damage grade 4) represent more than half of the buildings belonging to all the vulnerability classes.

Important damage is observed at I = VIII where the damaged buildings (considering the five grades of damage) account for around a 90% of the buildings in the vulnerability classes, where the evolution of the damage grades 2 and 3 show an increment in the percentage of buildings equal or greater to those undergoing damage grade 1. The superior damage grade 4 occurs in ten out of the twelve vulnerability classes being absent in the two least common vulnerability classes: 0.642 and 0.802. Damage grade 5 is not present in the distribution.

In the last scenario event considered (I = IX), damaged buildings (with damage grades from 1 to 5) account for a 100% of the buildings in ten out of the twelve vulnerability classes. The superior damage grades 3 and 4 account for more than half of the buildings belonging to all the vulnerability classes, and damage grade 5 occurs in eight of them (from 0.685 to 0.786); this damage grade is greater in percentage (around a 0.5%) in the most common vulnerability classes in the distribution (class 0.714, class 0.729 and class 0.743).

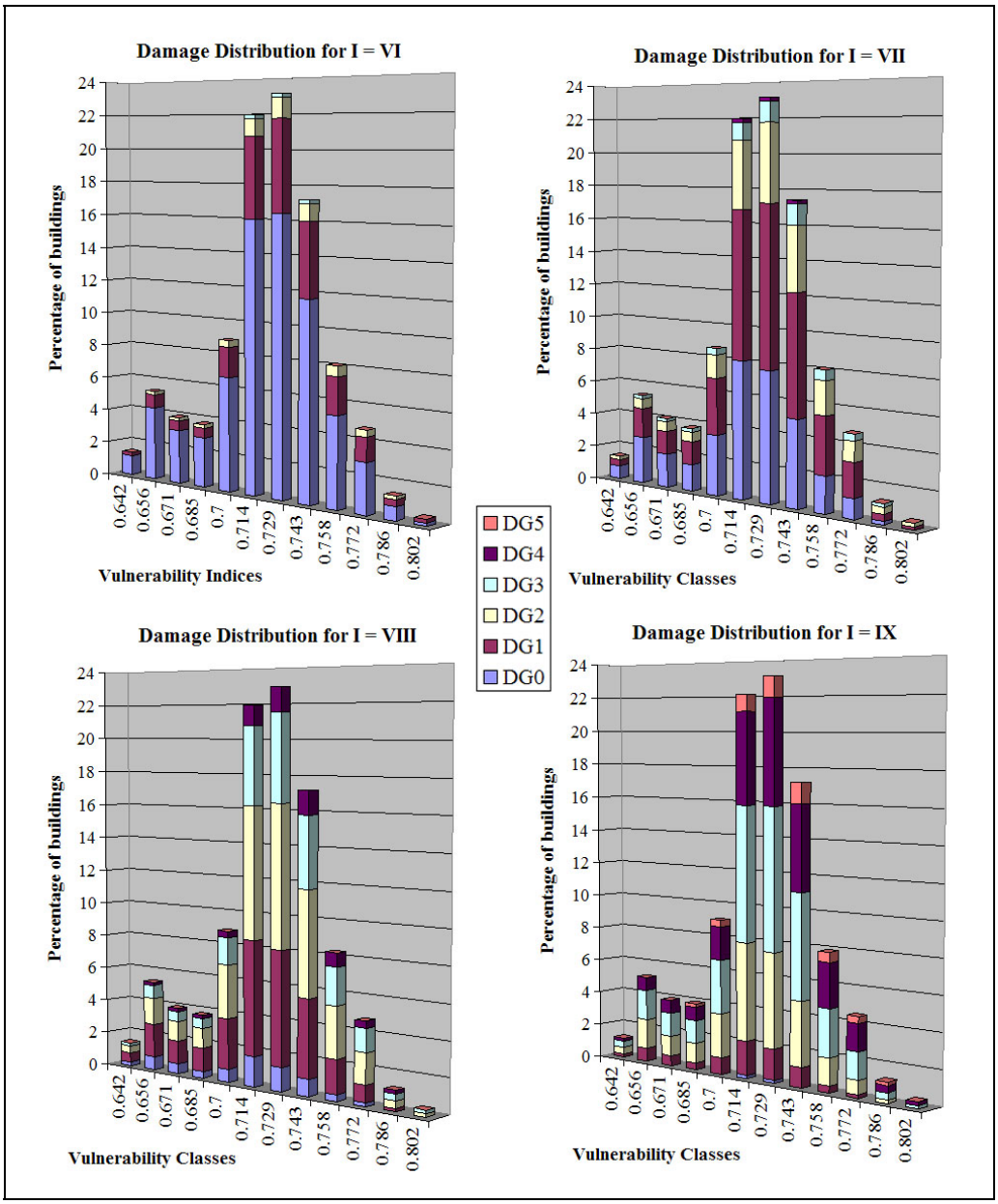

Figure 6.32: Damage distribution by vulnerability classes.

The mean semi-empirical functions used to forecast damage in the La Milagrosa Barrio may be represented also as a unique curve corresponding to a single vulnerability index, which may be estimated by the use of Equation 6.1, where the result yields a vulnerability index V_I = 0.69, which is the value found as representative of the vulnerability class for the Non-Engineered Reinforced Concrete Buildings typology (NENG-RC) studied in this dissertation. The mean semi-empirical vulnerability function for this typology is shown in Figure 6.33, and the Damage Probability Matrix in Table 6.29.

The damage representation may be directly obtained in terms of fragility curves for each of the macroseismic intensities, where the curves represent the probability that the expected damage of the building will reach or exceed a fixed damage grade during the seismic event [Giovinazzi and Lagomarsino, 2004]. The expression to obtain such curves is:

$$P(D \geq D_k) = \sum_{j=k}^{5} p_j \qquad \text{eq. 6.21}$$

where $P(D \geq D_k)$ is the probability of reaching or exceeding certain damage grade D_k, and p_j is the discrete beta density probability (equation 3.10) associated with damage grade j (for j = 0, 1, 2, 3, 4, 5). The obtained fragility curves for the vulnerability class VI = 0.69 representing the non-engineered reinforced concrete buildings typology are shown in Figure 6.34.

Intensity	DG0	DG1	DG2	DG3	DG4	DG5
I=V	0.924	0.066	0.01	0	0	0
I=VI	0.772	0.185	0.038	0.005	0	0
I=VII	0.429	0.38	0.152	0.035	0.003	0
I=VIII	0.105	0.344	0.339	0.172	0.039	0.001
I=IX	0.01	0.114	0.291	0.35	0.205	0.03
I=X	0	0.015	0.096	0.268	0.406	0.215
I=XI	0	0.001	0.016	0.088	0.301	0.595
I=XII	0	0	0.002	0.021	0.121	0.856

Table 6.29: Damage Probability Matrix for V_I = 0.69 (NENG-RC).

In spite the vulnerability function for the studied typology is not expressed as an IVIM function (of the kind shown in Figure 3.6), the parameters in the Mean Semi-empirical vulnerability function, the DPM, and the Fragility Curves may be used for damage forecast of the building typology, with an open possibility of future calibrations if additional data on the building typology may be obtained.

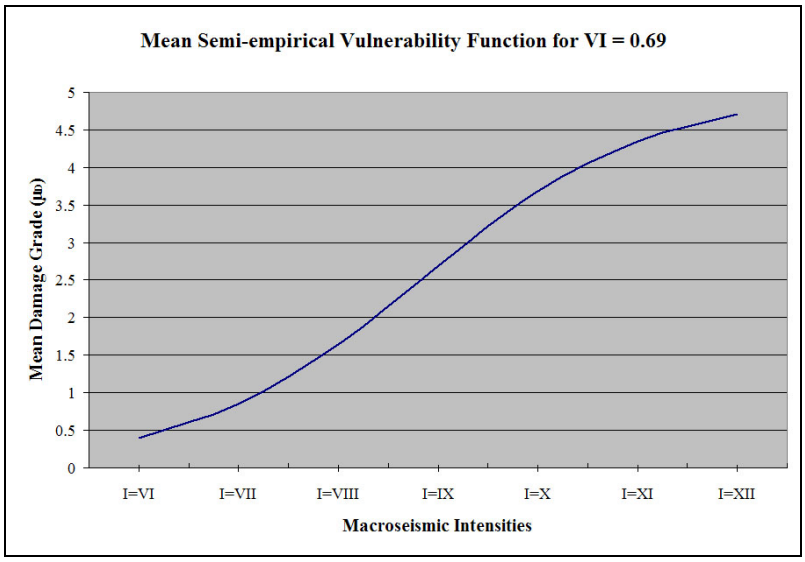

Figure 6.33: Mean Semi-empirical vulnerability function for V_I = 0.69 (NENG-RC typology).

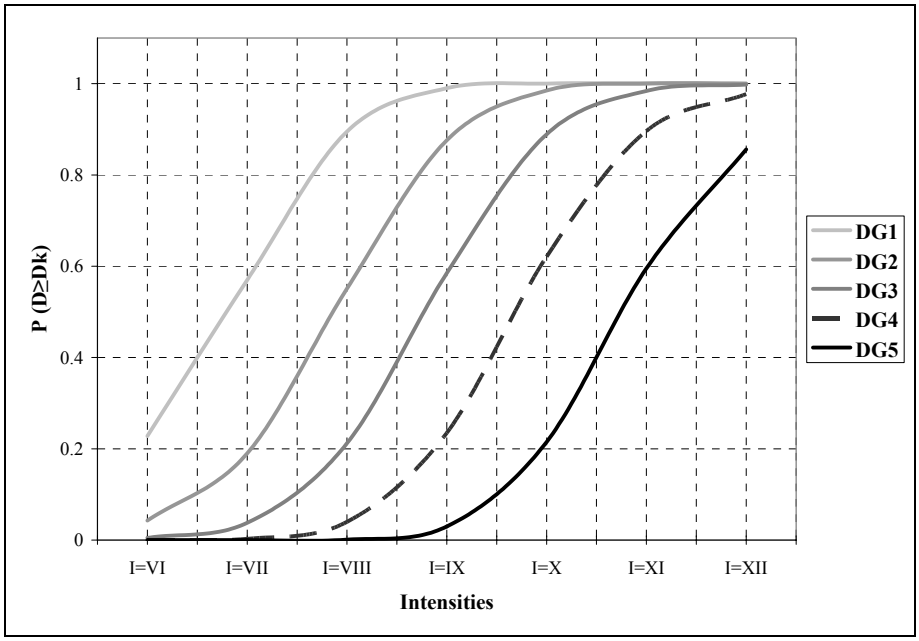

Figure 6.34: Fragility Curves for V_I = 0.69 (NENG-RC typology).

6.4 Summary

Two selected vulnerability assessment methodologies (IVIM and LM1) are used in this chapter. The LM1 approach provides vulnerability distributions for Mérida allowing concluding preliminarily that most of the constructions at "La Milagrosa" (and other similar settlements are highly vulnerable). A more detailed vulnerability evaluation of these constructions is performed through the IVIM; the required knowledge about them is acquired by studying the available damage reports for similar conditions, by trying to understand their seismic behavior and by performing a code type analysis (following the Venezuelan seismic code) on three prototype buildings (with one, two and three floors, respectively). The output of the evaluation by the IVIM is a classification of the constructions according their vulnerability indices. This information is used to perform a new study inside "La Milagrosa" with LM1 methodology providing local damage scenarios.